UNIVERSITY OF PRETORIA

FACULTY OF VETERINARY SCIENCE

DEPARTMENT OF PARACLINICAL SCIENCES

TITLE OF THE RESEARCH PROJECT:

Histopathology of cerebral babesiosis in dogs with naturally acquired *Babesia rossi* infection

THE DEGREE:

MMedVet (Pathology)

AUTHOR:

Dr Michelle Lewis

STUDENT NUMBER:

20115866

SUPERVISOR: Prof. Andrew Leisewitz

CO-SUPERVISOR: Dr Sarah J. Clift

© University of Pretoria

ACKNOWLEDGEMENTS

I am eternally grateful to so many supportive friends and family who have helped me along this journey, but firstly thank you Lord for blessing me with the ability to do this and for blessing me with the circle of people that I needed to carry me through it.

To my husband, Herman, I have no words to express how much your love and support have meant to me. Thank you Sweety.

To my children Caitlin and Ethan, thank you for being patient with me and supporting me in your own way, while I spent many hours working on this “pieces”.

To my parents, Lynn and Edmund, thank you for your support and for making a way for me to become a veterinarian. I know it was tough at times, but somehow you managed to get me through it.

To Sarah and Andrew, thank you for your mentorship, patience, guidance and for rooting for me when I needed it most. I dearly appreciate you both.

Thank you to the histopathology laboratory team at the Pathology Section, Faculty of Veterinary Science, University of Pretoria for processing the histology slides, special stained slides and immunohistochemistry. Mr. P Mokonoto, Mr. X Mtshali, Mrs RM Phaswane and especially Mrs N Timmerman for your patience, meticulous work and attention to detail. You are all greatly appreciated.

© University of Pretoria

DECLARATION

No conflicts of interest have been declared. Full funding has been received from an NRF research grant (Reference: CPRR13080726333, Grant No: 91572, 31 March 2014) obtained by Professor Andrew Leisewitz.

© University of Pretoria

ETHICS STATEMENT

This study was granted permission by the Animal Ethics Committee of the FVS, UP (Ref: V061-18).

This study was also granted permission by the Research Ethics Committee, FVS, UP (Ref: REC062-18).

Professor Andrew Leisewitz received authorisation from the Research Ethics Committee for larger protocol to investigate the use of canine babesiosis as a model or human malaria (V034-14).

© University of Pretoria

TABLE OF CONTENTS

ACKNOWLEDGEMENTS 2
DECLARATION 3
ETHICS STATEMENT 4
TABLE OF CONTENTS 5
LIST OF FIGURES 7
LIST OF TABLES 10
APPENDICES LIST 11
ABBREVIATIONS / ACRONYMS 11
CHAPTER 1 INTRODUCTION 13
CHAPTER 2: LITERATURE REVIEW 15
2.1 Protozoa as a cause of CNS disease 15
2.2 Babesia – introduction to the disease 15
2.3 Cerebral Babesiosis – canine and bovine 21
2.4 Babesiosis and Malaria – similarities and differences 26
2.5 Malaria 27
2.6 Proposed pathogenesis of cerebral babesiosis (CB) 34
2.7 Canine cerebral babesiosis as a model for cerebral malaria 37
CHAPTER 3: RESEARCH OBJECTIVES 39
3.1 Aims of this study 39
3.2 Hypothesis 39
3.3 Benefits arising from the project 40
CHAPTER 4: MATERIALS AND METHODS 41
4.1 Experimental Design 41
4.2 Data analysis and completing scoresheets 46
4.3 Facilities 51
4.4 Equipment 51
4.5 Records 52
CHAPTER 5: RESULTS 53
5.1 Selection of formalin-fixed paraffin-embedded (FFPE) tissue blocks 53
5.2 Summary of score sheets (HE, special stains and IHC) and statistical analyses 53
5.3 Histopathology descriptions of CCB and non-CCB cases 57
5.4 Immunohistochemistry 71
CHAPTER 6: DISCUSSION 82
6.1 Babesia rossi as the causative Babesia sp. in this study 82

© University of Pretoria

6.2 Macroscopic pathology of the brain 84
6.3 Histopathology of CCB and non-CCB cases 84
CONCLUSIONS 108
REFERENCE LIST 110
APPENDICES 122
Appendix A: Check sheet template and abbreviations used on check sheets 122
Appendix B: Histopathology grading and scoring criteria 124
Appendix C: Master summary check sheet for all cases (see attached) 131

© University of Pretoria

LIST OF FIGURES

Figure 1: Life cycle of canine babesiosis.

Figure 2: Brain of a dog demonstrating multifocal cerebral cortical haemorrhages typically associated with cerebral babesiosis caused by *B. rossi*. (Jacobson, 2006).

Figure 3: The brain of a bovine infected with *Babesia bovis* showing typical macroscopic changes in bovine cerebral babesiosis (a – b). There is diffuse congestion of the entire brain when visualised from an external perspective. Gyral widening, filling out and obliteration of the outline of sulci are noted (a). In coronal sections of the brain, bovine cerebral babesiosis typically displays severe congestion of the grey matter (b) when compared to a normal bovine brain (c) (adapted from images from UPSpace, 2009).

Figure 4: The malaria life cycle.

Figure 5: Case 1 (CCB). HE stain. Mononuclear cell leucostasis (oval dotted line) and congestion in a vessel with an intact wall (thin arrows). Note the small number of mononuclear cells in the vascular wall (vasculitis) in the bottom part of the vessel wall (thick arrows). 20 x magnification.

Figure 6: Case 1. HE stain. Moderate parasitaemia. Note the small intravascular, degenerating *Babesia* parasites (thin arrows) in an erythrocyte that has started showing lytic changes. 40 x magnification. *Insert* (top right): close-up of *Babesia* infected erythrocyte.

Figure 7: Case 1 (Cerebral babesiosis, treated). HE stain. Note the petechiae (thin arrows), ecchymoses (thick arrows) and suffusive haemorrhages (solid star) in the brain of a dog with cerebral babesiosis caused by *Babesia rossi*. Sub-macro, 2 x magnification.

Figure 8: From Appendix B (Histopathology Grading and Scoring criteria) illustrating how the distribution of inflammatory cells was evaluated in vessels displaying vasculitis.

Figure 9: Case 5 (CCB). HE stain. Vasculitis consisting of mononuclear cellular infiltrate, effacing the vessel wall with erythrocytes extending throughout the wall, indicating a loss of vascular integrity. 40 x magnification.

Figure 10: Case 1 (CCB). HE stain. Vasculitis consisting predominantly of mononuclear cellular infiltrate (thin arrows), completing effacing the vascular wall. Outline of vessel wall in dotted lines. 20 x magnification.

Figure 11: Control section, MSB stain. 20 x magnification.

© University of Pretoria

Figure 12: Case 1 (CCB). MSB stain. Haemorrhage, vasculitis and leucostasis transitioning from intralesional (IL, on right) to perilesional (PL, on left) with fibrin deposition (red staining filamentous material). 4 x magnification.

Figure 13: Case 1 (CCB). MSB stain. Higher magnification of the area highlighted in figure 12. Note the red staining fibrin (thick arrows) and yellow-green staining erythrocytes (thin arrows). 20 x magnification.

Figure 14: Case 1 (CCB). HE stain. Severe endothelial cell hypertrophy, as indicated in two hypertrophied endothelial cells (thin arrows). Note the blood vessel with mononuclear vasculitis and loss of vascular wall integrity. 40 x magnification.

Figure 15: Left: Control case, HE stain. Note neurons with fine nissl substance and clearly visible nucleus and nucleolus. Right: Case 2 (CCB). Neuronal injury in 3 neurons (thin arrows) typified by, shrunken and hypereosinophilic cytoplasm with indistinct to pycnotic nuclei. Note the perilesional location of neuronal injury in this image with haemorrhage and vasculitis in the blood vessel in the bottom left of the image (indicated by a solid star). 40x magnification.

Figure 16: Top left. Control case, cerebellum white matter and grey matter junction depicting even staining of white matter. LFB stain. Top right: Case 3 (CCB). LFB stain. Cerebral white matter (WM) and grey matter (GM) junction, depicting decreased LFB staining in WM (dotted ovals). 4 x magnification. Bottom middle: Case 3 (CCB). LFB stain. Higher magnification of image in top right, showing pallor of LFB stain and neuropil spongiosis (thin arrows). 40 x magnification.

Figure 17: Left: MAC-387 control section. Case 1 (CCB). MAC-387 IHC. Note the numerous MAC-387 positive labelling cells (thin arrows) in the neuropil. One blood vessel wall is filled with MAC-387 positive labelling cells, forming a distinct outline of the affected blood vessel (thick arrow). Intralesional (IL) area. 20 x magnification.

Figure 18: Case 11 (CCB). MAC-387 IHC. Note the perilesional (PL) haemorrhage with MAC-387 positive labelling monocyte-macrophage lineage cells in both perilesional and intravascular areas. The intact blood vessel wall is outlined (- - - -) in the top half of the image (BV). 4 x magnification.

Figure 19: Case 20 (non-CCB). MAC-387 IHC. Note the numerous intravascular MAC-387 positive labelling leucocytes in a thrombus of a large meningeal blood vessel (star) as well as leucostasis in the smaller adjacent blood vessel (thick arrow). 4 x magnification.

© University of Pretoria

Figure 20: Left: IBA1 IHC control section with scattered positive labelling of resident microglia (thin arrows). Right: Case 11 (CCB). IBA1 IHC showing numerous positively labelled extravascular cells associated with an area of microvascular haemorrhage (thin arrows). Note the intact larger blood vessel to the left (dotted line). 10 x magnification.

Figure 21: Case 1 (CCB). IBA IHC. Note the low number of IBA1 positive cells (thin arrows) in an area with multiple acute haemorrhages (dotted lines).

Figure 22: Case 20 (non-CCB). IBA1 IHC. Note the positive labelling of resident IBA1 positive cells in the neuropil (thin arrows), displaying thin cytoplasmic processes and small angular cell outlines, compared to plump, round activated intravascular IBA1 positive immunolabelling mononuclear cells (thick arrows). 20 x magnification.

Figure 23: Top: VCAM-1 control section with no VCAM-1 immunoreactivity present in the endothelial cells (thin arrows). Below: VCAM-1 IHC showing small bead-like areas of positive immunoreactivity in activated endothelial cells (thin arrows). (a) Case 12 (CCB group). (b) Case 20 (non CCB group). 40 x magnification.

Figure 24: Left: CD3 control section showing a lack of CD3-positive immunoreactivity. Right: Case 7. CD3 IHC showing scattered rare intravascular CD3-positive T lymphocytes (thin arrows). 20 x magnification.

Figure 25: Left: CD20 control section showing a lack of CD20- positive immunoreactivity. Right: Case 17 (non-CCB) CD20 IHC showing rare, isolated intravascular positive labelling of a B lymphocyte (thin arrow). 20 x magnification.

Figure 26: Atomic force field microscopy of red cell surfaces from two different dogs (a & b), naturally infected with *Babesia rossi*. Note the absence of abnormal red cell surface knobs or ridges as described in *Plasmodium falciparum* and *Babesia bovis* infected red cells. The arrow denotes a bump in the red cell surface as a result of a *Babesia* parasite within the cell (Leisewitz AL and Russell BM, unpublished data).

© University of Pretoria

LIST OF TABLES

Table 1: A summary of the vectors, distribution and severity of disease caused by the three currently recognised dog *Babesia* species.

Table 2: Postmortem findings in a series of 25 cases of confirmed mono-infections of *Babesia rossi* in dogs that died as a result of the infection (GIT - gastrointestinal tract; ALI – acute lung injury; ARDS – acute respiratory distress syndrome).

Table 3: Summary of the similarities and differences between *Babesia* and Malaria haemoparasites and the diseases they cause.

Table 4: List of special stains used and the target feature/s that are highlighted.

Table 5: List of antibodies used, including the clone, source, catalogue number and cell-line / feature targeted.

Table 6: Scores per individual case for the 4 broad histological categories and test statistics results for the Mann-Whitney U test and p-values per category. Group 1 = treated CCB cases; group 2 = non-treated CCB cases; group 3 = non-CCB cases.

Table 7: Descriptive statistical analyses per group, including. Group 0 = controls; group 1 = treated CCB cases; group 2 = non-treated CCB cases; group 3 = non-CCB cases.

Table 8: Summary of average scores and percentages of possible maximum score in CCB versus non-CCB cases.

Table 9: Bar graph depicting the numerical data in table 8.

Table 10: Leucostasis details per case, including distribution within the brain, cell type/s, severity and distribution relative to haemorrhagic lesions.

Table 11: Differences between the 3 babesiosis groups in this study, i.e. CCB treated, CCB not treated and non-CCB.

© University of Pretoria

APPENDICES LIST

A: Check sheet template and abbreviations used on check sheets

B: Histopathology grading and scoring criteria

C: Master summary check sheet for all cases

ABBREVIATIONS / ACRONYMS

BBB:	blood-brain barrier
BCB:	bovine cerebral babesiosis
CCB:	canine cerebral babesiosis
CM:	cerebral malaria
CNS:	central nervous system
DIC:	disseminated intravascular coagulation
DPS:	Department of Paraclinical Studies
EL:	extralesional (away from haemorrhages)
FFPE:	Formalin-Fixed Paraffin-Embedded
FVS:	Faculty of Veterinary Science
HCM:	human cerebral malaria
HE:	haematoxylin and eosin
HIV:	human immunodeficiency virus
ICAM1:	intercellular adhesion molecule-1
IHC:	immunohistochemistry
IFN-γ:	interferon gamma
IL:	intralesional
IL-1, 6, 8, 10:	interleukin-1, 6, 8, 10
iNOS:	inducible nitrous oxide
LFB:	luxol fast blue stain
MSB:	martius scarlet blue
MCM:	murine cerebral malaria
MCP-1:	monocyte chemotactic protein-1
MN:	mononuclear leucocyte
Non-CCB:	non-cerebral canine babesiosis
NO:	nitric oxide
OVAH:	Onderstepoort Veterinary Academic Hospital

© University of Pretoria

PfEMP1:	*P. falciparum* erythrocyte membrane protein 1
PL:	peri-lesional
pRBCs:	parasitised red blood cells
SP:	Section of pathology
TNFα:	tumour necrosis factor alpha
TSP:	thrombospondin
VCAM1:	vascular cell adhesion molecule-1
VESA1:	variant erythrocyte surface antigen 1

© University of Pretoria

CHAPTER 1 INTRODUCTION

Canine babesiosis, caused by *Babesia rossi* in Southern Africa is the most severe babesial disease affecting dogs and often results in a multisystemic disease with a high morbidity and mortality (Welzl et al., 2001, Jacobson, 2006, Penzhorn, 2011, Leisewitz et al., 2019a, Leisewitz et al., 2019b). Canine cerebral babesiosis (CCB) is a central nervous condition that develops as a rare and acute complication with a mortality rate approaching 100%. In South Africa, CCB is only associated with *B. rossi* infection. Outside of Southern Africa, there are isolated documented cases where *Babesia canis* has been implicated in CCB (Adaszek et al., 2012, Strobl et al., 2020).

There is virtually no published literature describing the cerebral-complicated form of the disease. That which is published is antiquated and describes individual cases. In 2000 a study was completed by Pardini and presented as a dissertation for a Masters of Science (MSc) in Pathology degree at the University of Pretoria (Pardini, 2010). In this study Pardini described the macroscopic, histological and ultrastructural lesions of CCB in dogs presented at the Onderstepoort Veterinary Academic Hospital (OVAH), Faculty of Veterinary Science (FVS), University of Pretoria (UP) over the period 1996 to 1998. This Masters thesis was never published. In addition, the understanding of haemoprotozoal cerebral disease pathology and pathophysiology has advanced since then. Immunohistochemistry (IHC) techniques that were not available at the time of Pardini's study are now fairly easily obtainable and routinely used in veterinary pathology.

Molecular diagnostic techniques were not readily available in the 1990s and the *Babesia* species infecting the dogs in these cases could not be confirmed on a molecular level. Molecular diagnostic techniques have been used routinely at the OVAH since 2010 and to date, CCB has not been diagnosed in a dog infected with *B. vogeli* or any other *Babesia* species. *B. rossi* is responsible for over 95% of all babesia cases presented to the OVAH and *B vogeli* has never been responsible for severe disease in dogs examined in the OVAH (Matjila et al., 2004).

The archived tissue samples collected by Pardini were used in this study to conduct a retrospective cross-sectional study of the microscopic pathology in CCB. In Pardini's study a total of 54 fatal canine babesiosis cases were postmortemed, of which 32 cases had microscopic cerebral involvement and the remaining 22 cases did not. All samples

© University of Pretoria

were collected from dogs that were presented at the OVAH and originated from Pretoria and the immediate surrounding areas.

Blood samples were collected from 56 dogs at the OVAH as part of a study to determine the prevalence of *Babesia* infection in dogs in South Africa (Matjila et al., 2004). PCR testing showed that 19 of the 56 dogs were positive for *Babesia* and out of these 1 was infected with *B. vogeli* while the remaining 18 were infected with *B. rossi* (Matjila et al., 2004). Unpublished data gathered at the OVAH strongly support the finding that *B. rossi* appears to be the only *Babesia* species in South Africa to cause complicated canine babesiosis. Given the distribution of the vectors, distribution of *B. rossi* and the severity of the clinical symptoms, it is assumed that the dogs included in this (and Pardini's) study had a mono-infection of *B. rossi* or coinfection of *B. rossi* and *B. vogeli*.

In this study the definition of CCB was pathological, not clinical and hence the focus was on a selection of the 32 cases that showed microscopic cerebral morphological changes. This study included a review of the histopathology as seen on haematoxylin and eosin (HE) staining, applied special staining to highlight demyelination and fibrin, as well as IHC to accurately identify the cellular and inflammatory responses associated with the central nervous lesions.

© University of Pretoria

CHAPTER 2: LITERATURE REVIEW

2.1 Protozoa as a cause of CNS disease

Protozoan parasites that infect and cause disease in the central nervous system (CNS) of mammals include *Babesia, Theileria, Trypanosoma, Toxoplasma, Neospora, Sarcocystis, Acanthamoeba, Balamuthia* and *Plasmodium* species (Elsheikha and Khan, 2010, Cantile and Youssef, 2016). In humans, neuropathogenic protozoa include *Acanthamoeba, Toxoplasma*, *Trypanosoma* and *Plasmodium* (Elsheikha and Khan, 2010, Chimelli, 2011). Clinicopathological presentation of these conditions include encephalopathy (cerebral malaria), meningoencephalitis (trypanosomiasis) and nodular lesions (toxoplasmosis in reactivated Chaga's disease) (Chimelli, 2011). In animals, neuropathogenic protozoa have been found in a wide variety of domestic and wildlife species (Penzhorn, 2011). Immunosuppression has been suggested as a contributing factor for more severe manifestations and failure of treatment in human *Plasmodium* cases (Chimelli, 2011). Similar findings are mentioned in animal species, such as increased severity of babesiosis infections in young puppies and dogs with co-infections (Irwin, 2010) and neosporosis in immunologically immature foetuses versus closer to term foetuses (Andrianarivo et al., 2001). The blood-brain barrier (BBB) consists of the vascular endothelial cells with their intercellular tight junctions, the underlying basement membrane and the astrocyte foot processes. The manner in which protozoal organisms cross the BBB has been speculated on for a number of years and is not completely understood. Mechanisms include transcellular and paracellular movement as well as the "Trojan horse" method i.e. via infected leucocytes, but the details on a molecular level are not completely unravelled yet (Elsheikha and Khan, 2010). The intra-erythrocytic protozoa that also cause CNS disease include *Babesia, Plasmodium* and *Theileria* species (Cantile and Youssef, 2016). The focus of this literature review is babesiosis and the related disease caused by malaria parasites.

2.2 Babesia – introduction to the disease

Babesia species can infect a wide range of vertebrate hosts by parasitising the erythrocytes and causing a variety of clinical symptoms, including haemolytic anaemia, icterus and haemoglobinuria. The severity of clinical signs depends mainly on host susceptibility and the virulence of the *Babesia* species involved. Infection requires an

© University of Pretoria

invertebrate vector. To date the only vectors identified are ixodid ticks (Homer et al., 2000).

In summary, the *Babesia* lifecycle is as follows:
Sporozoites are transmitted from the salivary glands of feeding ticks into the host's bloodstream and subcutaneous tissue (Irwin, 2010, Shortt, 1973). Within the host's bloodstream the parasites enter erythrocytes and repeatedly multiply asexually, releasing merozoites, which in turn invade more erythrocytes. As merozoite numbers increase, the parasite numbers in the bloodstream become elevated and the host becomes capable of transmitting parasites, in the form of piroplasms within infected erythrocytes, back to the tick vector. Within the tick vector, piroplasms undergo sexual reproduction, followed by maturation. Mature parasites migrate either to the tick's salivary glands, ready for the next blood meal or to the tick's ovaries, where transovarial transmission to the next generation of ticks can occur (Irwin, 2010, Mehlhorn and Schein, 1985, Uilenberg, 2006). A brief summary of the life cycle is depicted in figure 1 below.

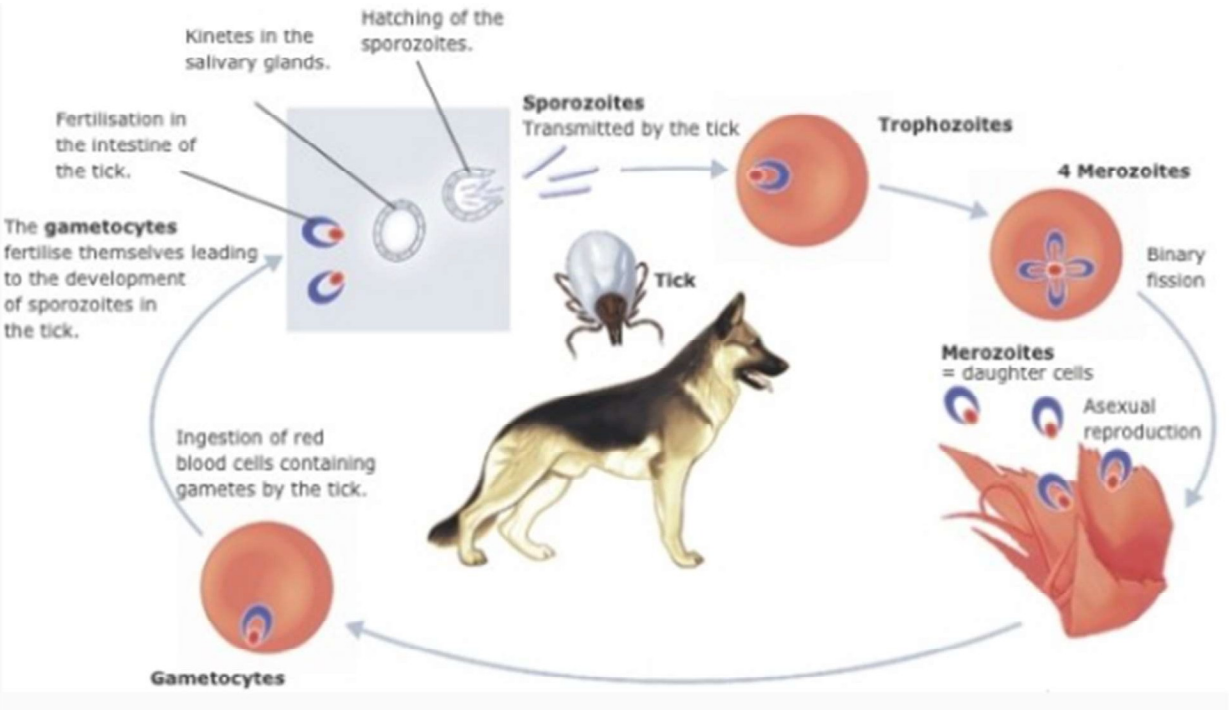


Figure 1: Life cycle of canine babesiosis. Pathvets (n.d.).

© University of Pretoria

2.2.1 Canine babesiosis

The first occurrence of canine babesiosis (CB) in South Africa is thought to date back to the 1790's, but was only linked to "redwater" (babesiosis in cattle) in the late nineteenth century when parasitised red blood cells (pRBCs) were identified on blood smears (Penzhorn, 2020). Following this discovery, inoculation studies proved that transmission of the disease occurred by injection of infected blood via the intravenous and subcutaneous routes. In 1901 Lounsbury, an American entomologist based at the Cape of Good Hope (Cape Town), was the first to demonstrate that CB was transmitted by *Haemaphysalis leachi*, now correctly identified as *H. elliptica,* the southern African yellow dog tick (Apanaskevich et al., 2007, Penzhorn, 2011).

Historically, based on morphology, the *Babesia* parasites that infect dogs have been divided into two main groups, i.e. large and small canine babesias (Uilenberg et al., 1989).

Due to differences in vector specificity, antigenicity, genetic make-up, serology and a lack of cross-immunity, large babesias were re-categorised in the late 1990s to the currently recognised three *Babesia* species, i.e. *Babesia vogeli, B. canis* and *B. rossi* (Carret et al., 1999, Zahler et al., 1998, Depoix et al., 2002, Uilenberg, 2006). Table 1 summarises the differences between these three canine *Babesia* species.

Table 1: A summary of the vectors, distribution and severity of disease caused by the three currently recognised dog *Babesia* species (Carret et al., 1999, Zahler et al., 1998, Depoix et al., 2002, Uilenberg, 2006, Uilenberg et al., 1989, Jacobson, 2006, Penzhorn, 2011, Leisewitz et al., 2019b).

	Babesia vogeli	***Babesia canis***	***Babesia rossi***
Vector	*Rhipicephalus sanguineus* * (kennel tick)	*Dermacentor reticulatus* (ornate dog tick)	*Haemaphysalis elliptica* (southern African yellow dog tick)
Distribution	Worldwide, tropics and subtropics mainly	Europe	Southern Africa
Severity of disease	Mild	Moderate	Severe

* In South Africa the vector, *R. sanguineus*, is more commonly associated with *Ehrlichia canis* infection (Groves et al., 1975).

© University of Pretoria

Small babesias include *Babesia gibsoni*, *B. annae* and *B. conradae* (Kjemtrup and Conrad, 2006). *B. gibsoni* has been identified in North and South America, Australia, the Middle East, Asia and parts of Europe (Muhlnickel et al., 2002, Schoeman, 2009). *B. annae* (also known as *Theileria annae*) was initially identified in Spain, but has since been found in red foxes on Prince Edward Island, Canada and, more recently, *B. annae* DNA has been isolated in lung exudates of red foxes in Great Britain (Bartley et al., 2016).

A recent study on 91 black-backed jackals in southern Africa included both free-ranging and captive jackals. It proved that the vast majority (84.6%) of this population of indigenous canid species harboured haemo-parasites of the *Babesia* genus and that *B. rossi* was present in almost one third of the jackals (Penzhorn et al., 2017). The study suggested that black-backed jackals are the likely natural reservoir host for *B. rossi* (Penzhorn et al., 2017). This was further supported by evidence in a follow-up study which showed a lack of evidence for African wild dogs serving as reservoir hosts for *B. rossi* (Shabangu et al., 2021).

Babesia rossi and complicated canine babesiosis

Much like human malaria infections, canine babesiosis has been classified clinically into either the uncomplicated or complicated form of the disease. Uncomplicated babesiosis is characterised by mild to moderate haemolytic anaemia and hypoxia in a dog that is ambulatory and judged to be well enough to be treated on an outpatient basis. Complicated disease is characterised by single or multiple organ dysfunction/failure as a result of systemic inflammation in a dog that requires in-hospital treatment (Leisewitz et al., 2019b) (Table 3).

For over a century CB in South Africa has maintained a reputation for being a particularly severe clinical disease when compared to CB in other parts of the world. Various underlying reasons for this highly virulent form of the disease have been attributed to poor adaptation of relatively recently introduced European and North American dog breeds to South Africa, and inadequate opportunity for natural selection of resistant dogs due to intense treatment (Penzhorn, 2011).

Macroscopic lesions vary depending on the form of the disease and organ systems affected when the dog develops complicated babesiosis. Table 2 lists common postmortem findings in canine babesiosis cases presented to the SP, FVS, UP.

© University of Pretoria

Table 2: Postmortem findings in a 25 case series with confirmed mono-infections of *Babesia rossi* in dogs that died as a result of the infection (Leisewitz et al., 2019b).

Macroscopic lesions	**Proportion of postmortem cases in which each lesion was observed (percent). n = 25.**
Splenomegaly due to red pulp hyperplasia	25 (100%)
Hepatosis	25 (100%)
Visceral haemorrhages (excluding GIT, lung and brain)	22 (88%)
Anaemia	20 (80%)
Icterus	17 (68%)
Acute interstitial pneumonia (ALI and ARDS)	16 (64%)
GIT haemorrhage	6 (24%)
Pericardial effusion	9 (36%)
Thoracic effusion	4 (16%)
Abdominal effusion	3 (12%)
Pericardial and thoracic effusion Abdominal and thoracic effusion	2 each (16%)
Cerebral babesiosis	4 (16%)
Acute kidney injury (nephrosis)	4 (16%)

Abbreviations: GIT, gastrointestinal tract; ALI, acute lung injury; ARDS, acute respiratory distress syndrome.

In South Africa, particularly in the area surrounding the OVAH, complicated babesiosis is associated with *B. rossi* infection (Jacobson, 2006) and includes clinical manifestations such as nervous signs ("cerebral babesiosis"), acute renal failure, pulmonary oedema, hepatopathy with icterus, haemoconcentration, immune mediated haemolytic anaemia, disseminated intravascular coagulation (DIC), systemic inflammatory response syndrome (SIRS) and shock (Jacobson and Clark, 1994, Leisewitz et al., 2019b, Leisewitz et al., 2019a). The two most fatal complications in South Africa, with mortality rates up to 80%, are cerebral babesiosis and the "red" haemoconcentrated form (Leisewitz et al., 2019b).

Canine cerebral babesiosis (CCB) was first described in Kenya (Purchase, 1947) and historically characterised by cerebral haemorrhages, high numbers of extracellular parasites in cerebral capillaries, heavily parasitised erythrocytes in cerebral tissue and severe cerebral congestion (Pardini, 2010). Cerebral babesiosis was first described in

© University of Pretoria

South Africa in the 1960s by a private practitioner in Port Elizabeth (Botha, 1964) and later at the Onderstepoort Veterinary Research Institute in Pretoria (Basson and Pienaar, 1965).

Clinicians have come a long way in investigating prognostic indicators and have made substantial progress with treatment protocols for CCB, but there are still many unanswered questions and mortality rates in this disease remain high, close to 100% (Collett, 2000, Welzl et al., 2001, Jacobson, 2006, Leisewitz et al., 2019b).

2.2.2 Babesiosis in cattle

Bovine babesiosis and anaplasmosis are considered to be the most economically important diseases of cattle worldwide (de Castro, 1997, Bock et al., 2004). *Babesia divergens*, transmitted by *Ixodes ricinus* ("castor bean/deer tick"), is the species prevalent in Europe and, unlike other bovine *Babesia* spp., it is a zoonosis (Zintl et al., 2003).

In South Africa, *Babesia bigemina* (African redwater), *B. bovis* (Asiatic redwater; also previously called *B. argentina*) and *Anaplasma marginale* are the three intraerythrocytic parasites involved in a highly prevalent disease complex. All three pathogens are transmitted by the ixodid tick *Rhipicephalus microplus* ("Asian blue tick") previously known as *Boophilus microplus*. This tick has spread rapidly on the African continent, adapting well to African conditions while competing with and replacing the indigenous *R. decoloratus* ("African Blue tick") in some areas. *R. decoloratus* transmits *B. bigemina* and *A. marginale* but has not been shown to transmit *B. bovis*. It is currently more widespread than *R. microplus*, but this may change as *R. microplus* continues to spread through the continent (Tønnesen et al., 2004, Madder et al., 2011, Nyangiwe et al., 2017).

Despite the close phylogenetic relationship between the two bovine *Babesia* parasites, *B. bovis* and *B. bigemina*, clinically the differences are striking. As is the case in dogs infected with *B. canis* or *B. vogeli*, *B. bigemina* infection in cattle typically causes a far milder form of bovine babesiosis, characterised mainly by anaemia. Likewise, as with *B. rossi* infections in dogs, *B. bovis* infection in cattle is known to cause a severe form of bovine babesiosis, characterised by symptoms such as severe anaemia, fever, haemoglobinuria, and nervous signs due to bovine cerebral babesiosis (BCB) (Brown and Palmer, 1999).

© University of Pretoria

2.2.3 Babesiosis in other vertebrate species

Although over 100 *Babesia* species have been identified, of which more than 70 species affect mammals, the most numerous being in rodents (Levine, 1988, Homer et al., 2000), the list of *Babesia* parasites that have been described to cause CNS disease is significantly shorter and is limited to *B. rossi, B. canis, B. bovis, B. divergens, B. duncani* and *B. microti.* Of these *Babesia* species, only *B. rossi* (previously *B. canis / B. canis rossi*) and *B. canis* (a single case documented in Europe) have been associated with CNS disease in dogs (Reyers et al., 1998, Jacobson, 2006, Schoeman, 2009, Adaszek et al., 2012, Callow and McGavin, 1963). In cattle, *B. bovis* has been described as causing CNS lesions (Rogers, 1971, Uilenberg, 2006, Callow and McGavin, 1963) and *B. divergens, B. duncani* and *B. microti* have been reported in association with cerebral disease in humans (Usmani-Brown et al., 2013). In South Africa, a variety of *Babesia* spp. have also been detected in wildlife. Clinical signs are not always present in wildlife species but when present, these are typically haemolysis-related, as seen in babesiosis in domestic animals. Infected wildlife species include roan antelope (*Hippotragus equinus*), giraffe (*Giraffa camelopardalis*), lions (*Panthera leo*) and black rhinoceros (*Diceros bicornis*) (Penzhorn et al., 2001, Nijhof et al., 2003, Oosthuizen et al., 2009). None of these wildlife species have, to date, been described to develop cerebral babesiosis.

2.3 Cerebral Babesiosis – canine and bovine

2.3.1 Clinical aspects

Following the first description of a case of CCB in Kenya (Purchase, 1947), CCB cases started appearing in South Africa in the 1950s. Neurological abnormalities and pathology were initially attributed to damage of both the central and peripheral nervous systems in canine babesiosis cases (Malherbe and Parkin, 1951, Botha, 1964) but there has never been any evidence to support peripheral nerve lesions as a contributing factor to the pathogenesis of CCB. Central nerve damage (neuronal injury) has, however, been described and was thought to be a result of ischaemia (Pardini, 2010).

Establishing a suitable definition for cerebral babesiosis is problematic. Human cerebral malaria (HCM) is diagnosed based purely on a clinical definition and is distinguished from non-cerebral malaria based on the absence of those clinical signs (Newton et al., 2000). Some severely affected canine babesiosis cases can demonstrate CNS clinical

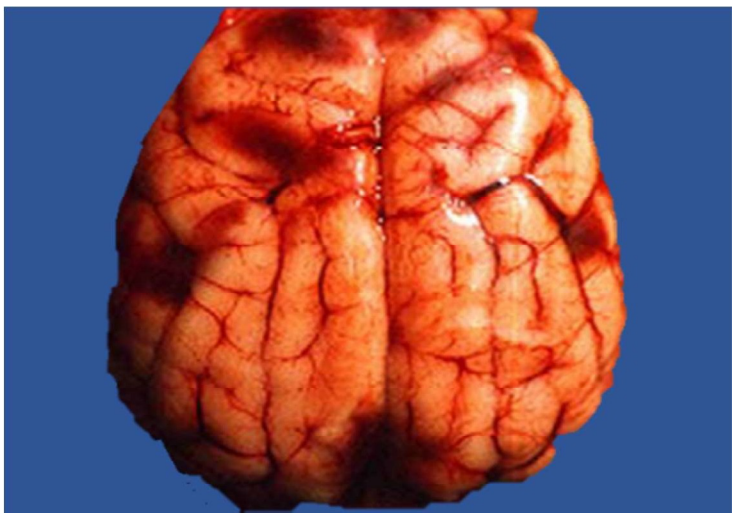
© University of Pretoria

signs that include seizures, profound depression or coma and nystagmus, which may be secondary to factors such as severe anaemia, acidosis, hypoglycaemia or other metabolic encephalopathies. CCB was defined by Basson based on both clinical and histopathological findings as: “an atypical manifestation of babesiosis, characterized by nervous symptoms; sludging of pRBCs in the smaller vessels and capillaries of the brain” (Basson, 1965). In this study an attempt was made to avoid potential selection bias by including animals who do / do not have neurological signs, those with / without cerebral pathology and controls.

The pathology of BCB in cattle has been well-studied (Rogers, 1971, Patarroyo et al., 1982, Callow and McGavin, 1963, Commins et al., 1988) and various researchers have paid particular attention to similarities between BCB and HCM (Hutchings et al., 2007, Aikawa et al., 1985, Allred et al., 2000). In cattle with BCB the course of the disease is typically fatal and neurological clinical aspects include hyperaethesia, nystagmus, circling, head pressing, aggression, convulsions and paralysis (De Vos et al., 2004).

2.3.2 Macroscopic pathology in CCB

Literature describing the macroscopic pathology of CCB is scarce. The available data described macroscopic haemorrhages that ranged from petechiae to suffusive and were often bilaterally symmetrical, most commonly present in the cerebral hemispheres (Piercy, 1947, Basson and Pienaar, 1965, Leisewitz et al., 2019b) (Figure 2).



© University of Pretoria

Figure 2: Brain of a dog demonstrating multifocal cerebral cortical haemorrhages typically associated with cerebral babesiosis caused by *B. rossi*. [adapted from (Jacobson, 2006)].

2.3.3 Histopathology of CCB

Few studies have offered detailed histological descriptions of cerebral babesiosis in dogs. Those that exist are dated and have considered individual cases only. In the first documented cases of CCB, histopathological descriptions included blood vessels packed with pRBCs and uneven distribution of capillary filling; however, there was no mention of localised cellular reaction or haemorrhage (Purchase, 1947). In other reports, common histopathological findings included oedema (perivascular or perineuronal), "sludging" of pRBCs erythrocytes in smaller calibre vessels and variably sized haemorrhages (Piercy, 1947, Maegraith et al., 1957, Basson and Pienaar, 1965, Okoh, 1978, Moore and Williams, 1979, Pardini, 2010). Less commonly, fibrin thrombi (Botha, 1964, Moore and Williams, 1979, Pardini, 2010), margination of pRBCs in larger vessels, infiltration of leucocytes into perivascular spaces, neuropil necrosis and glial cell reactivity (Basson and Pienaar, 1965, Leisewitz et al., 2019b) have been described.

In Pardini's cases the most common histopathological findings, found in more than 50% of cases with cerebral lesions, included the following which are listed in order of most to least frequent:

i. Haemorrhages primarily limited to the grey matter, including petechiae, ecchymoses and suffusive haemorrhages
ii. Visible *Babesia* parasites
iii. Neutrophil infiltration on periphery of haemorrhages
iv. Oedema (cortex, subcortical grey matter and/or white matter)
v. Monocytic leucostasis
vi. Microvascular necrosis
vii. Endothelial nuclear swelling

The remainder of the findings, recorded in less than 50% of cases with cerebral lesions, were intra- and extra-vascular fibrin polymerisation, Alzheimer type 2 cells, perivascular neutrophilic cuffing, neutrophilic margination, lymphocytes and plasma cells (Pardini, 2010).

© University of Pretoria

Due to the challenges in defining CCB, it was decided to limit the definition of CCB in this study to histological lesions only and not to include clinical signs. All cases selected for this study were naturally infected dogs that originated from the area surrounding the OVAH in Pretoria, South Africa. The CCB cases had been diagnosed as canine babesiosis on thin peripheral capillary blood smears and had macroscopic and/or microscopic cerebral lesions with concurrent central nervous signs.

2.3.4 Macroscopic pathology of BCB

Macroscopically, bovine cerebral babesiosis (BCB) descriptions include the most outstanding feature as being diffuse congestion of the grey matter (Bock et al., 2004, De Vos et al., 2004) (refer to Figure 3).

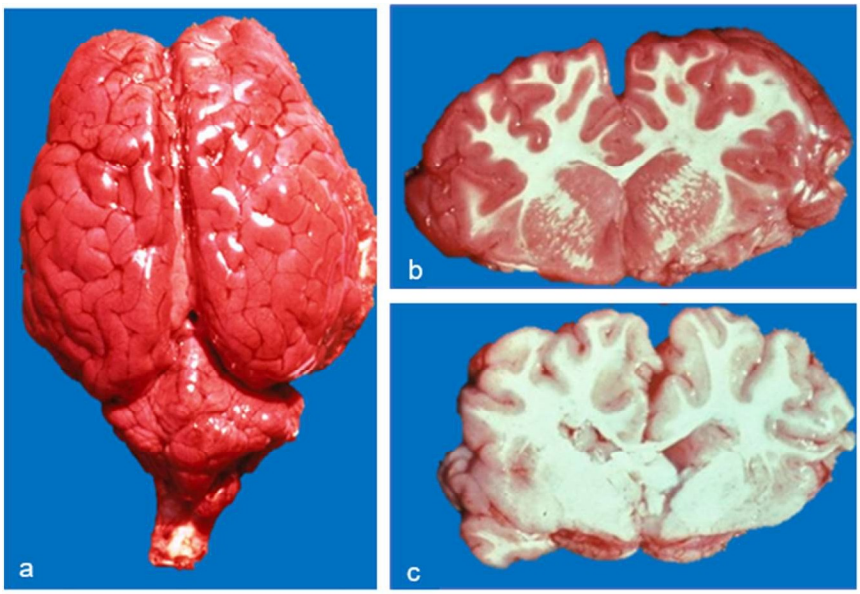


Figure 3: The brain of a bovine infected with *Babesia bovis* showing typical macroscopic changes in bovine cerebral babesiosis (a – b). There is diffuse congestion of the entire brain when visualised from an external perspective. Gyral widening, filling out and obliteration of the outline of sulci are noted (a). In coronal sections of the brain, bovine cerebral babesiosis typically displays severe congestion of the grey matter (b) when compared to a normal bovine brain (c) (adapted from images from UPSpace, 2009).

2.3.5 Histopathology of BCB

Histologically the primary brain lesions in BCB, due to both natural and experimental *B. bovis* infection, have been described as diffuse marked distension of capillaries by pRBCs which is more prominent in the grey matter (Rogers, 1971, Patarroyo et al., 1982,

© University of Pretoria

Callow and McGavin, 1963, Commins et al., 1988). Perivascular oedema and histopathological lesions in the vascular endothelium have not been described in BCB.

The extent of perivascular, perineuronal and interstitial oedema has been described as variable, (Callow and McGavin, 1963, Patarroyo et al., 1982). There is very limited literature regarding vascular endothelial injury in BCB and the data that are available, indicate a lack of injury to endothelial cells in experimental cases (Everitt et al., 1986). As with CCB, thrombosis, neuronal degeneration and malacia were not typical features of BCB cases (Callow and McGavin, 1963, Rogers, 1971, Patarroyo et al., 1982). In contrast to CCB, perivascular haemorrhage was a rare exception in BCB and in a study done on 10 experimentally infected cattle, only one animal had this lesion (Callow and McGavin, 1963).

Virulent *B. bovis* strains have been shown to be associated with neutrophilic leucostasis in pulmonary capillary beds, but infiltration of neutrophils in the CNS has not been documented in bovine babesiosis (Wright et al., 1988). In the lungs, the leucostasis was thought to be the result of a chemoattractant reaction to various proteases released by the parasites. Similar findings have been noted in *P. falciparum* (malaria) infections in humans (Wright et al., 1988) and in the lungs of *B. rossi*-infected dogs (Martin, 2020). The terms “cytoadherence”/ “sequestration” have been used extensively in human malaria research and was adopted by some BCB researchers (Allred and Al-Khedery, 2004, Ho and White, 1999, Smith et al., 2013). It refers to the ability of pRBCs to adhere to capillary and postcapillary venular endothelial cells. Cytoadherence is considered a survival mechanism utilising the microaerophilic conditions in venous blood for optimal maturation and avoiding clearance by the spleen (Smith et al., 2013). Cytoadherence was central to these observations but the underlying pathophysiological mechanisms are not fully understood.

Atomic force microscopy is a very high resolution type of scanning probe microscopy, with resolution in the order of fractions of a nanometer and its application in *B. bovis* pRBCs has shown surface changes that reveal the formation of numerous ridge-like protrusions (ridges) (Hutchings et al., 2007, Aikawa et al., 1985). In contrast, examination of RBCs parasitised by *B. bigemina* using this technology displayed the absence of ridges (Hutchings et al., 2007). The exact protein/s expressed on *B. bovis*-infected RBCs have not yet been identified on the basis of its structure, although a parasite-associated protein that possibly increases interaction between endothelial cells

© University of Pretoria

and pRBCs has tentatively been named *B. bovis* variant erythrocyte surface antigen 1(VESA1) (Allred et al., 2000).

2.4 Babesiosis and Malaria – similarities and differences

There are several similarities between babesiosis and malaria. From a socio-economic aspect, both diseases have a wide global distribution but are most prevalent in third world or developing countries, mainly in Africa and Asia. Both diseases can cause high morbidity and mortality in their respective vertebrate hosts; both pathogens require an invertebrate vector to infect the vertebrate host; both are intraerythrocytic apicomplexan protozoal parasites and both can cause severe multi-organ complications, such as cerebral babesiosis and cerebral malaria (CM). Differences include the vectors, life cycle phases and production of blood pigment.

It is important, at this point, to note the difference between sludging of pRBCs (noted in CCB) and sequestration of pRBCs (noted in HCM and thought to be present in BCB). Sludging is considered a passive process where microvascular obstruction by parasitised and non-parasitised erythrocytes occurs (Malherbe and Parkin, 1951, Malherbe, 1956, Maegraith et al., 1957, Moore and Williams, 1979, Pardini, 2010, Basson and Pienaar, 1965). In sludging there is an accumulation of RBCs in capillaries in the absence of evidence for adhesions between RBCs and the capillary endothelium. In sequestration, on the other hand, there is accumulation of RBCs in capillaries with proven active biomechanical cytoadherence, where pRBCs attach to each other and to the endothelium of small calibre blood vessels. Sequestration has been described in HCM cases and is suspected to have the same or similar mechanism in BCB. Further details are described in pathogenesis and pathophysiology of human malaria (section 2.5.2).
Similarities and differences are summarised in table 3.

© University of Pretoria

Table 3: Summary of the similarities and differences between *Babesia* and Malaria haemoparasites and the diseases they cause (Wright et al., 1988, Abdullahi et al., 1990, Schetters and Eling, 1999, Mota et al., 2001, Krause et al., 2007, Dorovini-Zis et al., 2011, Penzhorn, 2011, Pardini, 2010).

Similarities	**Differences**	
• Intra-erythrocytic apicomplexans • Vector borne • Anaemia • Haemolysis • High parasite density • Lactic acidosis with hypoglycaemia • Multiple organ dysfunction and failure • Red cell sequestration (suspected, not proven in CCB) • Cytokine storm-associated pathology • Immunity is spleen and T cell dependant • Neutrophil accumulation in capillary beds	***Babesia***	**Malaria**
	• Tick vector • No tissue phase in parasite life cycle • No pigment	• Mosquito vector • Tissue phase in parasite life cycle • Haemozoin pigment

It has been shown that babesiosis, like malaria, induces an inflammatory sepsis-like state (Clark et al., 2008, Goddard et al., 2016, Leisewitz et al., 2019a).

2.5 Malaria

In summary the malaria life-cycle is as follows:

The first phase is the pre-erythrocytic phase, which starts when a female anopheline mosquito takes a blood-meal from a human and inoculates *Plasmodium* sporozoites from its salivary glands into the human host. The sporozoites are motile and are transported to the liver via the bloodstream. In the liver they invade hepatic cells, signalling the start of the asexual production phase. During this phase of schizogony, a single sporozoite can produce between 10 000 to over 30 000 daughter merozoites, causing massive swelling and eventual rupture of infected hepatocytes, with subsequent release of motile merozoites into the bloodstream. The intraerythrocytic phase follows, where merozoites invade RBCs and become trophozoites. In some *Plasmodium* spp.

© University of Pretoria

the intrahepatic forms remain dormant in the liver and do not divide immediately (hypnozoites), which can lead to relapses. Over a period of time the trophozoites enlarge and haemozoin pigment is produced as a by-product of haemoglobin consumption. By the end of the intraerythrocytic phase, the parasite has consumed about two-thirds of the RBCs haemoglobin and now forms a multinucleated schizont. Infected RBCs rupture, releasing 6-30 merozoites from the schizont, each of which has the potential to invade a new RBC and repeat the cycle. The malaria life cycle is depicted in figure 4 below.

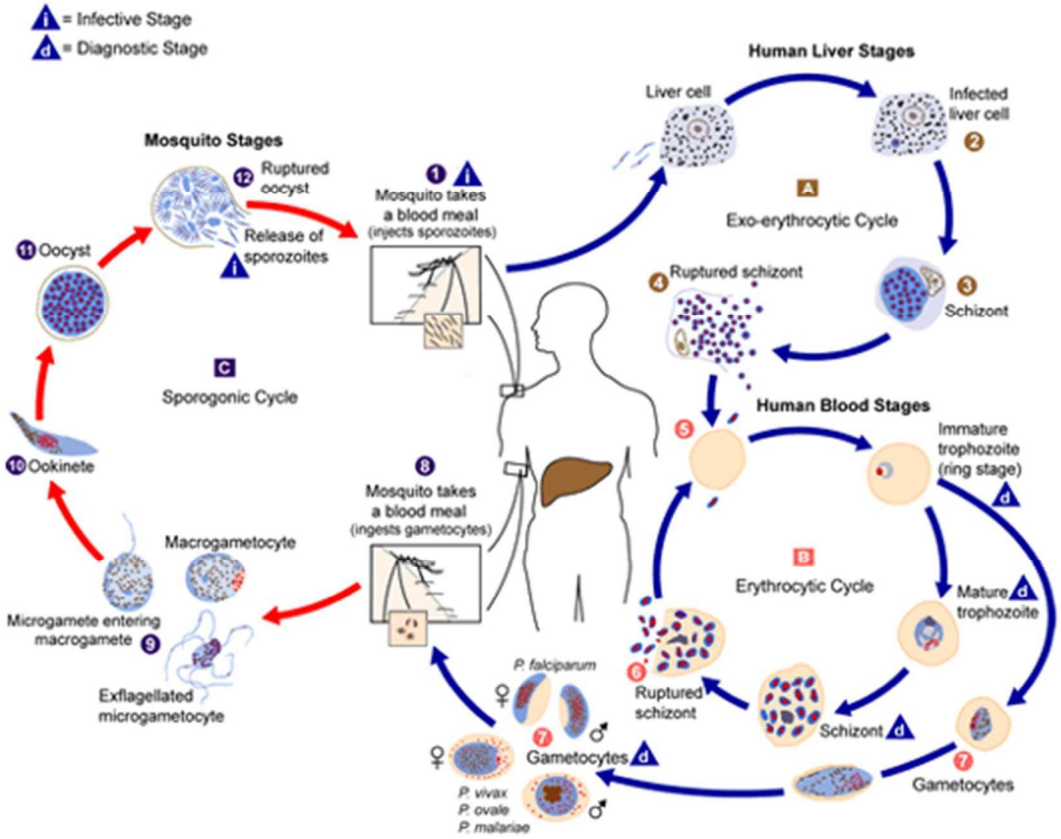


Figure 4: The malaria life cycle. Centers for Disease Control and Prevention (n.d.).

Malaria is caused by the direct effects of the asexual parasite and by the host's immune reaction. Some blood-stage parasites will become longer-lived sexual forms (gametocytes) that can transmit the disease. Once ingested by a feeding female anopheline mosquito, the male gametocyte exflagellates, dividing rapidly into motile male gametes which fuse with female gametocytes and undergo sexual division to form a zygote in the insect's midgut. The zygote matures and encysts into an oocyst, expands

© University of Pretoria

via asexual division and bursts to release numerous motile sporozoites which migrate to the salivary gland, awaiting the mosquito's next blood meal (White and Ashley, 2022).

2.5.1 Malaria in humans, background

In humans, malaria is caused by the genus *Plasmodium* which is chiefly represented by five species, with one species (*Plasmodium ovale*) split into two subspecies. All species are transmitted by the anopheles mosquito vector. These species are *Plasmodium falciparum*, *P. vivax*, *P. malariae*, *P.ovale wallickeri*, *P. ovale curtisi* and *P. knowelsi*. Ninety percent of human malaria mortalities are attributed to *P. falciparum* (Snow, 2015, Milner, 2018).

In human malaria, as in canine babesiosis, a multi-syndromic form of the disease develops in a proportion of the clinically infected population and is referred to as "severe malaria". It is associated with a high mortality rate.

Children under the age of 5 years are at highest risk of developing cerebral malaria. In 2020, 77% of malaria deaths were attributed to children in this age group (Monroe et al., 2022). Severe malaria clinically manifests as life-threatening anaemia, cerebral malaria, respiratory failure and/or acute renal failure (Bartoloni and Zammarchi, 2012).

2.5.2 Pathogenesis and pathophysiology of human malaria

The malaria parasite's biology is generally stable, but it is the human immune response, specifically an inappropriately amplified response, that appears to be the deciding factor for whether a person will develop clinical illness or remain asymptomatic. The final clinical outcome of infection is ultimately considered to be a result of the parasite's pre-programmed biology interacting with the human host's pathophysiological response. The variation in interaction between these two role-players is influenced by genetic diversity of the parasite, human polymorphism, host comorbidities, timing of treatment and environmental factors. The result is a variation in clinical disease including fever, anaemia, coma and respiratory distress. Attempts to eradicate malaria are therefore more complicated than simply reducing the burden of the disease. Factors such as drug availability and shifting of genetically stable parasite populations between low and high endemic areas also need careful consideration (Milner, 2018).

In uncomplicated malaria the initial schizonts rupture, releasing merozoites into the peripheral circulation. The parasites then multiply asexually and the life-cycle progresses from merozoite reinvasion to trophozoite development and more schizonts

© University of Pretoria

that rupture. After 1-2 days the parasitaemia reaches a level where the human host's immune response causes the first symptoms of feeling unwell (Oakley et al., 2011, Milner, 2018). The consequent fever is mainly attributed to tumour necrosis factor-alpha (TNF-α), while interleukin-10 (IL-10) and interferon gamma (IFN-γ) also contribute to the inflammatory response (Clark et al., 2008, McCall and Sauerwein, 2010, Milner, 2018).

Various *Plasmodium* species have different mechanisms of infecting erythrocytes. *P. falciparum* produces the *P. falciparum* erythrocyte membrane protein 1 (PfEMP1), which causes changes on the surface of the pRBCs resulting in it becoming cyto-adherent ("sticky") and adhering to endothelium, platelets or uninfected RBCs (Aikawa et al., 1992b, Baruch et al., 1996, Rowe et al., 1997). This cyto-adherent nature permits pRBCs to sequester in microvasculature, causing vasculitis and obstruction as well as avoiding splenic clearance (Milner, 2018, Fairhurst and Wellems, 2006). In contrast, the other four *Plasmodium* species (*P. vivax, P. malariae, P. ovale and P. knowlesi*) do not induce the presentation of an erythrocyte surface protein and as a result, infection with one of these four species does not result in prolonged periods of pRBC sequestration. It is thought that this difference between *P. falciparum* and the four less pathogenic *Plasmodium* species not only allows for more frequent splenic exposure for clearance of infection in the four less virulent species, but also results in the parasites being more readily visible on peripheral blood smears. In addition, *P. vivax* has a preference for reticulocyte invasion, leading to a lower parasitaemia than *P. falciparum* (Milner, 2018). Progression from typical malaria symptoms to cerebral malaria can be rapid and take place within minutes to hours of the patient displaying the initial clinical symptoms. Differential diagnoses for CM, as for CCB, are thus important to consider such as coma, head trauma, meningitis, hypoglycaemia and bacterial sepsis, among others.

The unique ability of *P. falciparum* to produce PfEMP1 and initiate cytoadherence, particularly with the endothelium, is considered the key factor that permits *P. falciparum* to cause the unique clinicopathological syndrome, cerebral malaria (CM) (Milner, 2018). An equivalent membrane protein has not, to date, been described in canine cerebral babesiosis, although a gene that may have a similar function (BrEMA1) has been identified in *B. rossi* and in a preliminary study it was suggested that it may play a role in disease severity (Matjila et al., 2009).

© University of Pretoria

Similar to ridge formation in BCB, freeze fracture electron microscopy has proven that *P. falciparum*-infected RBCs undergo ultrastructural membrane changes to form knob-like structures (Allred et al., 1986).

2.5.3 Histopathology of cerebral malaria

- General changes

Typical histological lesions of HCM include oedema, sequestration of pRBCs with intravascular and perivascular damage associated with ring haemorrhages and vascular thrombosis, axonal and myelin changes, as well as varying age-related leucocyte reactions. Cerebral oedema is a common non-specific lesion, not unique to HCM and is seen in various non-malaria encephalopathies (Dorovini-Zis et al., 2011). In a study of a series of 103 paediatric autopsies done over a period of 14 years in Malawi, brain swelling was however found in all (100%) of the cerebral malaria cases (Milner Jr et al., 2014).

- Haemozoin pigment and sequestration

In contrast to *Babesia*, *Plasmodium* spp. produce a crystalline pigment (haemozoin) as a product of haemoglobin degradation by the parasite. This is a notable and distinguishing feature between the two haemoprotozoal genera (Uilenberg, 2006) (refer to Table 3). Sequestration of pRBCs is described in most HCM cases and is found in the grey and white matter (Dorovini-Zis et al., 2011). In the Malawi study, two histological patterns were noted in the brain of clinically defined CM cases. Firstly, there was a pattern displaying sequestration of pRBCs only and no other cerebral histological changes. The second pattern was more prevalent and included sequestration of pRBCs together with cerebral microthrombi, ring haemorrhages and extra-erythrocytic haemozoin pigment (Milner Jr et al., 2014).

- Vascular changes, haemorrhage and thrombosis

In HCM of young children, fibrin-platelet thrombi have been described in association with blood vessels sequestered with red blood cells and pigment-laden monocytes, while endothelial cells showed reactive hypertrophy, typically characterised by plump cell nuclei. Endothelial cell injury has been attributed by some to cause microvascular thrombosis, which in turn, is thought to be associated with perivascular ring haemorrhages. Some authors consider pRBCs to be the main driving force behind the vascular changes, ultimately leading to activation of the coagulation cascade,

© University of Pretoria

disseminated intravascular coagulation (DIC), fibrin deposition and thrombosis (Milner Jr et al., 2014, Nishanth and Schlüter, 2019). Ring haemorrhages were often associated with a thrombosed, ruptured capillary at the centre of the lesion with fibrin deposition and centrally located pRBCs (Dorovini-Zis et al., 2011, Milner Jr et al., 2014). On the edge of the ring haemorrhages, non-parasitised RBCs were admixed with scattered leucocytes. The lesions were mainly present in the white matter. Vascular damage was not considered a pre-requisite to increased permeability of the blood-brain barrier (BBB), and blood vessels did not routinely have thrombi present in HCM of young children (Dorovini-Zis et al., 2011). In adults with clinical HCM, typified by premortal coma, a significant association was noted in patients with increased microvascular congestion (with pRBCs or non-pRBCs) and sequestration of pRBCs (Ponsford et al., 2012). There was, however, no significant correlation between patients with premortal coma and cerebral oedema or localised loss of vascular integrity (Medana et al., 2011).

- Myelin changes

In HCM, myelin damage was demonstrated using a Luxol fast blue (LFB) stain, and it varied from total myelin loss to patchy, vacuolated myelin degeneration with loss of structure (Medana et al., 2002). Degradation of myelin was frequently associated with areas of ring haemorrhages, but not restricted to those areas. The extent of axonal injury was assessed using IHC for the beta-amyloid precursor protein (β-APP), which is a reliable and sensitive method for early detection of axonal injury (Hortobagyi et al., 2007). The results showed that early axonal injury was closely associated with ring haemorrhages and sequestered capillaries, varying from large clusters to small foci (Dorovini-Zis et al., 2011).

- Glial cell changes

In HCM, reactive astrocytes were described as being distributed in the subcortex and deep white matter regions but lacking in the cortex. The distribution of astrocyte reaction was not found to overlap with areas of sequestration, RH or axonal or myelin degeneration (Dorovini-Zis et al., 2011).

- Inflammatory response

In young children with CM, there was a lack of a typical extravascular immune response to damaged vasculature, myelin and axons. Intravascular monocyte accumulation was, however, described as being pronounced, causing distention of some capillaries. Phagocytosed haemozoin was a common finding at the centre of RH areas. This was in

© University of Pretoria

contrast to histological changes in adults, where localised accumulations of reactive microglia, lymphocytes and astrocytes (Dürck's granulomas) were noted, suggesting that an immune response had developed with age. In adults, haemozoin-laden monocytes were found only within the micro-vessel lumens and did not appear to have migrated through or beyond the vessel walls, and macrophage phagocytosis was not a consistent feature (Dorovini-Zis et al., 2011).

2.5.4 Mouse model: pathology and pathogenesis of cerebral malaria

The murine model of cerebral malaria (MCM) has been widely used for over two decades and involves *Plasmodium berghei* ANKA (PbA) infection of C57BK/6 or CBA mice, showing a number of shared characteristics with human CM (Carvalho et al., 2000, De Souza and Riley, 2002, De Souza et al., 2010, Penet et al., 2005, Lackner et al., 2006, Hunt et al., 2010, Craig et al., 2012). The mortality rate in affected mice is documented as being between 80-90%, with deaths typically occurring within 6-9 days of infection (Carvalho et al., 2000). Clinical signs include ataxia, seizures, respiratory distress and coma, followed by rapid death, often within 4-5 hours of the initial neurological signs (De Souza and Riley, 2002). There are few studies that describe the macroscopic lesions in MCM and the information available indicates that the largest haemorrhages are present in the deep white matter of the rhinencephalon ("olfactory brain" i.e. the most rostral portion of the brain) with fewer lesions in the grey matter of the outer cortex (Lackner et al., 2006).

Histopathological features in MCM have been described as being inconsistent, with no clear topographical association between intravascular plugging of pRBCs and haemorrhagic foci (Carvalho et al., 2000, Lackner et al., 2006). Adherence between adjacent monocytes (monocyte-monocyte adherence) as well as between monocytes and endothelial cells (monocyte-endothelium adherence) has been shown to vary during the stages of infection and has been described as the most prominent feature in MCM (Carvalho et al., 2000, Miu et al., 2008). Vascular plugging and monocyte-endothelium adherence are noted as being most evident at 6-8 days post-infection. Although similar adherences have been noted in vascular beds outside the brain, haemorrhages are described as being limited to the CNS and are mainly present in the cerebellum and olfactory brain. Haemorrhages are found to be variably sized, including perivascular layered micro-haemorrhages as well as subarachnoid haemorrhages. The

© University of Pretoria

haemorrhage locations are not directly associated with congested vessels which, given the lack of haemorrhages in other organs, is considered an indication that endothelial damage in the CNS is the main underlying cause for the haemorrhages, rather than rupture of vessels due to increased pressure. Perivascular oedema has been noted as a common feature of MCM (Carvalho et al., 2000).

Leucocyte involvement in MCM includes not only monocytes, but lymphocytes too. Natural killer (NK) cells are cytotoxic granular lymphocytes involved in the innate immune response that, when activated, can produce a range of cytokines resulting in T cell recruitment. This reaction has been observed in MCM cases (Hansen et al., 2007).

Less common histological features of MCM include extravasated mononuclear inflammatory cells, damaged Purkinje cells and vascular plugging by pigment-containing monocytes (Carvalho et al., 2000).

As in humans, genetic and environmental factors determine the susceptibility of mice to experimental CM (De Souza et al., 2010). It has been suggested that MCM is not primarily due to hypoxia associated with vascular sequestration, but rather a consequence of a strong immune reaction and that the release of nitric oxide (NO) is a key contributing factor (Clark et al., 1997). The role of NO is thought to possibly activate some secondary neuropathological mechanisms (Maneerat et al., 2000) and pro-inflammatory cytokine release is a shared contributing factor in both murine and human CM (Clark et al., 1997, Miller et al., 2002). A more recent viewpoint is that CM, whether in humans or mice, develops as a result of a combination of biomechanical effects (sequestration) and the host cytokine response (Moxon et al., 2020).

2.6 Proposed pathogenesis of cerebral babesiosis (CB)

The pathogenesis of CB is poorly understood. A number of contributing factors have been postulated over the decades since CB was first described. These factors frequently overlap or are extrapolated from hypotheses put forward to understand the pathogenesis of HCM. Some of the more common contributing factors include: endothelial cell injury with subsequent increased vascular permeability; microvascular obstruction by parasitised and non-parasitised erythrocytes (“sludging”); and infarction

© University of Pretoria

leading to localised hypoxia (Malherbe and Parkin, 1951, Malherbe, 1956, Maegraith et al., 1957, Basson and Pienaar, 1965, Moore and Williams, 1979, Pardini, 2010).

- Endothelial cell injury

In Pardini's study, endothelial cell injury was interpreted as a central initiating event that led to a cascade of pathological changes, including microvascular necrosis, haemorrhage, leucocyte infiltration, perivascular oedema and malacia (Jacobson, 2006, Pardini, 2010). Reperfusion injury and infarction were also considered as consequences of endothelial damage.

- Sludging

Sludging of pRBCs in smaller calibre blood vessels has been widely described in *Babesia* cases, with or without neurological signs (Maegraith et al., 1957, Basson and Pienaar, 1965, Okoh, 1978). As in CM, parasitic emboli within the microvasculature was suspected to be the cause for obstruction. RBC shape change (distortion) was suggested as a contributing factor to impeding blood flow and causing sludging of both pRBCs and non-pRBCs, especially in smaller vessels (Jacobson, 2006, Pardini, 2010).

- Hypoxia

In haemoprotozoal diseases such as babesiosis, hypoxia is generally attributed to severe anaemia resulting from intravascular haemolysis of RBCs. In a study on 60 dogs infected with *Babesia canis* (Maegraith et al., 1957) it was found that, despite severe anaemia developing in some babesiosis cases, the blood continued to deliver adequate oxygen to the brain, thus excluding brain hypoxia as a likely primary cause for the neurological signs. This finding has, more recently, been supported in human neuropathology texts (Kalaria et al., 2018). In addition, compromised pulmonary function and physiological disturbances due to a marked inflammatory reaction are required for cerebral hypoxia to develop (Leisewitz and Berry, 1996, Kalaria et al., 2018).

In *Babesia bovis* infections, it has been postulated that anoxia can be caused when parasites release proteases which attract polymorphonuclear leucocytes to capillary beds, resulting in sequestration of erythrocytes and neutrophils (Commins et al., 1988). Similar protease / trypsin-like enzymes have been demonstrated in humans with *P. falciparum* infections (Cooke et al., 2005, Miller et al., 2002).

- Cytoadherence

Cytoadherence of infected red cells has the potential to allow the multiplication of parasites, resulting in high local parasite burdens. This is a consequence of the infected

© University of Pretoria

red cells' unique ability to adhere to capillary and postcapillary venule endothelium (Commins et al., 1988, Ho and White, 1999, Miller et al., 2002). Bovine *Babesia* parasites and malaria parasites have been found to form surface ridges and knobs respectively, which induce cytoadherence (Wright et al., 1988, Hutchings et al., 2007). These changes have, however, not been found in relation to canine *Babesia* species (Figure 5).

In *P. falciparum,* only virulent parasites form knobs. In comparison, both virulent and avirulent *B. bovis* strains can cause vascular adhesions, however, vascular sequestration occurs in the virulent strain only (Wright et al., 1988). This difference between *B. bovis* and *P. falciparum* is an indication that erythrocytes infected with avirulent malaria parasites lack cytoadherence receptors, while erythrocytes infected with both avirulent and virulent *B. bovis* species display cytoadherence receptors. In both *B. bovis* and malaria infections, *in vitro* studies have shown that these ridge/knob-formations have cytoadherence characteristics that lead to cell-cell and cell-endothelium interactions and are associated with the expression of the protein thrombospondin (TSP) (Roberts et al., 1985, Parrodi et al., 1989). TSP 1 and 2 are known as anti-angiogenic proteins (Lawler and Lawler, 2012). Another protein, laminin, has also been implicated as a promoter of cytoadherence in *B. bovis* infections (Parrodi et al., 1989) while, in *P. falciparum* infections where knob formation occurs, a parasite-derived histidine-rich protein has been associated with cytoadherence (Wright et al., 1988, Taylor et al., 1987).

Bovine cerebral babesiosis studies suggest that the sequestration cascade is notably more complex when compared to malaria, involving multiple proteins and molecules, including fibronectin, conglutinin, parasite antigens, IgG and cryofibrinogen. Of these, fibronectin is likely the key factor, as it is not only an integral part of the endothelial membrane, but also freely circulates in the plasma and has receptors for fibrin monomers which are abundant in acute babesiosis, forming complexes on infected erythrocyte surfaces. These complexes form cross-links between infected erythrocytes and endothelium membrane-fixed fibronectin, causing vascular stasis. The sudden decrease in fibronectin levels is further evidence of the consumption of fibronectin during the acute stage babesiosis infection (Wright et al., 1988). In addition to increased "stickiness" between the endothelium and RBCs, another cytoadherence factor described in *B. bovis* infections is lipid peroxidation of erythrocyte membrane lipids,

© University of Pretoria

which ultimately leads to increased rigidity and a decreased deformability of infected erythrocytes, resulting in difficulty navigating narrow capillaries (Commins et al., 1988).

The very limited ultrastructural investigation of CCB cases has not shown evidence of ridge/knob formation (Pardini, 2010). Unpublished atomic force field microscopy evaluation of the red cell surface on *B. rossi* infected red cells from naturally infected dogs has not revealed any red cell surface changes suggestive of ridges or knobs (Leisewitz AL and Russell BM, unpublished data) (figure 26). This finding questions how vital the role of sequestration and knob-formation is in haemoparasitic infections that cause severe CNS disease. It suggests that rather than sequestration playing the pivotal role in these diseases, other more important factors are most likely at play.

2.7 Canine cerebral babesiosis as a model for cerebral malaria

Endothelial cell injury is thought to be the key initial change in canine cerebral babesiosis and the central driving force behind a catastrophic cascade of subsequent pathological events, including microvascular necrosis, perivascular oedema, haemorrhage, malacia and leucocyte infiltration (Pardini, 2010). Similarly, in cerebral malaria, the central lesion is thought to be localised endothelial cell injury within and around cerebral microvasculature in association with pRBCs, microvascular ring haemorrhage and thrombosis (Dorovini-Zis et al., 2011, Brown et al., 2000, Medana and Turner, 2006). In young children with CM, as in dogs with CCB, leucocyte involvement is documented as being confined to the intravascular compartment, involving mainly mononuclear cells. In adults with cerebral malaria the inflammatory response included collections of reactive microglia, astrocytes and lymphocytes, suggesting that the immune reaction develops with age (Dorovini-Zis et al., 2011). This difference in immune reaction in association with the age of the host has not been demonstrated in dogs with CCB.

The vast majority of fatal CM cases are in young children. There are undeniable histological similarities between CM and CCB cases. The need for an in-depth review of the histopathology of CCB is long overdue and has represented a void in babesiosis research for a number of years. This CCB histopathology review, which includes a thorough description of the specific leucocytes, endothelial changes and myelin degeneration in naturally infected dogs, contributes significantly to the debate on mechanisms underlying lesion development in the brains of humans with CM. This

© University of Pretoria

project further demonstrates that there is a place for CCB to possibly be used as a model for some aspects of future CM research.

© University of Pretoria

CHAPTER 3: RESEARCH OBJECTIVES

3.1 Aims of this study

1) To perform and report detailed microscopic descriptions of the brain in *B.rossi*-infected dogs diagnosed pathologically with cerebral babesiosis and contrast these findings with published data on BCB and HCM.
2) To use IHC staining to semi-quantify and give detailed descriptions of some of the different cell populations and processes within the brain of dogs with canine cerebral babesiosis, including lymphocytes, macrophages, microglia and endothelial cells.

3.2 Hypothesis

Literature on the histopathological changes involved in cerebral malaria is readily available and similar descriptions on bovine cerebral babesiosis are available, but detailed histopathological studies of canine cerebral babesiosis are rare and none of these included immunohistochemical markers.

3.2.1 Histological features

It is expected that histological features in the brain of CCB cases would include, but not be limited to:

i. Erythrocyte changes such as anisocytosis and parasite invasion.
ii. Monocytic leucostasis.
iii. Endothelial changes.
iv. Vascular sludging of pRBCs.
v. Oedema (vasogenic and cytotoxic).
vi. Neuropil changes such as neuronal necrosis, neutrophil infiltration, and rarefaction.
vii. Haemorrhage, ranging from petechiae to ecchymoses to suffusive haemorrhages.
viii. Distribution within the CNS to mainly be in the deep sulci.
ix. Grey matter distribution to supersede white matter involvement.

3.2.2. Immunohistochemical reactions

Immunohistochemical reactions would be expected to mark specific cell types and contribute to understanding the pathogenesis of CCB using the following IHC antibody staining:

© University of Pretoria

i. CD3 (T cell) and CD20 (B cell) markers are expected to show presence of T and B lymphocytes in intact vasculature and be absent in areas of haemorrhage, myelin and axonal damage.
ii. IBA1 labels macrophages (including microglia and dendritic cells) and is expected to show mainly extravascular tissue macrophages in the haemorrhagic areas, possibly also phagocytosed *Babesia* organisms.
iii. MAC387 labels histiocytic cells, including monocytes / macrophages (mononuclear) and mature neutrophils (polymorphonuclear) that are intravascular or recently migrated and reactive within the tissue parenchyma. It is expected to show a similar but broader distribution to IBA1.
iv. VCAM-1 labels activated endothelial cells and is expected to show widespread distribution.

The similarities and differences between CCB, BCB and HCM will contribute to understanding the pathogenesis of these CNS diseases.

3.3 Benefits arising from the project

1. The project will provide the first detailed histological description of a cohort of CCB cases.
2. The project will provide the first detailed IHC description of a cohort of CCB cases.
3. The project will contribute to speculation around the pathogenesis of this form of canine Babesiosis.
4. The project will, for the first time, allow a cursory comparison between CCB, BCB and HCM.

This project was conducted to fulfil the requirement of a mini-dissertation for the MMedVet (Pathology) degree at the University of Pretoria. The study will result in at least one article in an acknowledged journal.

© University of Pretoria

CHAPTER 4: MATERIALS AND METHODS

Definition: For the purposes of this study, a cerebral babesiosis lesion was defined as haemorrhage with or without spongiosis and/or malacia. This definition of CCB was pathological, not clinical.

4.1 Experimental Design

This was a retrospective cross-sectional study of the histopathological changes in CCB. A total of ~~22~~20 cases were used, which included a selection of ~~19~~17 out of 54 cases sampled by Pardini between 1996 and 1998, and 3 cases collected in 2017. Samples that were collected between 1996 and 1998 were sourced from archive storage as formalin-fixed paraffin-embedded (FFPE) blocks, while the 2017 cases were presented as patients at the OVAH and sampled during routine post-mortem examination. Archived cases were selected based on the presence of macroscopic and / or microscopic cerebral lesions (refer to 4.1.1 – 4.1.3 for details). Some cases lacked brain lesions and were grouped as non-cerebral babesiosis cases. The 20~~22~~ cases were subdivided into 3 groups and a fourth (control) group was added. The 4 groups consisted of:

1. Dogs diagnosed on thin peripheral blood smear with babesiosis and histologically with CCB that were treated before death or euthanasia (11 cases).
2. Dogs diagnosed on thin peripheral blood smear with babesiosis and histologically with CCB that were not treated before death or euthanasia (5 cases).
3. Dogs diagnosed on thin peripheral blood smear with babesiosis but not having cerebral pathology, i.e. non-cerebral babesiosis, that were or were not treated (~~6~~4 cases).
4. Control group of healthy dogs (3 cases).

This study focused on reviewing the histopathological changes as seen on HE staining, a selection of special stains, as well as IHC. The latter was not as readily available at the time of Pardini's study and was used in this study in an attempt to accurately identify and describe the cellular responses and neuronal changes associated with the central nervous lesions.

© University of Pretoria

4.1.1 Study animals: Macroscopic inclusion criteria for groups 1 and 2

The essential criterion for inclusion in groups 1 or 2 was based on Pardini's definition of cerebral babesiosis (Pardini, 2010) that includes dogs diagnosed as suffering from babesiosis on stained thin peripheral capillary blood smear with microscopic cerebral lesions and a history of central nervous signs. For this study, macroscopic examination of the brain FFPE tissue blocks for these 2 groups was done on each case and further inclusion criteria were based on the following:

a) The presence of obvious macroscopic haemorrhage visible with the naked eye and

b) Wax blocks with sufficient (thick) tissue sections available for HE, special staining and IHC processing.

Based on these criteria, a subset of 1 to 5 blocks was selected per case and used for this study.

4.1.2 Study animals: Macroscopic inclusion criteria, group 3

The criteria for inclusion in Group 3 were based on Pardini's criteria for non-cerebral babesiosis (Pardini, 2010), i.e. dogs diagnosed as suffering from babesiosis on stained thin peripheral capillary blood smear but lacking in macroscopic and/or microscopic cerebral lesions and with no concurrent central nervous signs. Macroscopic examination of the brain FFPE tissue blocks for this group with the naked eye showed no haemorrhagic lesions.

4.1.3 Study animals: Exclusion criteria

For cerebral babesiosis cases listed as groups 1 and 2 above, exclusion was based on:

a) A lack of cerebral pathology, as observed by Pardini (Pardini, 2010) or
b) FFPE blocks with insufficient tissue.

For non-cerebral cases (group 3 above) cases were excluded if there was insufficient tissue embedded in the wax block/s.

4.1.4 Control animals: Exclusion criteria

Control cases were excluded if they tested positive on polymerase chain reaction (PCR) and reverse line blot (RLB) for any blood parasites (Matjila et al., 2004), if they had any significant co-morbid disease (based on history and clinical examination) and/or if the haematology test results indicated any abnormalities.

© University of Pretoria

4.1.5 Study animals: Sources

The dog carcasses were sourced by Pardini over the period of 1996 to 1998 (Pardini, 2010) and by Leisewitz during 2017. All dogs were patients of the OVAH.

4.1.6 Control animals: Sources

The control animals were sourced from a welfare organisation for another research project (University of Pretoria Animal Ethics certificate V050-13), managed by A. Leisewitz.

4.1.7 Postmortem and sample collection

The postmortem examinations were performed by Pardini at the Section of Pathology (SP), Department of Paraclinical Sciences (DPS), Faculty of Veterinary Science (FVS), University of Pretoria (UP) over the period of 1996 to 1998 (Pardini, 2010). Samples collected in 2017 were done by Leisewitz or Lewis. All fresh tissues were collected from carcasses of dogs that died or were euthanized and submitted to the SP with permission for a student training postmortem. A diagnosis of babesiosis was confirmed by peripheral thin blood smear (1996-1998) and/or PCR and RLB (for the samples collected in 2017).

4.1.8 Sample processing

Formalin fixed samples were routinely trimmed and placed into tissue cassettes then embedded in histology grade paraffin wax. Processing was done on the Histo -Tek VP1 tissue processor and embedded into wax blocks using the Thermo Scientific embedding machine. Cutting and staining of the samples were performed using standardised techniques (Suvarna and Layton, 2018) at the histopathology laboratory, SP, DPS, FVS, UP. Archived wax blocks (1996-1998 cases) were retrieved and selected according to the inclusion and exclusion criteria previously described. Tissue blocks from cases sampled in 2017 were selected based on the same criteria. The number of slides per case varied, depending on the number of wax blocks selected. A total of 72 tissue wax blocks were selected. Based on the HE findings, 1-2 areas of interest (“hotspots”) per case, displaying the most severe lesions, were demarcated with a permanent black marker on the histology glass slides. The corresponding FFPE block was melted, the tissue section was trimmed to isolate the area of interest corresponding to the markings on the glass slide and this section was re-embedded as part of a combination (“combo”)

© University of Pretoria

block for IHC and special staining. Combo blocks each included 1 to 4 areas of interest and case identities per block were recorded pictorially and with digital photography. A total of 11 combo blocks were prepared, of which 1 was a control combo block.

Tissue sections

The 72 wax blocks were sectioned for routine HE examination and the 11 combo blocks were utilised for the 2 x special stains and 5 x IHC immunomarkers.

Each case had the following sections:

- 1 x HE stained tissue section per selected wax block
- 2 x special stains (combo blocks)
- 5 x IHC-labelling (combo blocks)

Examination

A microscopic check-list (appendix A) was compiled and completed in detail, per case, to ensure thorough and consistent examination of the HE, special stains and IHC sections. Microscopic and IHC immunolabelling examinations were done using a CX21 Olympus light microscope. All tissue sections were surveyed by the co-supervisor following examination by the principal investigator.

4.1.9 Special stains

Special stains were performed in the histopathology laboratory at the SP, DPS, FVS, UP, according to standard accredited methods (Suvarna and Layton, 2018).

Table 4: List of special stains used and the target feature/s that are highlighted.

Special stain:	**Stain/highlight:**
1. Luxol fast blue (LFB)	Myelin stain, highlights demyelination
2. Martius scarlet blue (MSB)	Fibrin stain, delineates haemorrhage

4.1.10 Immunohistochemistry (IHC)

IHC was performed manually, following validated internal protocols. The standard immunoperoxidase procedure included deparaffinization and hydration of slides, incubation with 3% hydrogen peroxide for 15 minutes to quench endogenous peroxidase activity, enzymatic digestion or heat-induced epitope retrieval (HIER) followed by non-specific immunoglobulin binding, incubation with the primary antibody and application of the Expose® IHC detection system. For negative reagent controls, a buffer was substituted for the primary antibody in each case.

© University of Pretoria

A test run on the IHC labelling showed adequate labelling of tissue with 2 of the 5 IHC markers (MAC387 and IBA1). The remaining 3 markers (VCAM-1, CD3 and CD20) did not display satisfactory immunolabelling initially, thus optimisation was done and confirmed to be adequate by using lymphoid tissue (spleen and lymph node) for CD 3 and CD20 (sourced from FFPE blocks from the same group of animals sampled by Pardini in 1996-1998), and brain tissue from dogs affected by central nervous system arteritis for VCAM-1. The reason for the initial inadequate immunolabelling of CD3, CD20 and VCAM1 was attributed to the age of the tissue samples. The optimised methods were subsequently and routinely used to process the blocks for CD3, CD20 and VCAM-1 IHC.

Table 5: List of antibodies used, including the clone, source, catalogue number and cell-line / feature targeted.

Antibody:	**Clone:**	**Source:**	**Catalogue number:**	**Label/highlight:**
1. CD3	Polyclonal rabbit anti-human CD3 antibody	Dako	A0452	T cell marker
2. CD20	Polyclonal rabbit CD20 antibody	Thermo Fisher Scientific	MS4A1	B cell marker
3. IBA1	Polyclonal rabbit IBA1 antibody	Abcam	Ab153696	Labels activated microglia.
4. MAC387	Monoclonal mouse anti-human myeloid/histiocyte antigen antibody, clone MAC387	Dako	M0747	Labels histiocytes; also neutrophils, monocytes, tissue reactive macrophages, eosinophils and epidermis.
5. VCAM-1	Monoclonal mouse anti-human VCAM1 antibody, clone 3H10	Novus Biologicals	NBP2-03600	Expressed by cytokine-activated endothelium.

© University of Pretoria

4.2 Data analysis and completing scoresheets

This was a descriptive study that focused on cerebral lesions associated with CCB and non-CCB at light microscopic level, with the addition of special stains and immunohistochemistry to highlight the specific inflammatory cell infiltration and cellular changes associated with the lesions.

A grading system (appendix B) was developed, based on findings described in previous studies of cerebral babesiosis in dogs or cattle and *B. rossi* infected dogs, (Botha, 1964, Basson and Pienaar, 1965, Moore and Williams, 1979, O'Connor et al., 1999, Hutchings et al., 2007, Pardini, 2010, Henning et al., 2020) as well as findings in cerebral malaria studies in humans (David et al., 1983, Turner et al., 1994, Dorovini-Zis et al., 2011, Milner Jr et al., 2014). A data collection check-sheet (appendix A) was structured around this grading system and completed for each case. The check-sheets were used to semi-quantitatively establish the histological findings in this study (Appendix A).

4.2.1 Inflammatory cells and vasculitis

For the purpose of completing the score sheets, inflammatory cells were grouped based on visualisation with HE staining as either mononuclear (MN; monocytes, macrophages and lymphocytes) or neutrophils. Inflammatory cell distribution was recorded in association with lesions (see lesion definition above) as being intralesional (IL) when >50% of the inflammatory cells were within a lesion, perilesional (PL) when >50% of the inflammatory cells were at the edge of a lesion and extralesional (EL) when >50% of the inflammatory cells were away from a lesion. The severity of the vasculitis was rated based on the concentration of inflammatory cells, ranging from mild (single leucocytes, no expansion of vessels walls and less than ¼ of the wall affected) to moderate (monolayer of leucocytes, slight expansion of the vessel wall, approximately ½ of the wall affected) to severe (multiple layers of leucocytes, obvious expansion of the vessel wall and ¾ to whole wall affected).

4.2.2 Type of vasculitis and vascular necrosis

For the purposes of completing the grading sheets, vasculitis was classified as: fibrinoid vasculitis (if smudged eosinophilic exudate was noted on HE staining) or necrotic vasculitis (if evidence of necrotic debris was present) or inflammatory vasculitis (if there was a lack of fibrinoid and necrotic vasculitis, but inflammatory cells were clearly associated with the blood vessel). Vasculitis was also recorded in relation to the vessel

© University of Pretoria

wall as perivascular (>50% in the areas surrounding the vessel); vascular wall (>50% within the vessel wall) or intravascular (>50% within the vessel lumen). Lastly, vasculitis was recorded based on the remaining integrity of the affected vessel wall as: intact (may have rarefaction but wall remains intact); partial (part of the wall is homogenous and appears smudged, with or without endothelial nuclear pycnosis or karryorrhexis) or complete dissolution (loss of full circumference of vessel wall detail, with or without pycnotic endothelial cell nuclei, karyolysis and cell debris).

4.2.3 Fibrin and thrombi

The presence of fibrin was assessed on HE staining and MSB special stain. The severity of fibrin accumulation was based on the number of blood vessels in which fibrin was noted, using the MSB stain to more accurately identify the presence of fibrin. Mild cases had evidence of fibrin in less than one third of the vessels, moderate cases had fibrin present in one to two thirds of the vessels, while severe cases had fibrin in more than two thirds of vessels. The distribution of fibrin deposits was recorded based on association with lesions (as previously defined) which was recorded as IL, PL or EL fibrin deposition. Lastly, fibrin distribution was also observed in relation to the location of the exudate within or around blood vessels and was recorded as being intravascular, perivascular or both. The presence of thrombi was assessed on HE staining and included a survey of the entire tissue sample per case.

4.2.4 Endothelial cell hypertrophy

Endothelial cell hypertrophy was assessed on HE stain. Reactive endothelial cell changes were also assessed on IHC using VCAM-1 (refer to 5.4.1.3 for details). On HE, endothelial cell hypertrophy was assessed based on the nucleus width. If it was double or more the width of a normal endothelial cell nucleus, then it was classified as hypertrophied (figure 14). The severity of endothelial cell hypertrophy was based on the proportion of endothelial cells displaying the change. Where less than one third of endothelial cells were affected, the case was recorded as having mild endothelial cell hypertrophy, one to two thirds was moderate and more than two thirds was severe.

4.2.5 Leucostasis

Leucostasis was evaluated based on location, cell type, severity and distribution. Location was assessed based on whether leucostasis was observed in the grey matter,

© University of Pretoria

white matter and/or meninges. Cell type was determined according to whether the predominant inflammatory cells were MN or neutrophils or a combination of the two (refer to figure 5). Severity was recorded as mild if less than one third of the blood vessels displayed leucostasis, moderate if one to two thirds of vessels displayed leucostasis and severe if more than two thirds of vessels had leucostasis present. The distribution of leucostasis was determined by the association of leucostasis in relation to lesions.

4.2.6 Global changes

Oedema, congestion and parasitaemia were grouped as global changes as these changes are typically not localised to a specific area.

4.2.6.1 Oedema

Vasogenic oedema was identified as amorphous clear to eosinophilic extravascular material and the severity was assessed based on the thickness of the extravascular expansion. Mild vasogenic oedema was classified as approximately the thickness of 1 capillary wall; moderate as approximately the thickness of 2-3 capillary walls and severe vasogenic oedema as the thickness of more than 3 capillary walls. Cytotoxic oedema was identified as amorphous clear to eosinophilic material in the perineuronal areas and assessed based on absence or presence.

4.2.6.2 Congestion

Congestion was identified as intravascular accumulation of RBCs and scored based on the absence or presence. When scored as present, the criterion was that most blood vessels (>50%) displayed congestion when evaluating all available histology sections per case. Special attention was given to whether the congestion was present in venules, arterioles and capillaries, as presence in arterioles may signify hyperaemia and be associated with inflammation.

4.2.6.3 Parasitaemia

Parasitaemia was calculated as a percentage of pRBCs based on the total number of erythrocytes counted (figure 6), using an area of approximately 5mm^2 and a minimum of 150 erythrocytes in total. The percentage was interpreted as low parasitaemia for <20%; moderate parasitaemia for 20-50% and high parasitaemia for >50%. Aggregation of pRBCs was recorded as being present or absent.

© University of Pretoria

4.2.7 Neuronal injury and neurophagia

Neuronal injury was assessed on HE staining. A minimum of 3 out of a list of 5 neuronal changes were deemed necessary to classify changes as neuronal injury. The list of 5 neuronal changes were:

i. Hypereosinophilia
ii. Peripheralisation of nissl substance with irregular granular cytoplasm
iii. Shrunken cytoplasm
iv. Neurophagia
v. Karyolysis, karryorrhexis or chromatolysis

Neurophagia was assessed histologically based on the formation of nodules of phagocytosed neuronal material (neurophagia nodules) surrounding injured neurons. Both neuronal injury and neurophagia were recorded as being present or absent and there was no severity attributed to these changes, however, the proximity to lesions was recorded as IL, PL or EL.

4.2.7.1 Neuropil inflammation

On HE, neuropil inflammatory cellular infiltration was observed and recorded based on the predominant cell type (MN and/or neutrophils); association with lesions (IL, PL and/or EL) and severity of the infiltrate, which was classified as absent (no evidence of inflammatory infiltration), scant (up to 5 leucocytes per field of view) or obvious (more than 5 leucocytes visible per field of view).

4.2.7.2 Spongiosis

Spongiosis (demyelination) was assessed on routine HE staining and LFB special staining. The location of the change was recorded based on whether it was predominantly in the grey matter, white matter (>50% in either) or mixed (i.e. the predominant location could not be determined). The presence and severity of the spongiosis was assessed using the LFB special stain and was recorded based on the extent of demyelination, with mild demyelination assigned to cases with less than one third of the neuropil showing evidence of the change; moderate cases had demyelination in one to two thirds of the neuropil and severe cases had demyelination in more than two thirds of the neuropil. Lastly, spongiosis was assessed based on proximity to lesions, i.e. IL, PL or EL.

4.2.7.3 Immunohistochemistry - Descriptive

Immunohistochemistry was assessed by evaluating at least 3 areas of interest, where 50-100 positively labelled cells were present, i.e. “hot spots”. Not all cases had “hot

© University of Pretoria

spots", however, and in these cases the entire tissue sections were evaluated and the total number of cells of interest for that specific IHC was recorded. Cells of interest were dependent on the specific IHC stain being evaluated, i.e. leucocytes were cells of interest for MAC-387, IBA1, CD3 and CD20 whereas endothelial cells were cells of interest for VCAM-1. For cases with "hot spots" a total of at least 300 cells (with and without positive immunolabelling) were counted and for cases without "hot spots" the total number of cells of interest in the available sections were counted. Immunolabelling / immunoreactivity was interpreted as positive based on the visualisation of brown staining precipitate, which, depending on the IHC marker, was evenly distributed within the cell membrane or nuclear membrane (MAC-387, IBA1, CD3 and CD20), or formed small bead-like structures (VCAM-1). The number of positively labelled cells was recorded and a percentage was calculated based on the total number of cells of interest, using basic percentage calculations. The degree of IHC labelling was categorised based on the percentage of positive labelling cells compared to the total number of cells of interest. A mild IHC score was assigned to cases with <20%; moderate for 20-50% and severe for >50% positive IHC labelling.

4.2.7.4 Statistical Analysis

Data collected from the individual check-sheets were tallied for each of the 4 main groups and basic statistical analyses used to further investigate trends.

The following method was used to accurately quantify the proportion of pRBCs:

- "Lesions" were defined as areas of haemorrhage with or without spongiosis and/or malacia.
- A representative slide with good visibility of intra-capillary erythrocytes from each case was chosen.
- Two areas of approximately 5mm (millimetres) diameter were randomly chosen close to and away from lesions, respectively (if lesions were present).
- At least 150 erythrocytes were counted in total per case under the oil immersion objective (100x).
- The percentage of pRBCs was determined using standard percentage calculations and recorded in the case microscopy checklist (Appendix A).
- Details are outlined in Appendix B (grading and scoring criteria).

The following method was used to accurately quantify IHC labelling:

- As noted above, "lesions" were defined as areas of haemorrhage with or without spongiosis and/or malacia.

© University of Pretoria

- "Hotspots" were identified on HE sections as areas where there were one or more lesions present. IHC immunomarkers were applied to the hotspot areas to highlight accumulations of leucocytes and cellular changes of interest.
- In cases where hotspots were present, at least 3 hotspots were evaluated. Where fewer than 3 hotspots were present these were evaluated as representative for the case. Where no hotspots were present, evaluation of the leucocytes present was accepted as representative for the case. Notes were made in the check-sheet to reflect the presence / absence of hotspots findings.
- Within each hotspot at least 100 leucocytes were counted, resulting in a total of at least 300 leucocytes counted per case.
- For each immunomarker, positively labelled cells were calculated as a percentage (%) of the total cells counted, by applying standard percentage calculations.
- An allocation of negative, mild, moderate or severe was given depending on the percentage positive immunolabelling.
- Details are outlined in appendix B (grading and scoring criteria).
- All findings were recorded in the relevant check-sheet per case.

Data collected on scoresheets was analysed using the Mann Whitney test to determine significance between the babesiosis and control groups. The Kruskal test was used to determine whether there were significant differences between the scores for groups 1, 2 and 3.

4.3 Facilities

Facilities used at the SP, DPS, FVS, UP included the postmortem hall, histotechnology and immunohistochemistry laboratories.

4.4 Equipment

4.4.1 Macropathology

- Postmortem equipment: knives, scalpels, cutting boards, scissors, shears and hacksaws.
- Photography: Huawei P20 or Samsung Galaxy S10.

© University of Pretoria

4.4.2 Histology, Special stains and Immunohistochemistry

- Tissue sections were mounted on Superfrost® glass slides.
- Glass cover slips were fixed with Entellan™ mounting medium.
- Sundries included latex gloves, cutting blades, microtome blades.
- Antibodies (listed in Table 5).

4.5 Records

At completion of this study all FFPE wax blocks, HE stained slides, IHC labelled slides and special stained slides were archived in a designated storage facility at the SP, DPS, FVS, UP. All digital photos, data collection sheets and related documents were saved onto multiple external hard drives and Google drive files to which the principal researcher and supervisors have access.

© University of Pretoria

CHAPTER 5: RESULTS

5.1 Selection of formalin-fixed paraffin-embedded (FFPE) tissue blocks

All canine babesiosis cases were naturally infected and were diagnosed as suffering from babesiosis on stained thin peripheral capillary blood smear.

None of the 4 non-CCB cases had evidence of macroscopic haemorrhage. Sufficient tissue sample was present in all selected CCB and non-CCB cases.

The negative control FFPE blocks were devoid of macroscopically obvious haemorrhages.

5.2 Summary of score sheets (HE, special stains and IHC) and statistical analyses

Standardised check sheets and grading / scoring criteria (appendices A and B) were recorded per case. A master summary check sheet is included as appendix C. The scores were analysed using the Mann Whitney U test to determine the significance between the babesiosis and control groups. A p-value of ≤ 0.1 was used. The Kruskal test was used to determine whether there were significant differences between the scores for groups 1, 2 and 3 when compared to the control group (table 6). Mean, median, standard deviation (SD), minimum and maximum values were calculated and recorded (table 7).

5.2.1 Naturally infected cases

5.2.1.1 Vasculature

Overall, the naturally infected *Babesia* cases showed significantly higher scores for vascular changes (P value ≤ 0.1) when compared to scores for the control cases. The median scores for vascular changes were 8.00 (SD 2.115) for CCB treated; 8.00 (SD 2.588) for CCB not treated and 2.00 (SD 3.697) for the non-CCB cases (table 7).

Within the 3 *Babesia* infected groups, it was observed that the treated CCB group (group 1) showed higher scores for vascular changes, followed by the non-treated CCB group (group 2) and the non-cerebral babesia cases (group 3) had the lowest scores. Statistical comparison of these 3 groups was attempted with the Kruskal test but was not possible, due to the small number of cases.

5.2.1.2 Inflammation

The overall inflammation scores were not significantly higher for the *Babesia* infected cases (P value > 0.1) when compared to the control cases. The median scores for

© University of Pretoria

inflammation were 15.00 (SD 4.936) for CCB treated; 9.00 (SD 1.517) for CCB not treated and 10.00 (SD 2.872) for non-CCB cases (table 7).

Within the 3 *Babesia* infected groups, it was observed that the treated CCB group (group 1) showed higher inflammation scores, followed by the non-cerebral cases (group 3) and the non-treated CCB cases (group 2) had the lowest scores. Statistical comparison of the 3 groups was attempted with the Kruskal test but was not possible, due to the small number of cases.

5.2.1.3 Global

Oedema, congestion and parasitaemia were grouped as global (widespread) changes as these changes are typically not localised to a specific area. As for inflammation, global scores were not significantly higher in *Babesia* cases when compared to control cases (P value > 0.1). The median scores were 10.00 (SD 3.194) for CCB treated; 11.00 (SD 2.775) for CCB not treated and 9.50 (SD 3.162) for non-CCB cases (table 7).

It was observed that global changes showed the highest scores in the non-treated CCB cases (group 3) while the treated CCB (group 2) and non-cerebral babesia (group 3) cases had similar global scores. As for vascular changes and inflammation, the small numbers made statistical comparison of these 3 groups, with the Kruskal test, not possible.

5.2.1.4 Neuronal changes

Scores for neuronal changes were significantly higher in *Babesia* cases when compared to control cases (P value ≤ 0.1). The median scores were 1.00 (SD 0.603) for CCB treated; 1.00 (SD 0.447) for CCB not treated and 0.00 (SD 0) for non-CCB cases (table 7). It was observed that neuronal changes showed the highest scores in the treated and non-treated CCB cases (groups 1 and 2), while the non-cerebral babesia (group 3) cases had scored lower. The small numbers per group made statistical comparison of these 3 groups not possible.

5.2.2 Summary of statistical analyses

Tables 6, 7, 8 and 9 below list the statistical findings in a summarised format and per individual babesiosis case for each of the 4 broad categories of histological changes, i.e. inflammation, vascular changes, global changes and neuronal changes.

© University of Pretoria

Table 6: Scores per individual case for the 4 broad histological categories and test statistics results for the Mann-Whitney U test and p-values per category. Group 1 = treated CCB cases; group 2 = non-treated CCB cases; group 3 = non-CCB cases.

Group	Case number	Case identifier	Inflammation (max = 34)	Vascular Changes (max = 16)	Global Changes (max = 18)	Neuronal Changes (max = 3)	Total (max = 71)
1	1	S201-98	17	9	12	0	38
1	2	S598-97	7	4	8	0	19
1	3	S975-97	18	9	12	1	40
1	4	S965-97	16	7	8	1	32
1	5	S2575-97	9	9	10	1	29
1	6	S426-98	23	11	14	2	50
1	7	S1112-98	14	8	14	1	37
1	8	S1268-98	21	8	13	1	43
1	9	S1215-97	10	5	6	0	21
1	10	S3157-96	15	8	8	1	32
1	11	S1894-17	13	5	5	1	24
2	12	S1391-97	6	8	14	0	28
2	13	S923-97	10	9	8	1	28
2	14	S305-98	9	4	11	1	25
2	15	S2535-97	9	4	11	1	25
2	16	S1926-17	8	9	7	1	25
3	17	S2849-96	10	2	7	0	19
3	18	S2788-96	7	1	11	0	19
3	29	S1959-97	10	2	14	0	26
3	20	S3583-17	14	9	8	0	31
Mann-Whitney U [a]			25.000	12.500	31.000	8.000	16.000
Exact Sig. [2*(1-tailed Sig.)] P-value			0.554[b]	**0.064[b]**	0.963[b]	**0.022[b]**	0.148[b]

Abbreviations: CCB, canine cerebral babesiosis

a. The Mann Whitney U compares all the CCB cases (treated and non-treated together) to non CCB cases. b. Not corrected for ties.

© University of Pretoria

Table 7: Descriptive statistical analyses per group, including. Group 0 = controls; group 1 = treated CCB cases; group 2 = non-treated CCB cases; group 3 = non-CCB cases.

Group	Statistical analysis	Inflammation (max = 34)		Vascular Changes (max = 16)		Global Changes (max = 18)		Neuronal Changes (max = 3)		TOTAL (MAX 71)	
		Stat	Std. err	Stat	Std. err	Stat	Std. err	Stat	Std. err	Stat	Std. err
0 (n=3)	Mean	0.00	0.000	0.00	0.000	0.00	0.000	0.00	0.000	0.00	0.000
	Median	0.00		0.00		0.00		0.00		0.00	
	Std. Deviation	0.000		0.000		0.000		0.000		0.000	
	Minimum	0		0		0		0		0	
	Maximum	0		0		0		0		0	
1 (n=11)	Mean	14.82	1.488	7.55	0.638	10.00	0.963	0.82	0.182	33.18	2.888
	Median	15.00		8.00		10.00		1.00		32.00	
	Std. Deviation	4.936		2.115		3.194		0.603		9.579	
	Minimum	7		4		5		0		19	
	Maximum	23		11		14		2		50	
2 (n=5)	Mean	8.40	0.678	6.80	1.158	10.20	1.241	0.80	0.200	26.20	0.735
	Median	9.00		8.00		11.00		1.00		25.00	
	Std. Deviation	1.517		2.588		2.775		0.447		1.643	
	Minimum	6		4		7		0		25	
	Maximum	10		9		14		1		28	
3 (n=4)	Mean	10.25	1.436	3.50	1.848	10.00	1.581	0.00	0.000	23.75	2.926
	Median	10.00		2.00		9.50		0.00		22.50	
	Std. Deviation	2.872		3.697		3.162		0.000		5.852	
	Minimum	7		1		7		0		19	
	Maximum	14		9		14		0		31	

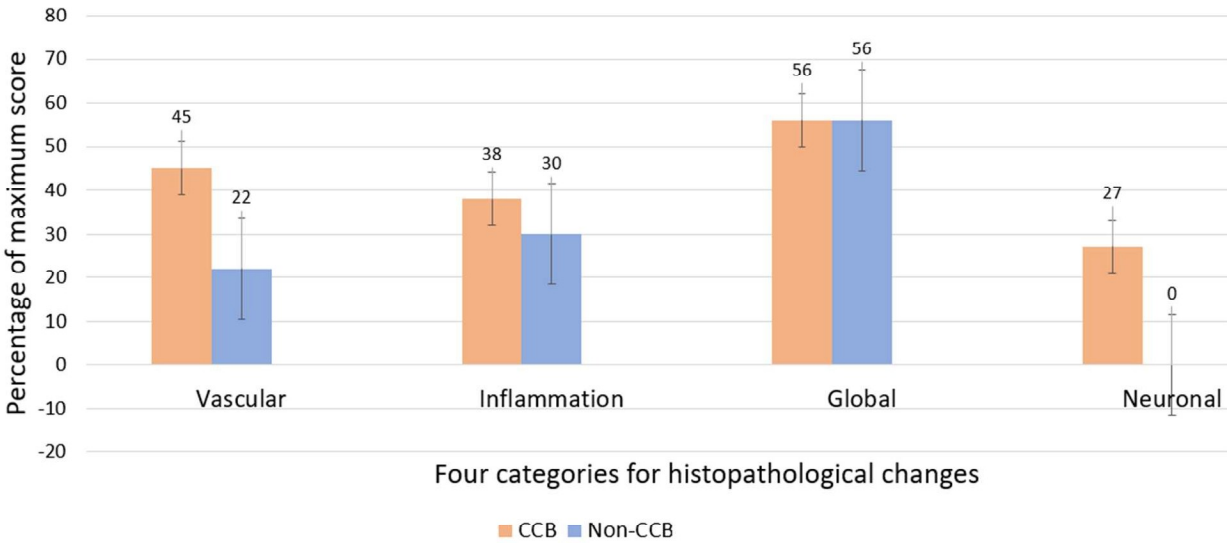
Abbreviations: Stat, statistical value; Std err, standard error; CCB, canine cerebral babesiosis.

© University of Pretoria

Table 8: Summary of average scores and percentages of possible maximum score in CCB versus non-CCB cases.

		CCB (n=16)	Non-CCB (n=4)
Inflammation	Average Score	13	10
	% of max (34)	38%	30%
Vascular	Average Score	7	4
	% of max (16)	45%	22%
Global	Average Score	10	10
	% of max (18)	56%	56%
Neuronal	Average Score	1	0
	% of max (3)	33%	0%

Table 9: Bar graph depicting the numerical data in table 8.



5.3 Histopathology descriptions of CCB and non-CCB cases

Below is a detailed and comprehensive description of the histological findings of the CCB (groups 1 and 2; cases 1 - 16) and non-CCB cases (group 3; cases 17 – 20). For the purpose of completing the score sheets, the definition of a "lesion" was: Haemorrhage with or without spongiosis and / or malacia. A master summary of the score sheets (appendix C) and detailed score sheets per case (appendix D) are included.

© University of Pretoria

5.3.1 Global changes

5.3.1.1 Leucostasis

The details of leucostasis findings per case are noted in table 10.

Table 10: Leucostasis details per case, including distribution within the brain, cell type/s, severity and distribution relative to haemorrhagic lesions.

Case	Leucostasis location (GM / WM / Men)	Leucostasis cell type (MN / NEUT)	Leucostasis severity (m, Mod, S)	Leucostasis distribution (IL, PL, EL)
1	GM > WM & Men	MN = NEUT	m (WM & Men); Mod (GM)	IL, PL & EL (global)
2	GM = WM	MN = NEUT (WM); M (GM)	m	IL = PL
3	GM > Men	MN > NEUT	S (GM); m (Men)	GM = IL; Men = EL
4	GM = WM = Men	MN = NEUT (WM & GM); MN = Men	m	GM & WM = IL; Men = EL
5	GM = WM	MN = NEUT	Mod	PL
6	GM = WM = Men	MN = NEUT	Mod	GM & WM = PL; Men = IL, PL, EL; (global)
7	GM = WM > Men	MN = NEUT	S (GM + WM); Mod (Men)	GM & WM = PL; Men = EL
8	GM > WM & Men	MN = NEUT	Mod (GM); m (WM & Men)	GM = IL,PL; WM & Men = PL (global)
9	WM = GM = Men	MN (WM & GM) MN = Neut (Men)	m	IL (GM & WM) PL, EL (Men)
10	GM > WM & Men	NEUT (GM & WM); MN (Men)	Mod (GM); m (WM & Men)	GM & WM = IL; Men = PL
11	GM = WM	NEUT (WM); MN (GM)	m (GM & WM)	GM & WM = IL
12	GM = WM	MN = NEUT	S (GM & WM)	IL, PL, EL (global)
13	GM = WM	MN = NEUT	S (GM & WM)	IL, PL, EL (global)
14	GM = WM	MN = NEUT	m	EL
15	GM = WM = Men	MN	Mod	IL, PL, EL
16	GM>WM & Men	MN = NEUT	Mod (GM) > m (WM & Men)	GM (PL, EL) WM (IL, PL) Men (EL)
17	GM	MN = NEUT	m	N

© University of Pretoria

18	GM & Men > WM	MN	Mod (GM & Men); m (WM)	N
19	Men > GM > WM	MN = NEUT	S (Men); Mod (GM); m (WM)	N
20	Men > GM & WM	MN & NEUT (Men); MN (GM & WM)	Mod (Men) *thrombi m (GM & WM)	Thrombi (Men) n/a (GM & WM)

Abbreviations: WM, white matter; GM, grey matter; Men, meninges; MN, mononuclear leucocytes; NEUT, neutrophils; N, none; m, mild; Mod, moderate; S, severe; IL, intralesional; PL, perilesional; EL, extralesional.

In summary, leucostasis in the CCB and non-CCB cases did not appear to be more dominant in certain parts of the brain and was distributed within the grey matter, white matter and meninges. There was no dominant leucocyte type involved in the majority of cases and the severity ranged from mild to severe.

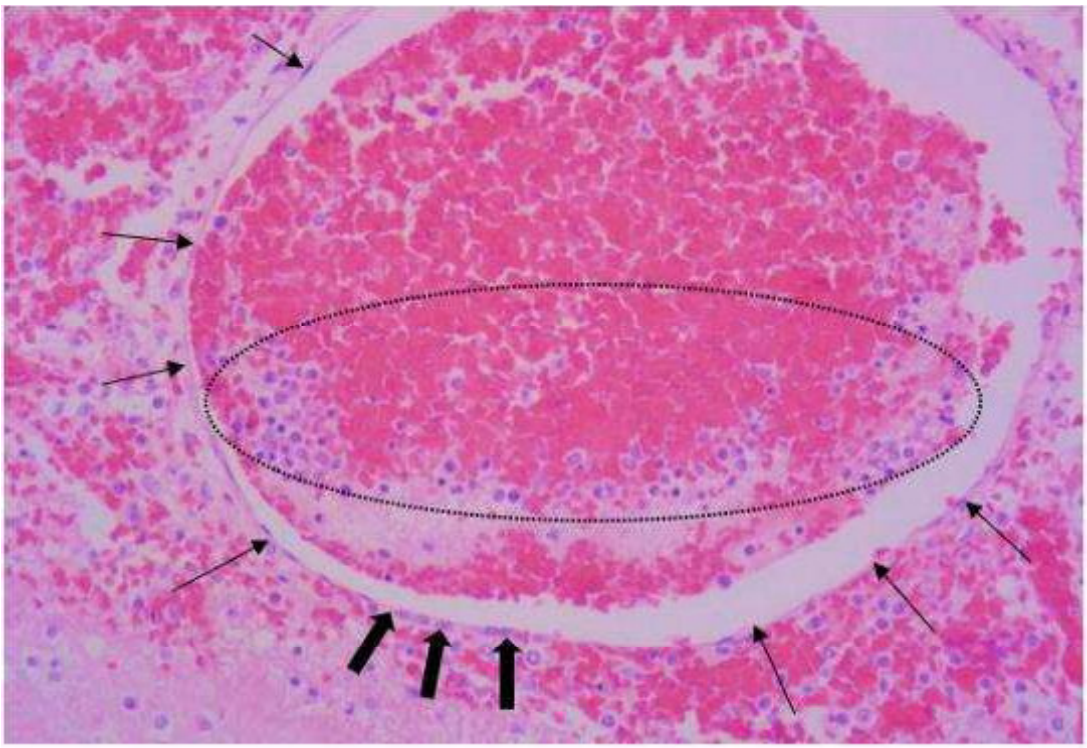


Figure 5: Case 1 (CCB). HE stain. Mononuclear cell leucostasis (oval dotted line) and congestion in a vessel with an intact wall (thin arrows). Note the small number of mononuclear cells in the vascular wall (vasculitis) in the bottom part of the vessel wall (thick arrows). 20 x magnification.

© University of Pretoria

5.3.1.2 Oedema

Vasogenic oedema was identified as amorphous clear to eosinophilic extravascular fluid and severity was scored based on the amount of fluid accumulation and expansion of the perivascular areas (appendix B). Within the CCB groups, 7 cases (cases 1, 2, 6, 8, 12, 13, and 14) had severe vasogenic oedema, as indicated by marked expansion (>3x capillary wall thickness) of the perivascular areas by oedema fluid. Moderate vasogenic oedema, indicated by perivascular accumulation of oedema fluid that was 2 - 3x capillary wall thickness was noted in 4 cases (cases 3, 4, 7 and 10). Mild vasogenic oedema, indicated by slight expansion (1 x capillary wall thickness) of the perivascular areas by oedema fluid, was present in 5 cases (cases 5, 9, 11, 15 and 16).

Cytotoxic oedema, as indicated by amorphous clear to eosinophilic perineuronal fluid, was noted in 7 cases (cases 1, 2, 3, 4, 6, 8 and 14) and absent in the remaining 9 cases (cases 5, 7, 9, 10, 11, 12, 13, 15 and 16).

In the non-CCB group, one case had severe vasogenic oedema (case 19); 2 had moderate vasogenic oedema (cases 17 and 20) and 1 had mild vasogenic oedema (case 18). None of the cases in this group displayed evidence of cytotoxic oedema.

In summary, vasogenic oedema was common in both CCB and non-CCB groups. Severe vasogenic oedema was present in the majority of CCB cases and in the minority of non-CCB cases. Cytotoxic oedema, on the other hand, was less common in the CCB group and absent in the non-CCB group.

5.3.1.3 Congestion

Congestion was present in all cases, CCB and non-CCB (figure 5), compared to being absent in all control cases.

5.3.1.4 Parasitaemia

Of the 16 CCB cases, 6 were scored as having high parasitaemia (cases 3, 5, 8, 12, 13 and 14). Of these 6 cases, half were from the CCB not treated group (n=5) and half were from the CCB treated group (n=11). The remaining 10 CCB cases had moderate parasitaemia (cases 1, 6, 7 and 15) and low parasitaemia (cases 2, 4, 9, 10, 11 and 16). Aggregates of pRBCs were noted in 10 of the 16 CCB cases, which included all 6 with high parasitaemia as well as another 4 (cases 1, 3, 5, 6, 7, 8, 12, 13, 14 and 15).

Of the 4 non-CCB cases, 2 had high parasitaemia (cases 18 and 19); 1 had moderate parasitaemia (case 17) and 1 had low parasitaemia (case 20). Aggregates of pRBCs were noted in 3 of the 4 cases in this group (cases 17, 18 and 19).

© University of Pretoria

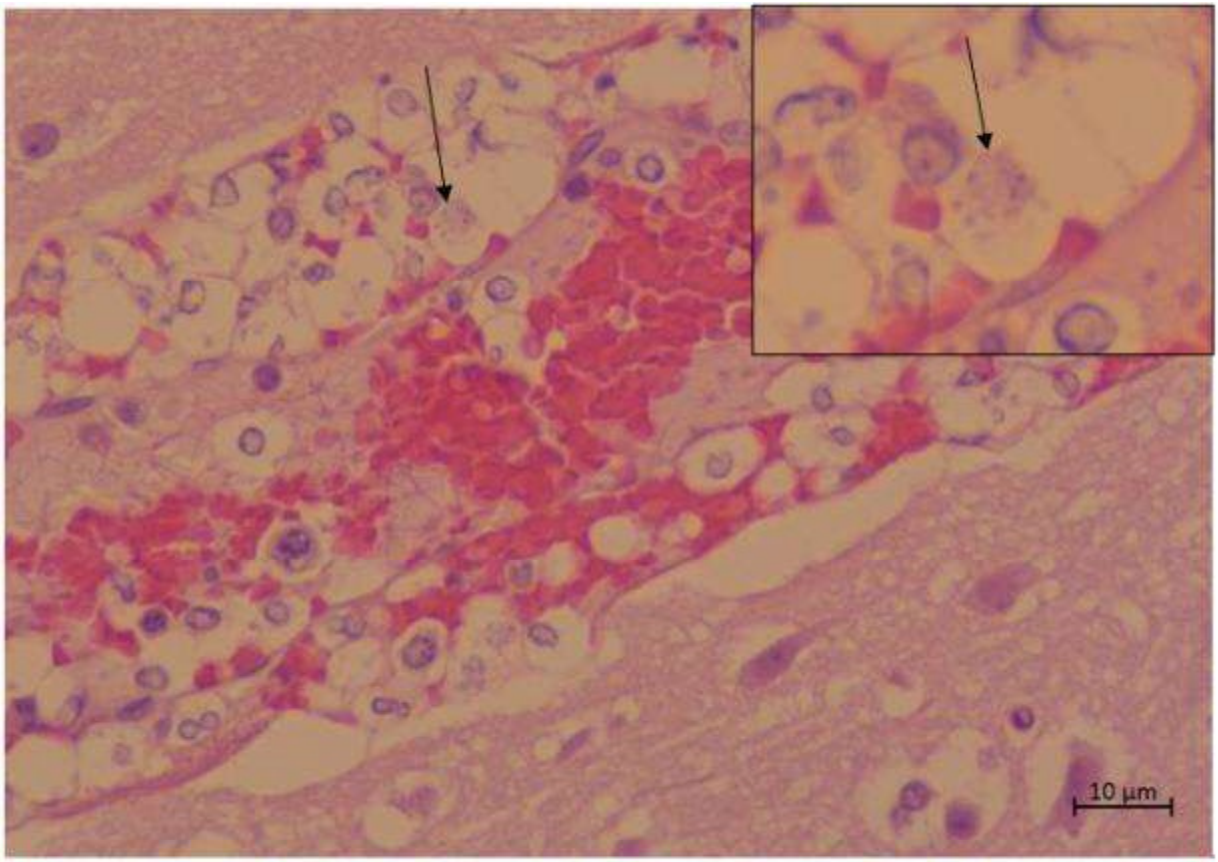


Figure 6: Case 1. HE stain. Moderate parasitaemia. Note the small intravascular, degenerating *Babesia* parasites (thin arrows) in an erythrocyte that has started showing lytic changes. 40 x magnification. *Insert* (top right): close-up of *Babesia* infected erythrocyte.

In summary, parasitaemia was high in approximately 37% of the CCB cases, which included more than half of the non-treated CCB cases, compared to just over one quarter of the treated CCB cases. Aggregation of pRBCs was noted in the majority of CCB cases. In the non-CCB group, high parasitaemia was noted in one third of cases and aggregations of pRBCs was present in just over one half of the cases.

5.3.2 Cerebral haemorrhages

Of the 16 CCB cases, 14 had petechiae as the primary haemorrhage size, (cases 1, 2, 3, 5, 6, 8, 9, 10, 11, 12, 13, 14, 15 and 16) while 2 cases had ecchymoses as the more prominent haemorrhage size (cases 4 and 7). A mixture of petechiae, ecchymoses and/or suffusive haemorrhages was noted in case 1, while ecchymoses and petechiae were noted in cases 6 and 10. Of the 16 CCB cases, 10 cases (cases 2, 4, 5, 7, 9, 10,

© University of Pretoria

11, 12, 13 and 15) had lesions in both the grey and white matter; 5 cases (cases 1, 3, 6, 8 and 16) had lesions in the grey matter only and 1 case (case 14) had lesions in the white matter only.

All 4 non-CCB cases had no evidence of lesions, as per the definition above and showed no evidence of haemorrhage.

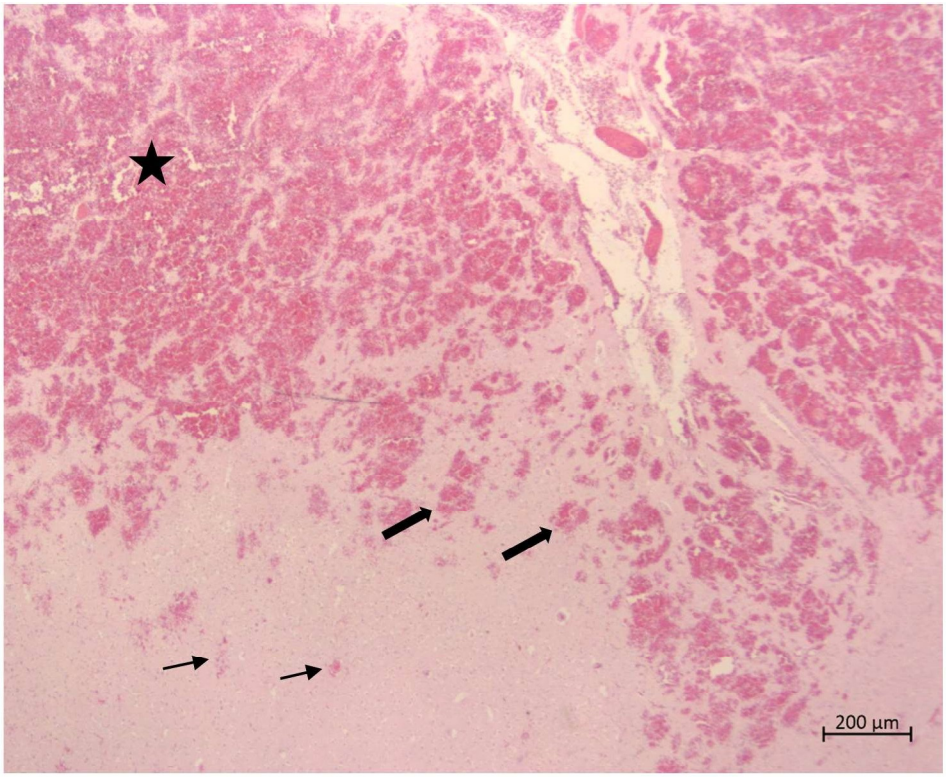


Figure 7: Case 1 (Cerebral babesiosis, treated). HE stain. Note the petechiae (thin arrows), ecchymoses (thick arrows) and suffusive haemorrhages (solid star) in the brain of a dog with cerebral babesiosis caused by *Babesia rossi*. Sub-macro, 2 x magnification.

In summary, the number of haemorrhages was significantly higher in CB cases compared to control cases; a higher number of CCB cases were observed to have haemorrhages compared to non-CCB cases, and petechiae were observed in more cases than ecchymoses or suffusive haemorrhages.

5.3.3 Vasocentric lesions

5.3.3.1 Inflammatory cells and vasculitis

All 16 CCB cases (groups 1 and 2), displayed inflammatory cells associated with vasculitis. The dominant cell type in 4 cases was neutrophils, with a combination of

© University of Pretoria

intramural, perivascular and intravascular distribution (cases 1, 4, 7 and 10) (figures 8, 9 and 10); 43 cases had dominant MN cells and fewer neutrophils, mainly distributed intramurally (cases 9, 12, 13 and 15). The remaining 8 cases had a mixture of neutrophils and MN cells, with no clearly dominant cell type visible on HE staining (cases 2, 3, 5, 6, 8, 11, 14 and 16), and intramural distribution was present in 5 of these 8 cases. The severity of 7 cases was scored as having severe inflammatory cell infiltrates (cases 1, 3, 4, 6, 7, 8 and 10) and these were all within the CCB-treated group (group 1). There were 6 cases with moderate inflammatory infiltration (cases 9, 11, 12, 13, 15 and 16). The remaining 3 cases were categorised as having mild inflammatory cell infiltrates (cases 2, 5 and 14). A total of 6 cases had inflammatory cells distributed intra-lesionally (IL) (cases 2, 3, 5, 8, 14 and 16), 4 cases were peri-lesional (PL) (cases 1, 4, 10 and 11) and 4 cases (cases 6, 7, 12 and 13) had a mixed distribution of inflammatory cells, found in 2 to 3 zones, i.e. IL and PL or IL, PL and extra-lesionally (EL). Intravascular stasis was present in 2 cases (cases 9 and 15).

The 4 non-CCB cases showed a predominantly MN inflammatory cell population in 3 cases (cases 18, 19 and 20) and 1 case (case 17) had no dominant inflammatory cell type, with MN and neutrophils numbers being approximately equal. Inflammatory cell numbers were graded as severe in 1 case (case 20), 2 were moderate (cases 18 and 19) and 1 was mild (case 17).

In summary, inflammation scores were significantly higher in the CB cases compared to control cases; more CCB cases had a mixture of MN cells and neutrophils and most were severe; more non-CCB cases had MN cells and moderate inflammation. Of the CCB cases, intramural inflammatory cell infiltrates in the IL and PL zones were most dominant, followed by perivascular and mixed distribution.

5.3.3.2 Type of vasculitis and vascular necrosis

Of the 16 CCB cases, 4 cases displayed necrotizing vasculitis with fibrin exudation (cases 5, 6, 10 and 16), 2 cases displayed necrotizing vasculitis without fibrin exudation (cases 4 and 14), 6 cases displayed vasculitis with fibrin exudation but no necrosis (cases 1, 3, 7, 11, 12 and 13) and 4 cases displayed vasculitis in the absence of both fibrin exudation and necrosis (cases 2, 8, 9, and 15). The location of the vasculitis was recorded using the diagram in figure 8. It was found that vasculitis occurred within the vessel walls (intramural) in 10 out of 16 cases (cases 1, 2, 3, 4, 5, 8, 9, 12, 13 and 16), perivascular in 3 cases (cases 10, 11 and 14), intravascular in 1 case (considered to be

© University of Pretoria

synonymous with leucostasis) (case 15) and in both the perivascular and vascular wall areas in 2 cases (cases 6 and 7).

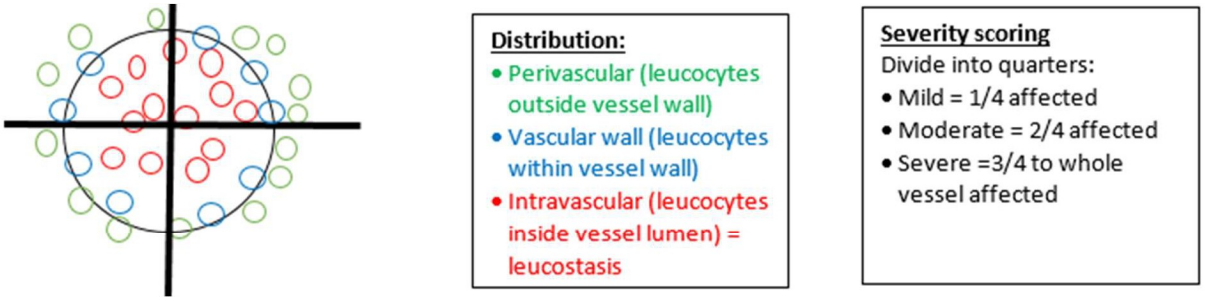
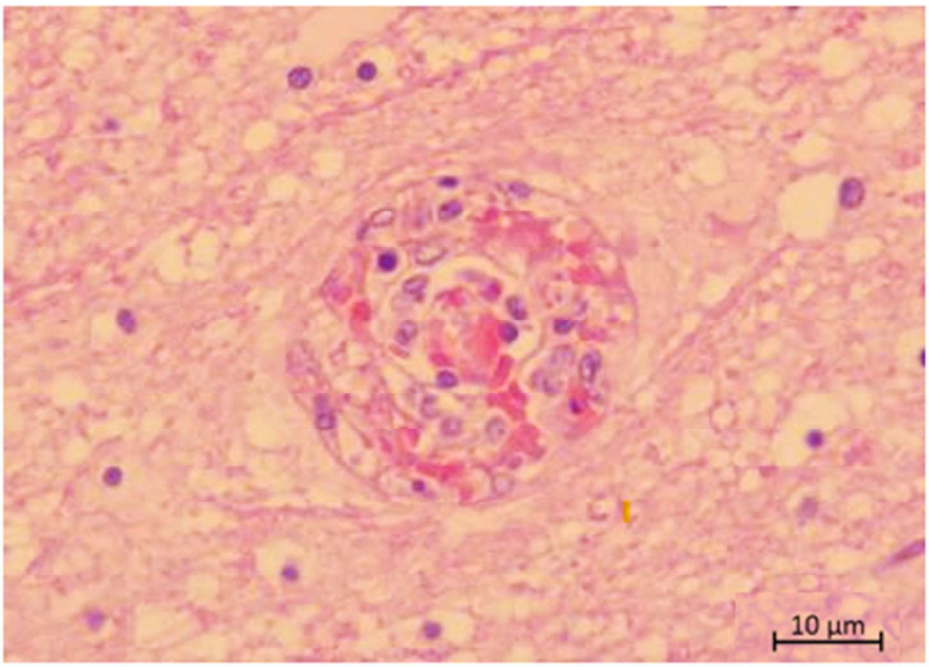


Figure 8: From appendix B (Histopathology Grading and Scoring criteria) illustrating how the distribution of inflammatory cells was evaluated in vessels displaying vasculitis.

The vessel walls remained partially intact in 9 of the 16 CCB cases (cases 1, 3, 4, 7, 10, 11, 12, 13 and 16) (figure 7), vascular integrity was completely lost in 5 cases (cases 5, 6, 8, 9 and 14) (figure 9) and the vascular walls remained intact in 2 cases (cases 2 and 15).

In the group of 4 non-CCB cases, there was no evidence of necrotizing vasculitis. All 4 cases had intravascular inflammatory cell accumulation (deemed to be synonymous with leucostasis) and all vessel walls remained intact.



© University of Pretoria

Figure 9: Case 5 (CCB). HE stain. Vasculitis consisting of mononuclear cellular infiltrate, effacing the vessel wall, with erythrocytes extending throughout the wall, indicating a loss of vascular integrity. 40 x magnification.

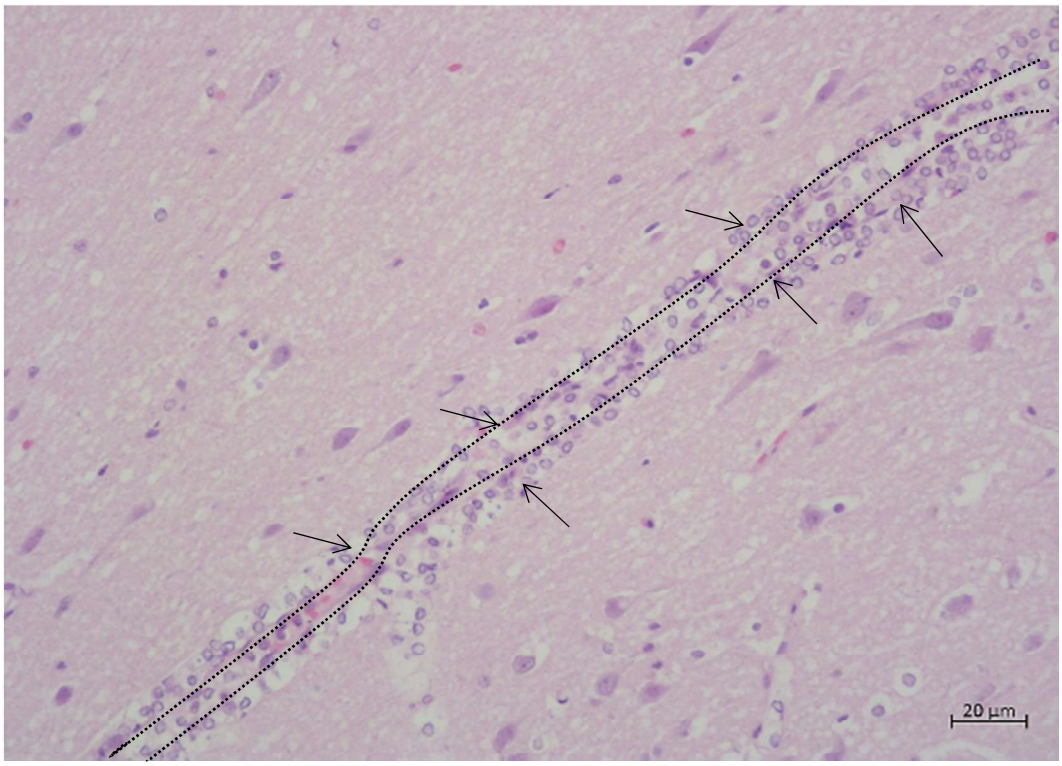


Figure 10: Case 1 (CCB). HE stain. Vasculitis consisting predominantly of mononuclear cellular infiltrate (thin arrows), completing effacing the vascular wall. Outline of vessel wall in dotted lines. 20 x magnification.

In summary, the non-CCB cases had no evidence of vasculitis involving vessel walls and only had leucostasis. The CCB cases all had evidence of vasculitis, with the majority displaying necrotizing vasculitis, with or without fibrin exudation and the minority of cases lacking evidence of vascular necrosis, with or without fibrin exudation. Most of these cases had partially intact vessel walls.

5.3.3.3 Fibrin and thrombi

Within the group of 16 CCB cases, there was no evidence of thrombosis. Fibrin was visualised in 10 cases on HE (cases 1, 3, 5, 6, 7, 10, 11, 12, 13 and 16) and in 15 cases when using the MSB special stain (all cases except case 9). Fibrin exudation varied in distribution, including intravascular (cases 13, 14, 15 and 16), within expanded vascular walls (cases 11 and 12), perivascular (cases 2 and 8) or mixed (cases 1, 3, 4, 5, 6, 7 and 10). Of the 15 cases that showed evidence of fibrin exudation, 12 cases were

© University of Pretoria

scored as moderate (cases 1, 3, 4, 5, 6, 7, 8, 10, 12, 13, 15 and 16) (figures 12 and 13) and 3 as mild (cases 2, 11 and 14). Of these cases the distribution in relation to lesions were: 5 with fibrin deposition in both IL and PL areas (cases 3, 5, 6, 7 and 12), 4 cases with IL fibrin (cases 2, 8, 11 and 14), 2 with PL fibrin (cases 1 and 10), 2 with fibrin deposition in both PL and EL areas (cases 4 and 16), 2 cases with fibrin in IL, PL and EL areas (cases 13 ad 15). Case 9 was the only CCB case that lacked evidence of fibrin exudation.

Within the non-CCB group 1 out of the 4 cases had evidence of fibrin on HE stain (case 20) and was confirmed on MSB special stain. The fibrin deposition was moderate and intravascular. Thrombus formation was noted in the meninges of this case with visible fibrin on HE and the predominant leucocytes within the thrombus were neutrophils. This was the only case with evidence of thrombus formation in this study.

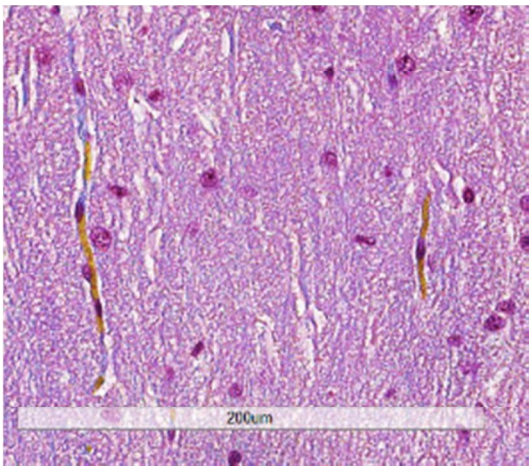
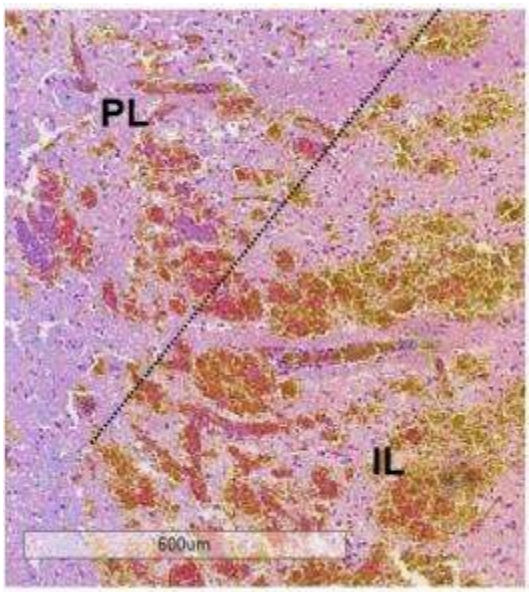


Figure 11: Control section, MSB stain. 20 x magnification.



© University of Pretoria

Figure 12: Case 1 (CCB). MSB stain. Haemorrhage, vasculitis and leucostasis transitioning from intralesional (IL, on right) to perilesional (PL, on left). 4 x magnification.

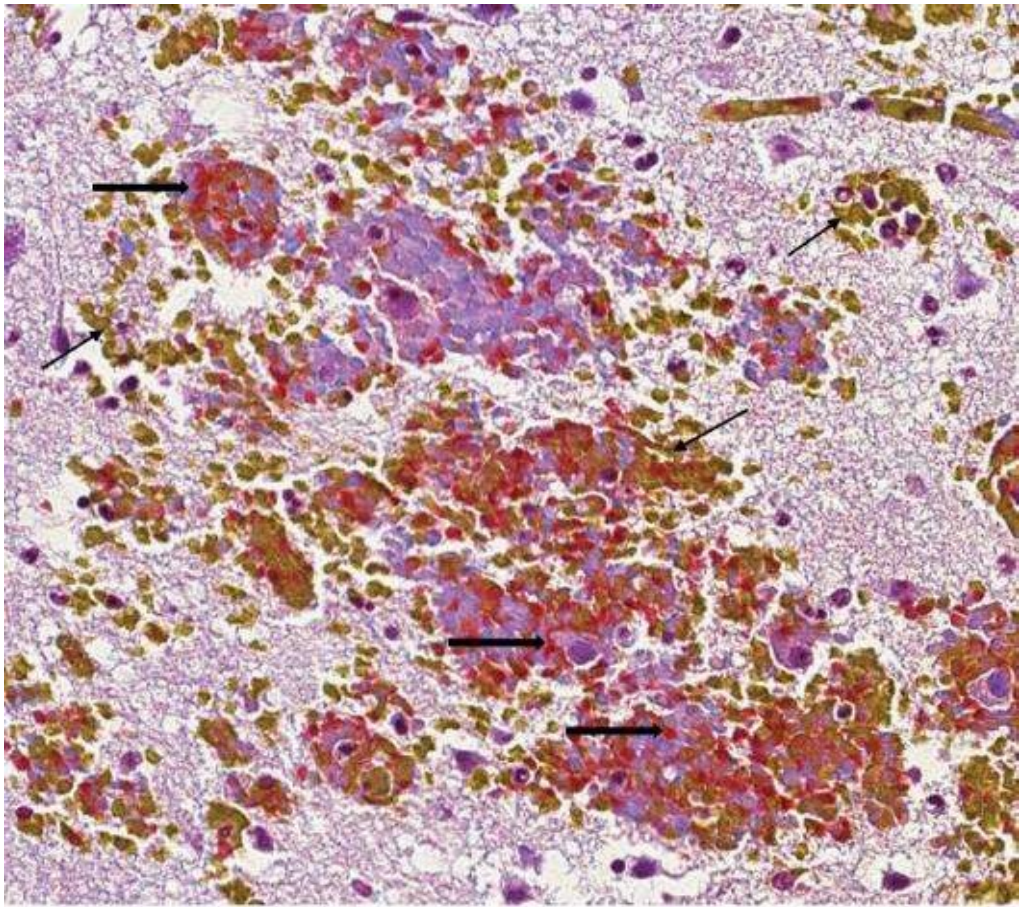


Figure 13: Case 1 (CCB). MSB stain. Higher magnification of figure 12. Note the red staining fibrin (thick arrows) and yellow-green staining erythrocytes (thin arrows). 20 x magnification.

In summary, the majority of the CCB cases had evidence of fibrin on HE staining. On MSB staining, an additional 5 cases in this group were confirmed to have fibrin present. The majority of cases had fibrin distributed intravascularly, extravascularly and within vessel walls, while the distribution in association with lesions was mainly in the IL and PL area. The majority of the non-CCB cases had no fibrin, however, the single case with evidence of thrombus formation was in the non-CCB group.

5.3.3.4 Endothelial cell hypertrophy

Endothelial hypertrophy was based on visualisation of the nucleus width being double or more the width of normal endothelial cells in the control groups. A mild score was attributed to cases with less than one third of the endothelial cells being affected, a moderate score for one to two thirds of the endothelial cells affected and a severe score

© University of Pretoria

was given to cases with more than two thirds of the endothelial cells displaying hypertrophy. In the group of 16 CCB cases, all cases had evidence of endothelial hypertrophy; 12 were moderate (cases 2, 3, 5, 6, 7, 8, 9, 10, 12, 13, 14 and 16), 3 were mild (cases 4, 11 and 15) and 1 was severe (case 1; figure 14).

In the group of 4 non-CCB cases, 2 had mild endothelial cell hypertrophy (cases 18 and 19), 1 moderate (case 17) and 1 was severe (case 20). The case with severe hypertrophy was the case that had thrombus formation (case 20).

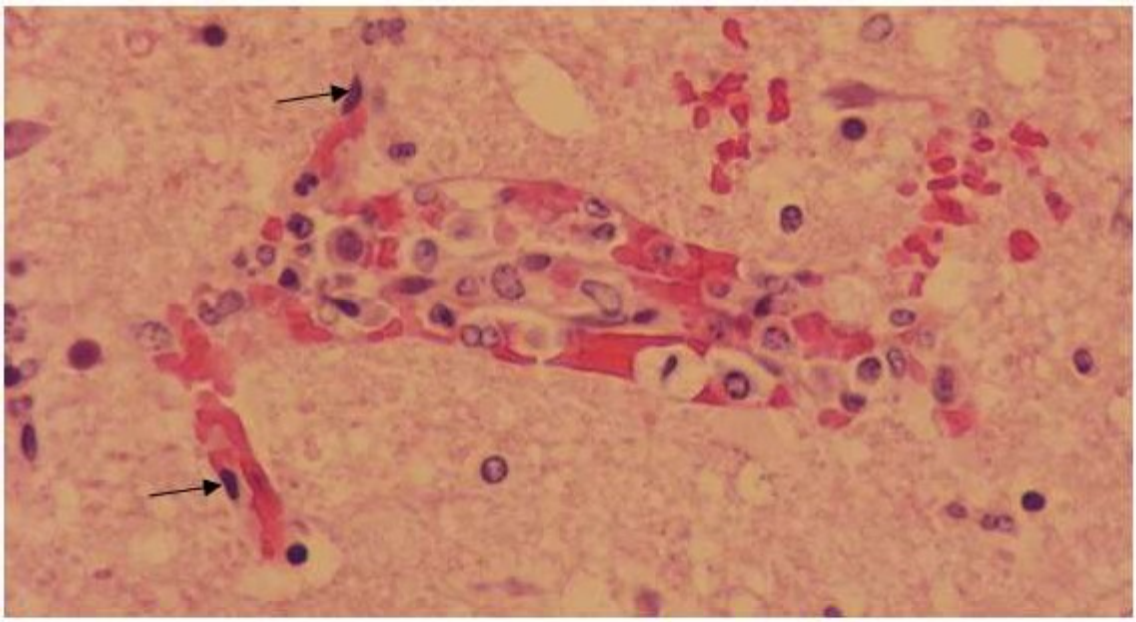


Figure 14: Case 1 (CCB). HE stain. Severe endothelial cell hypertrophy, as indicated in two hypertrophied endothelial cells (thin arrows). Note the blood vessel with mononuclear vasculitis and loss of vascular wall integrity. 40 x magnification.

In summary, on HE staining endothelial cell hypertrophy was present in the vast majority of CCB cases and a quarter of non-CCB cases. Further investigation into endothelial reactivity was done with VCAM-1 IHC immunolabelling (refer to 5.4.2.3 for details).

5.3.4 Neuronal changes

5.3.4.1 Neuronal injury and neurophagia

Neuronal injury was recorded on the score sheet when at least 3 of the following 5 neuronal changes were present: hypereosinophilia, peripheralisation of nissl substance with irregular granular cytoplasm, shrunken (angular) cytoplasm, neurophagia and/or pycnosis, karyolysis, karryorrhexis or chromatolysis. Within the CCB group, 8 out of the 16 cases had evidence of neuronal injury (cases 2, 3, 4, 5, 6, 7, 8, and 10). Of these 8

© University of Pretoria

cases, 1 case had neuronal injury in the IL zone only (case 7), 3 cases had neuronal injury in the PL zone only (cases 3, 6 and 10), 2 had neuronal injury in both the IL and PL zones (cases 4 and 8) and 2 cases had neuronal injury in all 3 zones (i.e. IL, PL and EL), (cases 2 and 5; figure 15). Neurophagia was observed in 4 of the 16 CCB cases (cases 5, 6, 7, and 8). The zones in which neurophagia was observed in these 4 cases included 1 in the IL zone only (case 5), 1 in the PL zone only (case 6), and 2 cases in both the IL and PL zones (cases 7 and 8).

The non-CCB group displayed neuronal injury in 1 (case 17) out of the 4 cases and no evidence of neurophagia was observed in any of the 4 cases.

In summary, neuronal injury was present in half the CCB cases and neurophagia was observed in one quarter of these cases. In the non-CCB cases, neuronal injury was rare and neurophagia was absent.

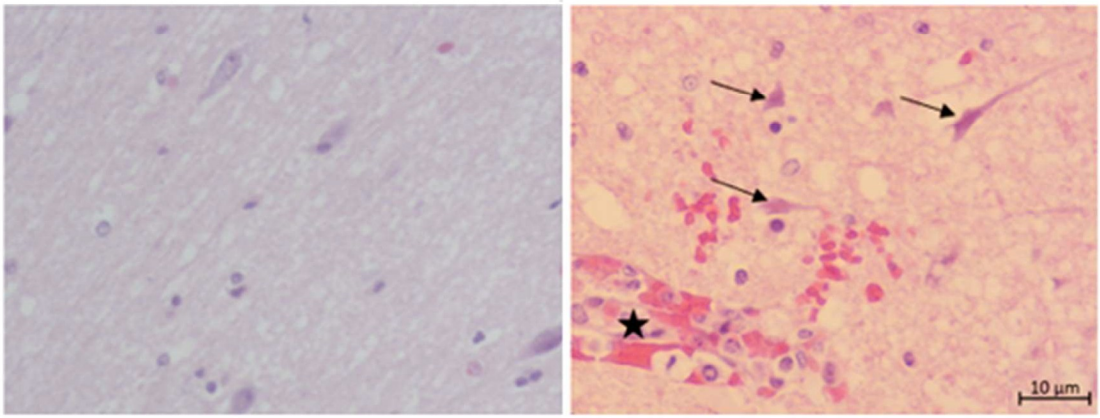


Figure 15: Left: Control case, HE stain. Note neurons with fine nissl substance and clearly visible nucleus and nucleolus. Right: Case 2 (CCB). Neuronal injury in 3 neurons (thin arrows) typified by shrunken and hypereosinophilic cytoplasm with indistinct to pycnotic nuclei. Note the perilesional location of neuronal injury in this image with haemorrhage and vasculitis in the blood vessel in the bottom left of the image (indicated by a solid star). 40 x magnification.

5.3.4.2 Neuropil inflammation

In the CCB group, a total of 11 out of the 16 cases had evidence of neuropil inflammatory infiltrates. Of these, 8 cases had obvious neuropil inflammatory infiltrate (cases 1, 3, 4, 5, 6, 7, 8, and 10) and 3 cases (cases 11, 14 and 15) had scant neuropil inflammatory infiltrate. No evidence of neuropil inflammatory infiltrate was noted in 5 out of the 16 cases in the group (cases 2, 9, 12, 13 and 16).

© University of Pretoria

Of the 11 cases that had evidence of neuropil inflammatory cellular infiltrate, 9 had equal numbers of MN and neutrophils (cases 1, 3, 4, 6, 7, 8, 10, 11 and 14). The other 2 cases had predominantly MN cells (case 5) or exclusively MN only (case 15) infiltrating the neuropil.

Within the non-CCB group, 2 cases had scant neuropil inflammatory cell infiltrate (cases 18 and 20) and 2 cases had obvious neuropil inflammatory cell infiltrate (cases 17 and 19). In all 4 cases MN cells were dominant (cases 17 and 19), or the only cell type (cases 18 and 20).

In summary, the majority of CCB cases and all non-CCB cases had evidence of inflammatory infiltrate in the neuropil. MN cells were the dominant cell type in both groups.

5.3.4.3 Spongiosis

On both HE and LFB special staining, there was no evidence of phagocytosed myelin within macrophages in any of the study cases. On HE staining, a total of 10 out of the 16 CCB cases had evidence of spongiosis. Of these 10 cases, 7 had spongiosis in both the grey and white matter (cases 3, 4, 5, 6, 7, 8, 14 and 15); 1 case had spongiosis in the white matter only (case 10) and another case had spongiosis in the grey matter only (case 11). There was no evidence of spongiosis on HE staining in the remaining 6 CCB cases (cases 1, 2, 9, 12, 13 and 16). With LFB staining, 11 CCB cases in total showed paler staining, of which 10 were mild, (cases 3, 4, 5, 7, 8, 10, 11, 14, 15 and 16) and 1 case was moderate (case 6). The remaining 5 cases (cases 1, 2, 9, 12, and 13) had no evidence of myelin changes on LFB staining. The distribution of paler LFB staining in relation to lesions showed that 3 cases had PL myelin pallor (cases 3, 7 and 10) and 1 case had IL myelin pallor (case 11). A mixture of PL and EL myelin pallor was observed in 3 cases (case 6, 14 and 16); IL and PL in 1 case (case 8) and a combination of IL, PL and EL myelin was affected in (cases 4 and 5).

In the non-CCB group, as in the control cases, there was no evidence of myelin pallor on HE and LFB stain.

In summary, the majority of CCB cases had evidence of spongiosis on HE staining and an additional case was shown to have pale staining with LFB special stain. Spongiosis was absent in the non-CCB cases on both HE and LFB special stain.

© University of Pretoria

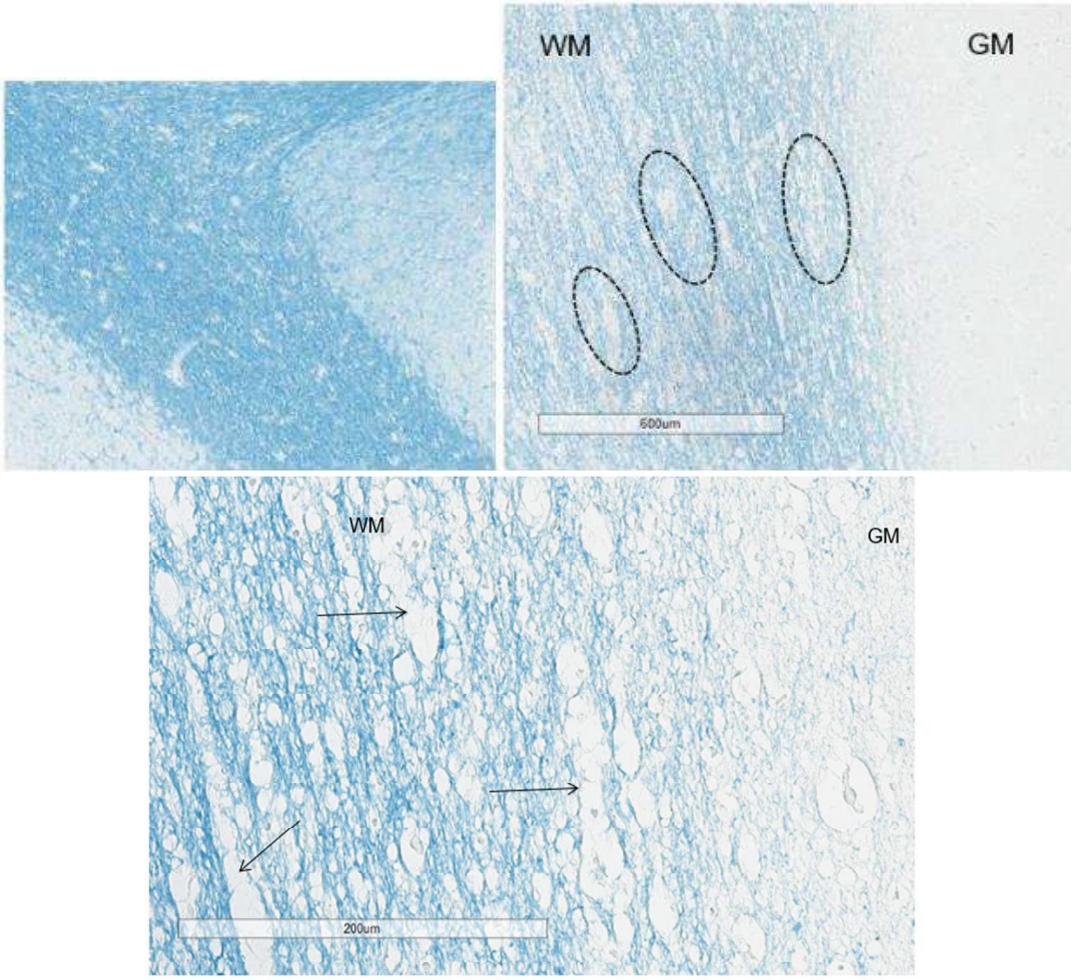


Figure 16: Top left. Control case, cerebellum white matter and grey matter junction depicting even staining of white matter. LFB stain. Top right: Case 3 (CCB). LFB stain. Cerebral white matter (WM) and grey matter (GM) junction, depicting decreased LFB staining in WM (dotted ovals). 4 x magnification. Bottom middle: Case 3 (CCB). LFB stain. Higher magnification of image in top right, showing pallor of LFB stain and neuropil spongiosis (thin arrows). 40 x magnification.

5.4 Immunohistochemistry

5.4.1 Control cases

5.4.1.1 MAC-387

MAC-387 labels histiocytes; also neutrophils, monocytes, tissue reactive macrophages, eosinophils and epidermis. The control cases showed no MAC-387 positive immunolabelling (figure 17).

© University of Pretoria

5.4.1.2 IBA1

IBA1 labels tissue macrophages and microglia as well as dendritic cells. The IBA1 positive labelling cells were primarily resident microglia cells (figure 20). No IBA1-positive labelling was noted in the remainder of the control tissue sections.

5.4.1.3 VCAM-1

VCAM-1 labels cytokine activated endothelium. The control cases displayed no VCAM-1 positive immunolabelling (figure 23).

5.4.1.4 CD3

CD3 labels T lymphocytes. CD3-positive labelling was rarely observed in the control cases; occasional CD3 positive T lymphocytes were observed in the intravascular compartment, considered to be part of the normal circulating leucocyte population (figure 24).

5.4.1.5 CD20

CD20 labels B lymphocytes, including plasma cells in dogs (Henning et al., 2020). There was no evidence of CD20-positive B lymphocytes in the control cases, except for very rare positive intravascular cells (figure 25). As noted with T lymphocytes reacting to CD3, here too the rare intravascular CD20-positive B lymphocytes were considered to be part of the normal circulating leucocyte population in the control dogs.

5.4.2 Naturally infected cases

5.4.2.1 MAC-387

Both CCB and non-CCB groups had variable numbers of MAC-387 positive labelling leucocytes observed in the intravascular and/or vascular wall (intramural) regions of all 20 study cases. MAC-387 positive leucocytes were observed within the neuropil of 9 out of the 20 study cases.

a) MAC-387 in association with vasculature

The CCB group had strong MAC-387 positive immunolabelling in 10 of the 16 cases, present in the intravascular and/or intramural regions (cases 1, 2, 3, 4, 6, 8, 9, 11, 14 and 15) (figure 18). Of these 10 cases, 6 had mixed distribution within all 3 zones, i.e. IL, PL and EL zones (cases 2, 3, 9, 11, 14 and 15) (figure 18); 2 cases were concentrated in the IL and PL zones (cases 4 and 8); 1 case had MAC-387 positive leucocytes concentrated in the PL zone only (case 1) and in 1 case they were present in the IL zone only (case 6). Moderate MAC-387 positive labelling of leucocytes was observed in 3

© University of Pretoria

cases (cases 5, 10 and 16) with distribution in IL and PL areas in case 5; PL and EL in case 10, and IL, PL and EL in case 16. Mild MAC-387 positive labelling was observed in 3 cases (cases 7, 12 and 13). The distribution was EL in case 7, while cases 12 and 13 had PL and EL distribution of MAC-387 positive labelling cells.

Within the non-CCB group all MAC-387 positive labelling leucocytes were restricted to the intravascular compartments. Leucocytes with strong MAC-387 positive labelling were observed in case 20, in association with thrombus formation (figure 19). Cases 18 and 19 displayed moderate MAC-387 positive labelling of leucocytes and case 17 had mild MAC-387 positive labelling.

b) MAC-387 in the neuropil

Strong MAC-387 positive immunolabelling of leucocytes within the neuropil was observed in 6 of the 16 CCB cases, (cases 1, 3, 4, 6, 8 and 9). Of these 6 cases, MAC-387 positive leucocytes were mainly distributed in the IL and PL zones of 3 cases (cases 1, 4 and 8) (figure 18), in IL zones in 2 cases (cases 3 and 6) and in all 3 zones (IL, PL and EL) in case 9. Moderate MAC-387 positive immunolabelling was present in the neuropil of 1 case (case 10), distributed in the PL and EL areas. Mild MAC-387 positive immunolabelling was noted in the neuropil of 2 cases (cases 11 and 16), with PL distribution in case 11 and IL in case 16 (figure 18).

In the non-CCB cases, similar to the observations described under vascular associated MAC-387 positive labelling, strong neuropil MAC-387 positive leucocyte labelling was restricted to case 20, in association with thrombus formation. Moderate (cases 18 and 19) MAC-387 positive labelling of leucocytes was restricted to intravascular compartments, and infiltration into the neuropil was absent.

© University of Pretoria

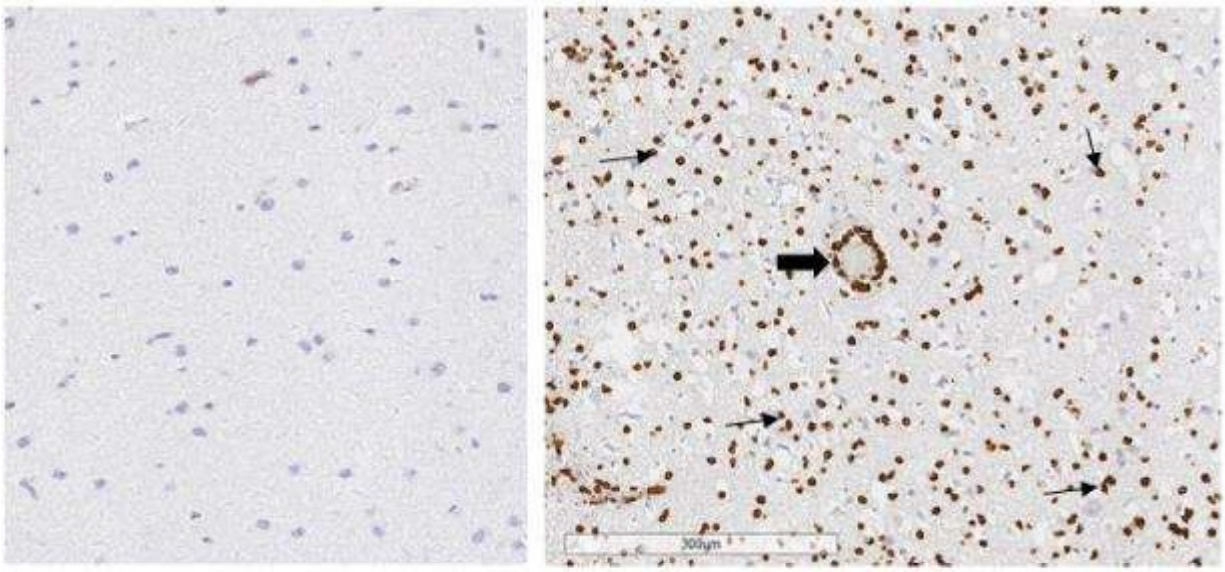


Figure 17: Left: MAC-387 control section. Right: Case 1 (CCB). Intralesional (IL) area. MAC-387 IHC. Note the numerous MAC-387 positive labelled cells (thin arrows) in the neuropil. One blood vessel wall is filled with MAC-387 positive labelled cells, forming a distinct outline of the affected blood vessel (thick arrow). 20 x magnification.

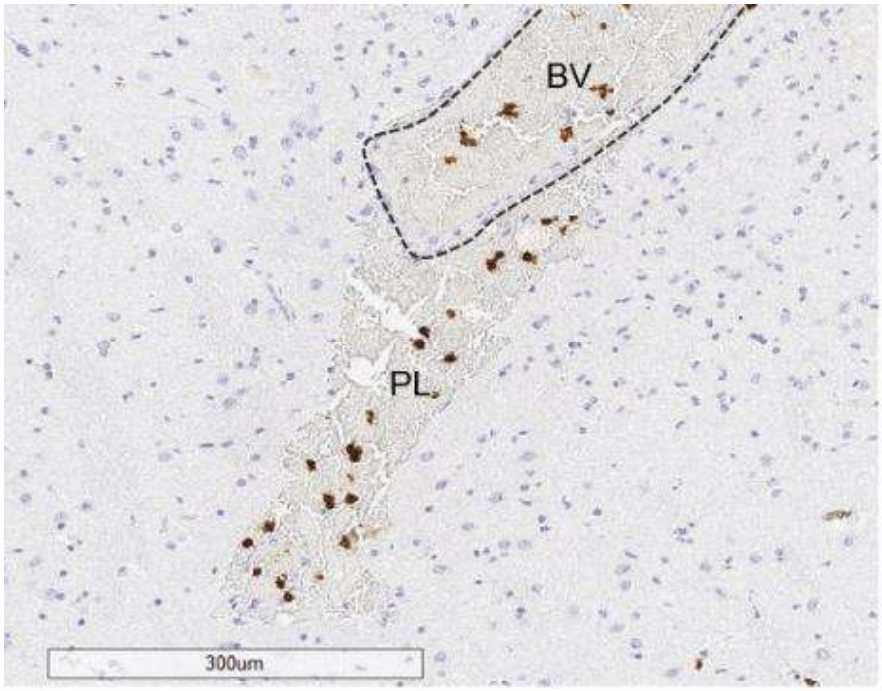


Figure 18: Case 11 (CCB). MAC-387 IHC. Note the perilesional (PL) haemorrhage with MAC-387 positive labelling monocyte-macrophage lineage cells in both perilesional and intravascular areas. The intact blood vessel wall is outlined (- - - -) in the top half of the image (BV). 4 x magnification.

© University of Pretoria

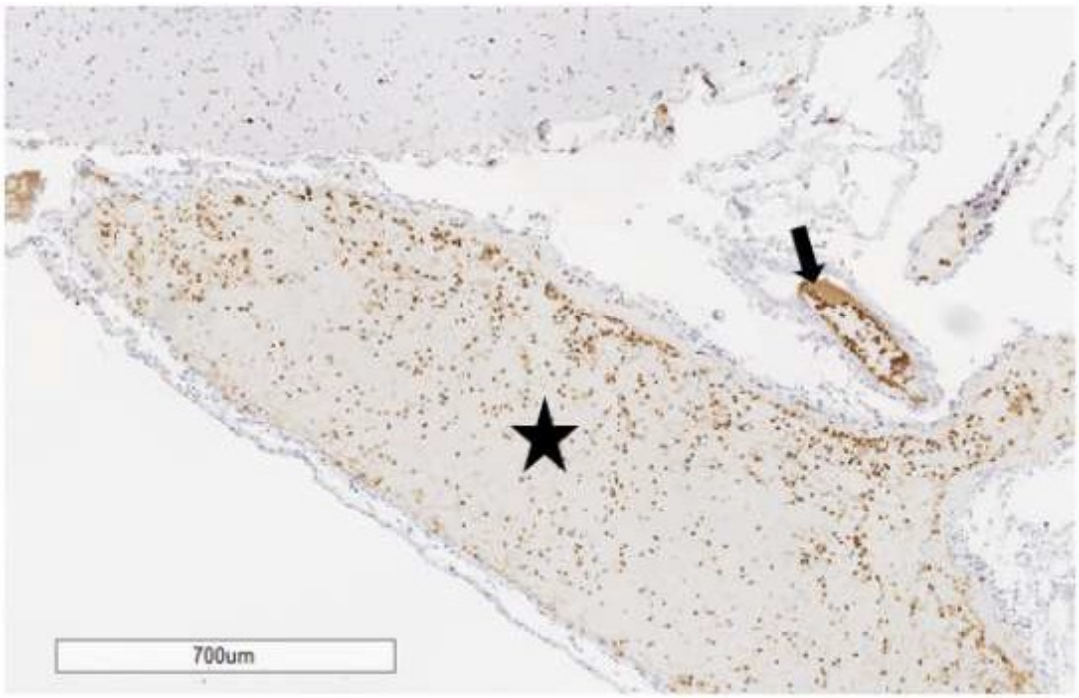


Figure 19: Case 20 (non-CCB). MAC-387 IHC. Note the numerous intravascular MAC-387 positive labelled leucocytes in a thrombus of a large meningeal blood vessel (star) as well as leucostasis in the smaller adjacent blood vessel (thick arrow). 4 x magnification.

In summary, MAC-387 IHC was widely distributed in intravascular, extravascular and intramural areas, with strong positive labelling observed in the majority of the CCB cases. In the neuropil, not associated with vasculature, randomly scattered MAC-387 positive leucocytes were observed in approximately one third of both the treated and non-treated CCB cases. In non-CCB cases, very few cases had strong positive MAC-387 immunolabelling associated with vasculature and it was absent in the neuropil.

5.4.2.2 IBA1

IBA1 positive labelling cells were primarily observed evenly dispersed within the neuropil and less frequently intravascularly. Vasocentric distribution of IBA1 positive cells was observed in the perivascular areas mainly and occasional IBA1 positive cells were also noted in the blood vessel walls of large meningeal blood vessels. The few cases where scattered intravascular IBA1 positive cells were noted were more commonly non-CCB cases.

a) IBA1 in association with vasculature

Within the CCB group, vasocentric perivascular IBA1 positive labelling was noted in all 16 cases to varying degrees. Strong IBA1 positive immunolabelling was observed in 1

© University of Pretoria

case and had a PL distribution (case 6). Moderate IBA1 positive immunolabelling was observed in 8 cases (cases 5, 7, 8, 9, 11, 12, 13 and 16). The distribution in these 8 cases included 3 cases in the EL zones (cases 7, 8 and 9), 2 cases in both PL and EL zones (cases 12 and 13), and 3 cases in IL, PL and EL zones (cases 5, 11 and 16) (figure 20). Mild IBA1 positive labelling was observed in 7 cases (cases 1, 2, 3, 4, 10, 14 and 15) (figure 21). The lesion-associated distribution of the 7 mild cases included: 4 cases with PL and EL distribution (cases 1, 2, 4 and 10); 1 case with IL and PL distribution (case 14) and 2 cases with IL, PL and EL distribution (cases 3 and 15).

The non-CCB group had mild vasocentric IBA1 immunolabelling in case 20, in association with thrombus formation (figure 22), similar to what was observed with MAC-387 immunolabelling.

b) IBA1 in the neuropil

Non-vasocentric IBA1 positive immunolabelling, focused in the neuropil, was strong in 2 CCB cases (cases 6 and 8) with PL distribution in case 6 and IL and PL distribution in case 8. Mild IBA1 positive immunolabelling was observed in the neuropil of 8 out of the 16 cases in this group (cases 1, 2, 3, 4, 7, 10, 11 and 16) (figure 21). The distribution of these mild cases included 1 case with IL distribution (case 16); 3 cases with PL distribution (cases 4, 7 and 11); 1 with EL distribution (case 3) and 3 cases with PL and EL distribution (cases 1, 2, and 10). There was no IBA1 labelling in the neuropil of the remaining 6 CCB cases.

In the non-CCB group, mild IBA1 positive immunolabelling was observed in the neuropil of case 20, in association with thrombus formation. IBA1-positive immunolabelling was absent in the remaining cases (case 17, 18 and 19).

© University of Pretoria

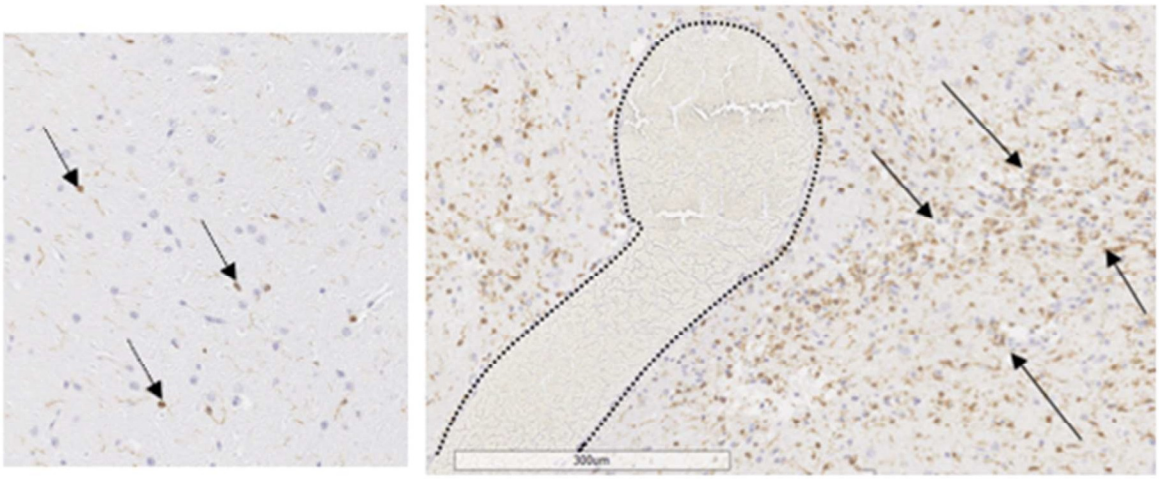


Figure 20: Left: IBA1 IHC control section with scattered positive labelling of resident microglia (thin arrows). Right: Case 11 (CCB). IBA1 IHC showing numerous positively labelled extravascular cells associated with an area of microvascular haemorrhage (thin arrows). Note the intact larger blood vessel to the left (dotted line). 10 x magnification.

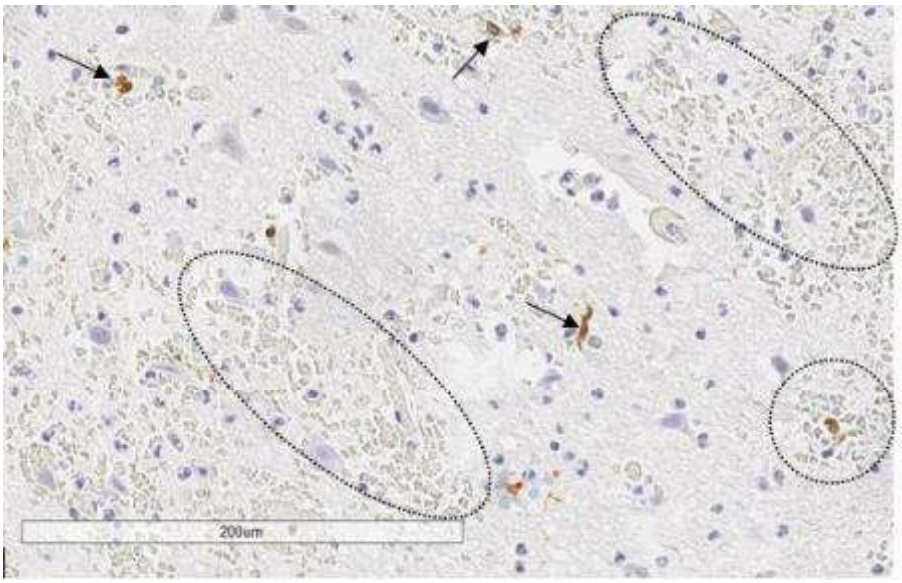


Figure 21: Case 1 (CCB). IBA IHC. Note the low number of IBA1 positive cells (thin arrows) in an area with multiple acute haemorrhages (dotted lines).

© University of Pretoria

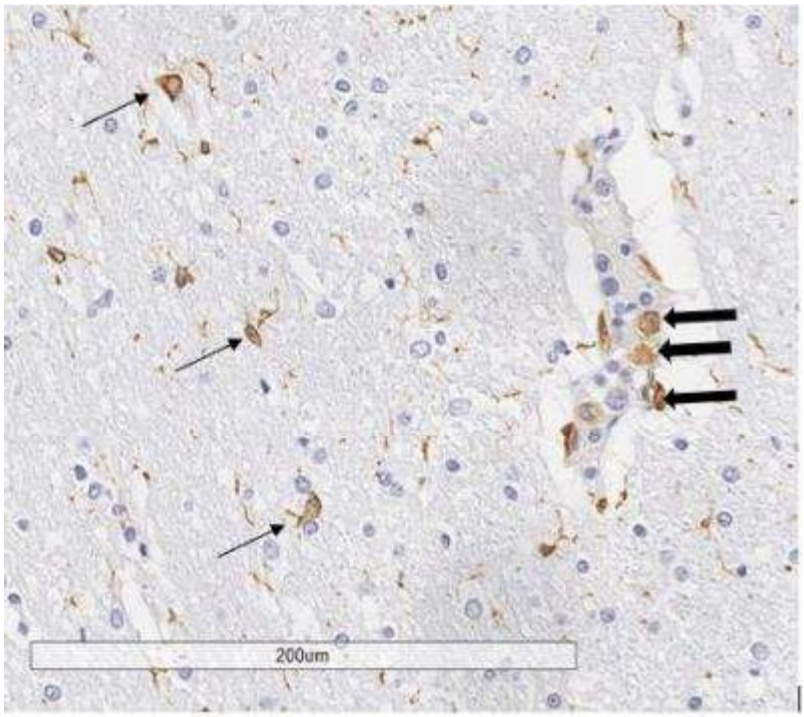


Figure 22: Case 20 (non-CCB). IBA1 IHC. Note the positive labelling of resident IBA1 positive cells in the neuropil (thin arrows), displaying thin cytoplasmic processes and small angular cell outlines, compared to plump, round activated intravascular IBA1 positive immunolabelled mononuclear cells (thick arrows). 20 x magnification.

In summary, IBA1 positive immunolabelling was predominantly observed to be rare and evenly distributed in the neuropil. Occasional cases had increased perivascular IBA1 positive cells with vessel walls that remained intact. Increased IBA1 immunolabelling did not appear to be associated with haemorrhages.

5.4.2.3 VCAM-1

Within the CCB group, 3 of the 16 cases showed evidence of moderate VCAM-1 positive immunolabelling that was restricted to the vascular endothelium (cases 3, 6 and 16). The distribution was in the IL and PL areas in cases 3 and 6, while case 16 had broad distribution of VCAM-1 positive endothelium labelling, including the IL, PL and EL areas. Mild VCAM-1 positive immunolabelling was present in 10 of the 16 cases in this group (cases 1, 4, 5, 7, 8, 10, 12, 13, 14 and 15). The distribution of these 10 cases included 5 cases with PL distribution (cases 8, 10, 12, 13 and 14) (figure 23a); 1 case with PL and EL distribution (case 1); 1 case with PL and IL distribution (case 7) and 3 cases with IL, PL and EL distribution (cases 4, 5 and 15). The remaining 3 out of the 16 cases in this group showed no evidence of VCAM-1 positive labelling (cases 2, 9 and 11).

© University of Pretoria

One non-CCB case had mild VCAM-1 positive immunolabelling (case 20), which was associated with thrombus formation (figure 23b. No immunoreactivity was observed in the other 3 cases in this group (cases 17, 18 and 19). The control cases also revealed no immunoreactivity to VCAM-1.

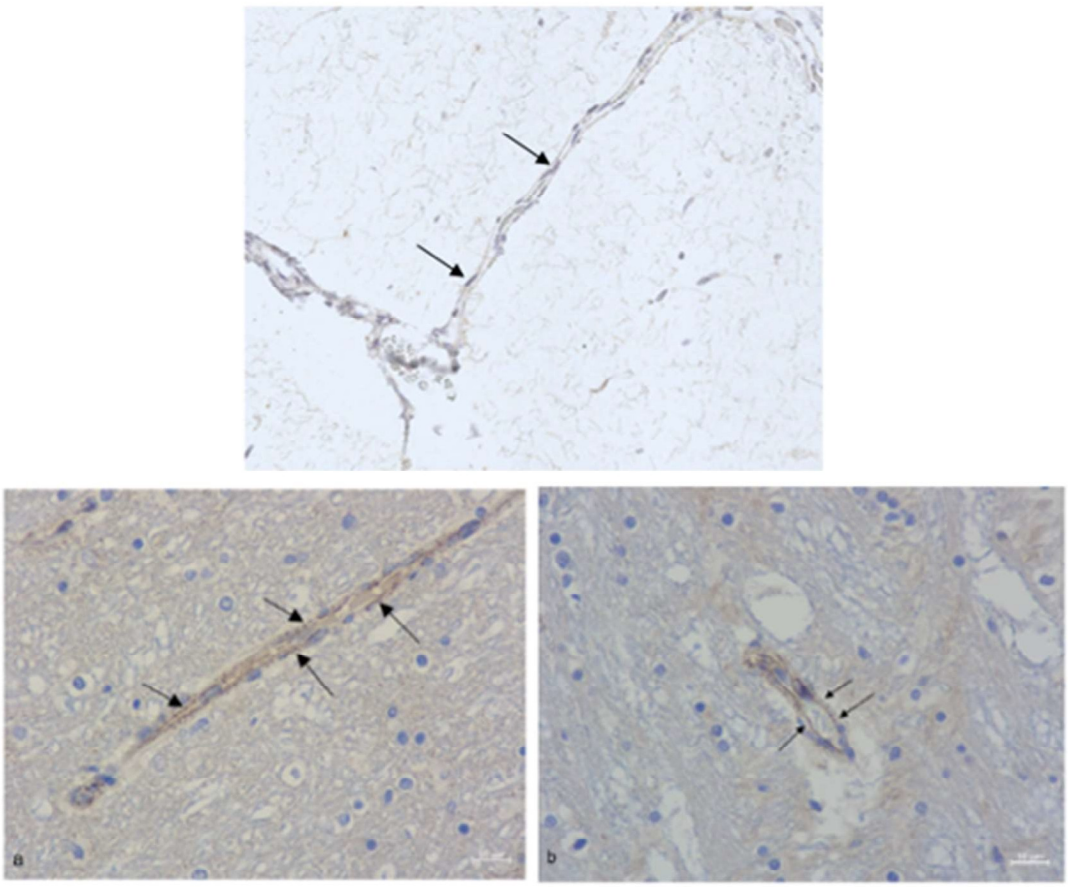


Figure 23: Top: VCAM-1 control section with no VCAM-1 immunoreactivity present in the endothelial cells (thin arrows). Below: VCAM-1 IHC showing small bead-like areas of positive immunoreactivity in activated endothelial cells (thin arrows). (a) Case 12 (CCB group). (b) Case 20 (non CCB group). 40 x magnification.

In summary, the majority of CCB cases exhibited positive VCAM-1 immunoreactivity, which was predominantly mild and mostly present in the IL and PL zones. The vascular endothelium in the majority of non-CCB cases failed to express VCAM-1.

5.4.2.4 CD3

Within the CCB group, 2 of the 16 cases revealed rare, scattered CD3-positive T lymphocytes immunolabelling, limited to the intravascular spaces only (cases 6 and 7) (figure 24). The distribution of positive labelling of T lymphocytes was EL in one case

© University of Pretoria

(case 6) and widely distributed in IL, PL and EL areas in the other case (case 7). The non-CCB group showed no evidence of CD3-positive T lymphocyte immunolabelling in any of the 6 cases. CD3 labelling within the neuropil was also assessed, with no positive labelling noted in any of the CB-positive cases (CCB and non-CCB cases).

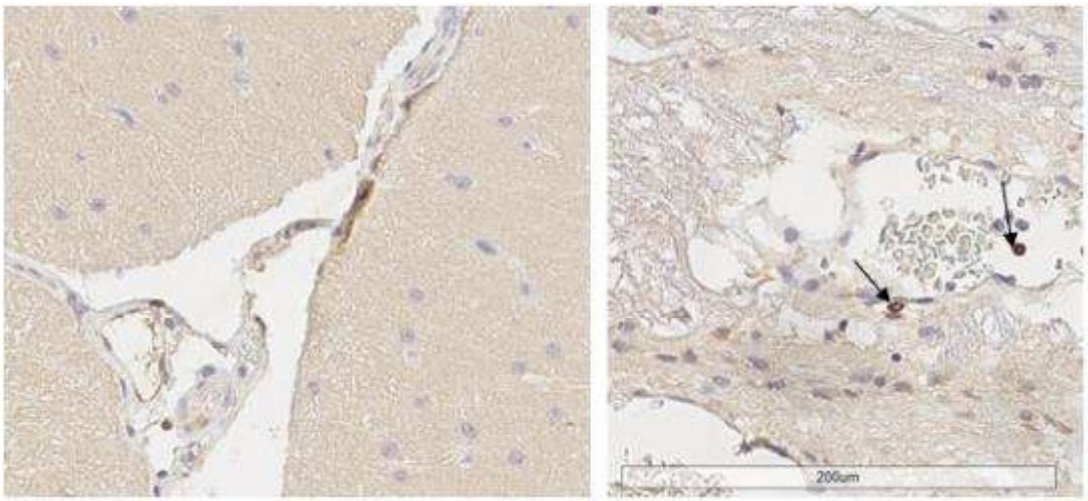


Figure 24: Left: CD3 control section showing a lack of CD3-positive immunoreactivity. Right: Case 7. CD3 IHC showing scattered rare intravascular CD3-positive T lymphocytes (thin arrows). 20 x magnification.

In summary, both CCB and non-CCB cases had no meaningful CD3 immunolabelling.

5.4.2.5 CD20

The CCB group had 2 cases with mild CD20-positive immunolabelling (cases 9 and 15), limited to the intravascular space of the EL zone in both cases.
The non-CCB group had 1 case with mild intravascular CD20-positive immunolabelling (cases 17).

© University of Pretoria

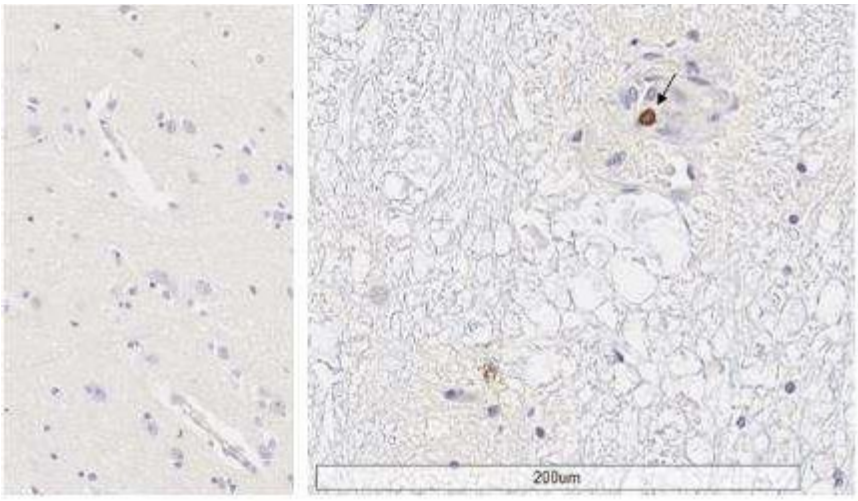


Figure 25: Left: CD20 control section showing a lack of CD20- positive immunoreactivity. Right: Case 17 (non-CCB) CD20 IHC showing rare, isolated intravascular positive labelling of a B lymphocyte (thin arrow). 20 x magnification.

In summary, both CCB and non-CCB cases had no meaningful CD20 immunoreactivity.

© University of Pretoria

CHAPTER 6: DISCUSSION

6.1 Babesia rossi as the causative Babesia sp. in this study

Canine babesiosis caused by *Babesia rossi* is the most severe babesial disease affecting dogs and is associated with complications in a small percentage of patients, resulting in multisystemic disease, high morbidity and high mortality (Welzl et al., 2001, Jacobson, 2006, Penzhorn, 2011, Leisewitz et al., 2019b). One of the complicated forms of this disease is CCB. Published literature describing the histopathological changes present in CCB is sparse and that which is published is mostly outdated and focuses on individual cases (Piercy, 1947, Purchase, 1947, Maegraith et al., 1957, Botha, 1964, Basson and Pienaar, 1965, Okoh, 1978, Moore and Williams, 1979). Pardini's Masters of Science (MSc) in Pathology thesis described the macroscopic, histological and ultrastructural lesions of CCB in dogs, but was not published (Pardini, 2010). A selection of the archived collection from Pardini's study (collected 1996-1998), was used for this project to conduct a retrospective cross-sectional study of the microscopic pathology in CCB. An additional 3 cases were sampled in 2017. In this study we focused on reviewing the histopathological changes as seen on HE staining, a selection of special stains and IHC. The last two were not as readily available at the time of Pardini's study, and were used in this study to enable a more accurate identification and description of the cell-type responses and neuronal changes associated with the central nervous lesions in CCB.

Archived material was used due to the scarcity of CCB cases. Overall, complicated babesiosis is a rare form of the disease and the cerebral form of complicated babesiosis, (i.e. CCB) is even scarcer. A notable decrease was seen in the number of canine babesiosis cases presented to South African veterinary hospitals for the period 2014-2016, which was attributed to increased host resistance, reduced pathogen virulence or a reduction in vector challenge (Lavan et al., 2018). Vector challenge reduction was thought to be linked to the release of new isoxazaline-containing acaricidal products and likely to be the main contributor to decreased numbers of canine babesiosis cases over this period (Lavan et al., 2018). In Gauteng province, where the OVAH is located, the babesiosis case numbers decreased from 120 to 44 over a 6 year period (2011-2016). Therefore, low numbers of CCB cases were available for sample collection at the start of this study in 2017 and thus archived material made up the bulk of the cases in this study.

© University of Pretoria

PCR testing for *Babesia* species identification was not routinely used at the OVAH until 2010, therefore PCR was not done on the archived cases. Despite this, we are confident that these dogs were infected with *B. rossi* because:

i. In South Africa, since routine PCR was initially introduced, CCB has only been diagnosed in *B. rossi* infected dogs (Penzhorn, 2011). *B. canis* has been associated with rare CCB cases, but is a southern European *Babesia* sp, (Strobl et al., 2020) and has not been associated with canine babesiosis in South Africa (Matjila et al., 2004, Penzhorn, 2011). *B. vogeli* has been found across the globe, including South Africa, but has never been found to be associated with complicated babesiosis (Matjila et al., 2004, Penzhorn, 2011). Therefore, complicated canine babesiosis in South Africa has to date only been diagnosed in *B. rossi* infected dogs. Small *Babesia* spp. (*Babesia gibsoni*, *B. annae* and *B. conradae*) are prevalent in North and South America, Australia, the Middle East, Asia and parts of Europe and have not been found in South Africa (Muhlnickel et al., 2002, Schoeman, 2009).

ii. Recent studies that were conducted in the last decade on dogs resident in the Onderstepoort and surrounding areas have all included PCR testing, and have confirmed *B. rossi* to be the overwhelmingly dominant *Babesia* species in this area, far outnumbering *B. vogeli* (Matjila et al., 2008, Scheepers et al., 2011, Goddard et al., 2016, Rautenbach et al., 2017, De Villiers, 2018, Leisewitz et al., 2019b, Defauw et al., 2020, Henning et al., 2020, Martin, 2020). *B. vogeli* is rarely identified in this geographical area and has never been demonstrated as a mono-infection in South Africa, neither has it been associated with severe clinical disease or CCB (Matjila et al., 2004, Irwin, 2009).

iii. All selected cases in this study were confirmed to have *Babesia* infections on thin film blood smear. Cerebral babesiosis cases were included based on macroscopically and/or visible haemorrhagic lesions.

iv. The 3 cases sampled in 2017 were confirmed to be infected with *B. rossi* on PCR testing.

v. The 3 control cases were confirmed on PCR to be negative for *Babesia,* as well as *Theileria*, *Ehrlichia* and *Anaplasma*.

© University of Pretoria

For these reasons we are confident that the cases in this study were infected with *B. rossi* and/or could rarely have had a combination of *B. rossi* and *B. vogeli* infection, although the latter is considered unlikely, given the results of the last decade of published babesia work from the Onderstepoort area (Scheepers et al., 2011, Goddard et al., 2016, Rautenbach et al., 2017, De Villiers, 2018, Leisewitz et al., 2019b, Defauw et al., 2020, Henning et al., 2020, Martin, 2020).

6.2 Macroscopic pathology of the brain

Although macroscopic pathology did not form part of this study, the majority of the cases in this study were described macroscopically in Pardini's thesis (Pardini, 2010). A short summary of the macroscopic findings recorded in the literature follows, as a reference to highlight the similarities and differences found in CCB, BCB, HCM and MCM. There is limited literature on the macroscopic pathological changes in all 4 of these diseases and it is particularly sparse in CCB, BCB and MCM.

In previous CCB studies, multifocal macroscopic haemorrhage was the most striking feature and varied in size from petechiae to ecchymoses to suffusive haemorrhages, most frequently affecting the grey matter of the cerebral cortex (Piercy, 1947, Basson and Pienaar, 1965, Pardini, 2010, Leisewitz et al., 2019b). Congestive brain swelling ("pink brain") was infrequently observed, in less than 10% of cases (Pardini, 2010). In BCB, typical macroscopic brain lesions were described as diffuse congestion of the grey matter with haemorrhage not being a feature of the disease in bovines (Bock et al., 2004).

In HCM, macroscopic lesions were described as frequently including brain swelling as a result of severe oedema (approximately 70% in one study) together with widespread petechial haemorrhages distributed in the cerebral and cerebellar white matter, as well as the brainstem (Dorovini-Zis et al., 2011). Macroscopic pathology in MCM cases indicated that petechial haemorrhages were predominantly located in the white matter of the rostral portion of the brain with scattered petechiae also noted in the grey matter (Lackner et al., 2006). The type of haemorrhage and location in the white matter was thus a common finding in HCM and MCM.

6.3 Histopathology of CCB and non-CCB cases

Tables 7 and 8 provide summaries of the scores for the 4 key histological changes (vascular, inflammation, global and neuronal) that were recorded in this study. A trend

© University of Pretoria

was seen with notably higher scores in the CCB cases versus the non-CCB cases in all 4 key histological categories. The most striking were the scores associated with the vasculature, which included vasculitis, vascular necrosis, fibrin exudate, endothelial hypertrophy and reactive endothelial cells (VCAM-1). Inflammation, global and neuronal scores were also higher in the CCB cases compared to non-CCB cases.

6.3.1 Cerebral haemorrhages

6.3.1.1 Causes for haemorrhages

This study, which was based on histological changes, confirmed the macroscopic picture seen in previous studies. Causes for haemorrhage include a loss of endothelium integrity, reduced platelet numbers (such as consumption coagulopathy), malfunction of platelets or malfunction of coagulation factors. Malfunction of platelets and coagulation factors are typically associated with inherited conditions or as a result of toxins or drugs (such as non-steroidal anti-inflammatories) (Mosier, 2017). Inherited conditions, toxins and drugs are routinely addressed upon admission of patients to the OVAH and are thus not considered likely to have been present in these cases. Based on these exclusion factors, it is probable that compromised endothelial integrity, together with thrombocytopenia, which is a common finding in haemoprotozoal disease (Grau et al., 1988, Scheepers et al., 2011, Gupta et al., 2013, Köster et al., 2015, Leisewitz et al., 2019b), were the likely primary contributing factors to haemorrhage in these cases. Whilst thrombocytopenia predisposes to haemorrhage, it does not cause vasculitis and vascular necrosis, as seen in the CCB cases (inflammation details are described later). Therefore, thrombocytopenia is considered to have exacerbated the haemorrhages once initiated, but not to be the cause for vascular damage. Endothelial injury remains the likely primary underlying initiator for haemorrhage and inflammation in the CNS of CCB cases.

6.3.1.2 CCB compared to HCM haemorrhages

In this study, haemorrhages in CCB cases ranged from petechiae to ecchymoses to suffusive haemorrhages, with petechiae being the most common form of haemorrhage. This suggests that there is an initial insult at the level of the small calibre blood vessels, which coalesce to form larger areas of haemorrhage, resulting in ecchymoses and eventually suffusive haemorrhages. Further to this, the treated CCB cases were thought to have survived for longer than non-treated CCB cases, which likely succumbed to the disease more acutely. This theory was supported by the evidence of treated CCB cases

© University of Pretoria

that were expected to survive for longer having larger areas of haemorrhage that included ecchymoses and suffusive haemorrhages, along with some petechiae, while non-treated CCB cases, with shorter expected survival, all had petechiae only. Similarly, in human cerebral malaria (HCM), cerebral haemorrhages were described as being centred around microvascular ring haemorrhages (Dorovini-Zis et al., 2011) and endothelial necrosis (Turner, 1997) however, no known literature describes larger cerebral haemorrhages such as ecchymoses and suffusive haemorrhages in HCM. This suggests that either early intervention and treatment prevents further haemorrhage and expansion of haemorrhages in HCM; or HCM patients succumb to the infection before progression of the disease can result in larger haemorrhages; or that the pathogenesis of the injury is slightly different, such as thrombosis-related or a pathomechanism specific to larger upstream vessels in babesia like damage to smooth muscle or stromal elements, rather than astrocytic support in the small vessel 'BBB' setting.

6.3.1.3 CCB compared to MCM haemorrhages

In MCM petechiae and larger haemorrhages were described but the anatomical location of the haemorrhages was localised in the rostral cerebrum in affected mice (Lackner et al., 2006, Miu et al., 2008, De Souza et al., 2010, Dorovini-Zis et al., 2011). This is possibly a result of the notable anatomical differences between dogs, humans and rodents. The range of haemorrhage sizes are similar to CCB and unlike HCM, and may be a result of endothelium-cytokine interaction.

6.3.1.4 CCB compared to BCB haemorrhages

Bovine cerebral babesiosis (BCB) is not associated with haemorrhages, which is unique, when considered in the context of the other 3 diseases discussed in this study, i.e. CCB, HCM and MCM (Bock et al., 2004, De Vos et al., 2004). It is suspected that, unlike CCB, HCM and MCM, endothelial cell membrane adhesion molecules are possibly not present or downregulated in bovines, which would result in a lack of vascular endothelial cell injury and the subsequent absence of haemorrhages. This is likely a direct effect of different or fewer inflammatory mediators or receptors involved in BCB, compared to HCM, CCB and MCM. These differences are likely to be on a molecular level and include reactivity of endothelium to cytokines.

6.3.1.5 Distribution of haemorrhages in the grey and white matter

In HCM and MCM, haemorrhages were described as being distributed widely in the white matter, whereas in this study the CCB cases showed a higher number with distribution in both the white and grey matter. This is possibly a result of differences in

© University of Pretoria

the pathomechanism between *Babesia* and *Plasmodium* and may be due to different affinities to adhesion proteins in the grey versus the white matter. It may also be a result of limitations in the material used in this study as we did not do macro-pathology and did not have access to a wide anatomical selection to do representative analyses of all regions of the brain.

6.3.2 Vasocentric lesions

6.3.2.1 Vascular “sludging” of parasitised red blood cells

In the few studies done to date describing histological changes in CCB, vascular changes have always included “sludging” of pRBCs or vasculature packed with pRBCs (Piercy, 1947, Maegraith et al., 1957, Basson and Pienaar, 1965, Okoh, 1978, Moore and Williams, 1979, Pardini, 2010, Leisewitz et al., 2019b). Pardini’s study included additional data and more in-depth analysis compared to the previous studies and some aspects of vasculitis, vascular necrosis, fibrin deposition, thrombi, endothelial hypertrophy and endothelial reactivity were addressed.

The CCB cases typically featured capillaries laden with pRBCs (sludging) together with petechiae, vasocentric inflammatory cell infiltration and reactive endothelial cells with plump nuclei. It was found that the pRBCs were frequently admixed with leucocytes intravascularly (leucostasis) and / or associated with vessel wall injury and inflammation (vasculitis). In HCM, the CNS lesions were described as being triggered by sequestered erythrocytes, pigment-laden monocytes and reactive endothelial cells, leading to petechiae and an inflammatory response that led to damage to the blood-brain-barrier, resulting in plasma leakage and oedema (Dorovini-Zis et al., 2011, Milner Jr et al., 2014, Trivedi and Chakravarty, 2022). BCB and HCM were associated with distended capillaries and with ridge-formation (in BCB) or knob-formation (in HCM) on the surface of pRBCs (Callow and McGavin, 1963, Aikawa et al., 1985, Taylor et al., 1987, Commins et al., 1988, Hutchings et al., 2007). MCM cases were documented as not showing clear association between sludging of intravascular pRBCs and haemorrhages, instead displaying a topographical prevalence in rostral areas (Carvalho et al., 2000, Lou et al., 2001, Lackner et al., 2006). As with CCB, there was no evidence in mice with MCM of ridge or knob formation on pRBC membranes (Lou et al., 2001).

Atomic force field microscopy images were captured of *B. rossi* infected red blood cells, and the cell membranes showed no evidence of “knobs” or “ridges” or any other form of membrane changes that could act as a point of ligand formation between the red cell

© University of Pretoria

membrane and the endothelium (figure 26) (Leisewitz, A.L. and Russell, B.M., unpublished data). There is evidence of haemorrhages of varying degrees occurring in CCB, HCM and MCM; similar overwhelming systemic inflammatory reactions in CCB, HCM, MCM and BCB, as well as similar plugging of capillaries by pRBCs in all four diseases, but there is a lack of evidence of knob or ridge formation in CCB and MCM. Endothelial injury is described in HCM and was present in CCB cases of this study. The need for knobs or ridges for cytoadherence to occur was questioned in a previous *P. falciparum* study, where parasitised cells adhered to each other, with or without knob formation (Udomsangpetch et al., 1989). A number of other HCM studies have, however, shown electron microscopic evidence of knob formation as the main points of adherence between pRBCs and endothelium with quantitative evidence that cases with more sequestration are more likely to show endothelial cell damage and cerebral symptoms (Aikawa et al., 1992b, Maier et al., 2009, MacPherson et al., 1985). Given the absence of true sequestration in CCB, i.e. an apparent lack of ligand formation between pRBCs and endothelial cells, this presents the question of what underlying pathomechanism is behind the endothelial damage and haemorrhage in CCB and how this differs or overlaps with HCM.

Details of the underlying pathomechanism for the haemorrhages is thus not clear and would require further investigation. The findings here suggest that endothelial injury is likely to occur as a result of factors functioning at a molecular level, such as cytokines or adhesion molecules engaging with the endothelial cell membrane, such as the *P. falciparum* erythrocyte membrane protein 1 (PfEMP1). The fact that there is a general lack of haemorrhage in BCB, even though pRBC ridges are present, and that BCB is frequently a fatal form of *B. bovis* infection, further supports the hypothesis that pRBC protrusions are not the primary cause for haemorrhage and that other factors are at play.

© University of Pretoria

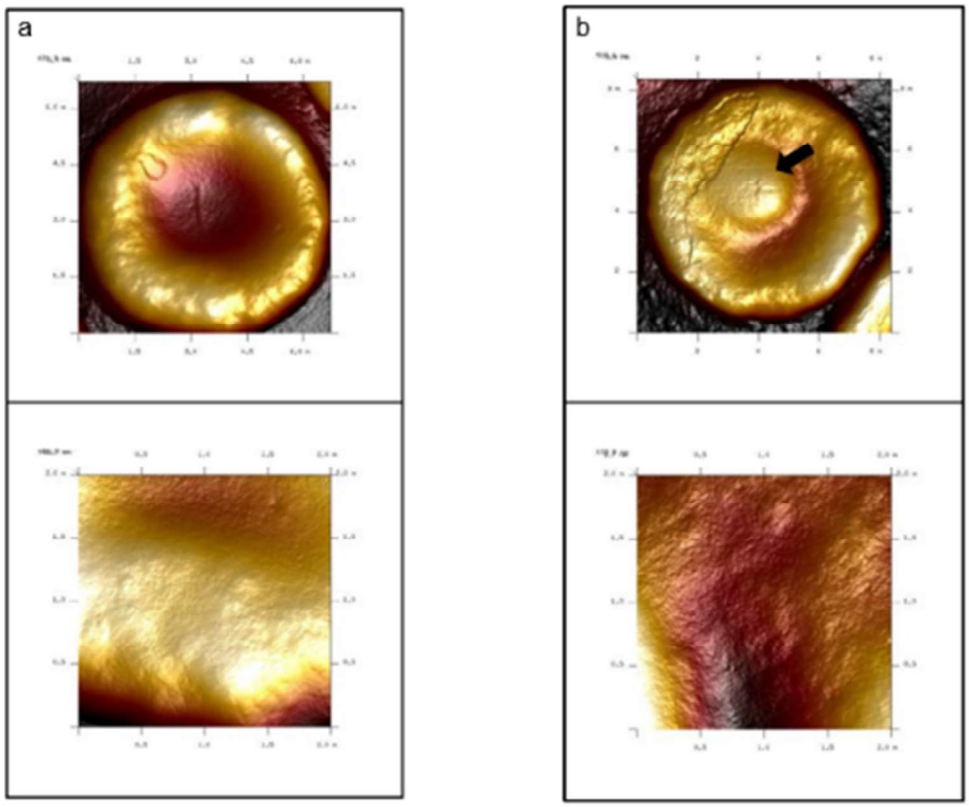


Figure 26: Atomic force field microscopy of red cell surfaces from two different dogs (a & b), naturally infected with *Babesia rossi*. Note the absence of abnormal red cell surface knobs or ridges as described in *Plasmodium falciparum* and *Babesia bovis* infected red cells. The arrow denotes a bump in the red cell surface as a result of a *Babesia* parasite within the cell (reproduced from Leisewitz AL and Russell BM, unpublished data).

6.3.2.2 Inflammatory cell types and vasculitis

In this study, vasculitis was present in all CCB cases (100%) and in all non-CCB cases (100%) leucostasis was present with intact blood vessel walls. In Pardini's study, vasculitis was recorded in only 11% of CCB cases (Pardini, 2010). The disparity between that study and this one can partly be attributed to the higher number of cases in that study compared to this study (n=20 in this study; n=54 in Pardini's study) as well as the selective case choices in this study, as we targeted cases that had macroscopically visible pathology. An older study of 3 individual cases mentioned perivascular cell infiltration with leucostasis confined to haemorrhagic lesions, which was indicative of vasculitis but no further details were documented (Basson and Pienaar, 1965). Unlike previous CCB studies, the present study recorded details such as cell type, severity and distribution in relation to lesions. Vasculitis was severe in most cases

© University of Pretoria

and predominantly included a mixture of both MN cells (monocytes / macrophages / lymphocytes) and neutrophils. It was most prominent in IL areas on HE staining.

Paediatric malaria patients coinfected with human immunodeficiency virus (HIV) were older and had a higher prevalence of developing CM. These coinfected patients had significantly greater intravascular monocyte and platelet accumulations than did HIV^- HCM cases. Minimal neutrophils were noted in all HCM children. This is considered to be a result of immune dysregulation in HIV^+ children and it exacerbates the pathological features of CM (Hochman et al., 2015). Adults with HCM, on the other hand, had an immune response that involved reactive microglia, lymphocytes and astrocytes (Turner, 1997). HIV therefore significantly adds to the complexity of malaria infections in humans. Similar granulomas were not evident in these CCB cases and has not been described in BCB or MCM. In MCM, the inflammatory response varied as the stages of infection progressed, but a prominent feature, as in HCM in children, was leucostasis. In MCM the leucocytes included both monocytes and lymphocytes. Leucostasis was associated with monocyte-monocyte and monocyte-endothelium adherence (Carvalho et al., 2000).

Neutrophils

Neutrophils were distinguished from mononuclear leucocytes on HE staining by visualising the polymorphonuclear (lobed) shape of neutrophil nuclei. The CCB cases mostly had a mixture of both neutrophils and MN leucocytes, which suggests that inflammatory triggers for both cell types were equally active in these cases. Neutrophils are produced in the bone marrow and circulate in the blood until being recruited into the tissue during an acute inflammatory response. Neutrophil pro-inflammatory cytokines include interleukin 1 (IL-1), interleukin 8 (IL-8), tumour necrosis factor (TNF) and various growth factors, amongst others. Activated neutrophils have enhanced ability to adhere to the endothelium, which further interferes with blood flow through the microvasculature, and neutrophils themselves cause tissue damage by degranulation, oxidative bursts and opsonisation, thus further contributing to ongoing cytokine release (Ackermann, 2017). The presence of neutrophils in brain sections of CCB cases was an indication of the acute nature of at least one quarter of cases where neutrophils were the dominant leucocytes, and acute to subacute inflammatory responses where neutrophils were mixed with MN leucocytes. Neutrophils were mainly confined to the intravascular compartment in the form of leucostasis in BCB (Commins et al., 1988). Although BCB is known to be associated with neutrophilic leucostasis in the lungs,

© University of Pretoria

leucostasis has not been demonstrated in the CNS of BCB cases (Commins et al., 1988). In HCM and MCM, neutrophil distribution was described as being primarily intravascular and cells were easily identifiable due to the presence of phagocytosed haemozoin pigment inside the cells (Carvalho et al., 2000, Miu et al., 2008, Dorovini-Zis et al., 2011).

The cause of a more prominent neutrophilic inflammatory response in CCB cases is not clear, but it is thought to be related to the presence of larger haemorrhages in CCB, compared to HCM, BCB and MCM. Larger haemorrhages may elicit more profound initial neutrophil infiltrates and there is possibly also some spillage of neutrophils with extravasation following rupture of neutrophil-rich leucostatic blood vessels. The combination of cytokines and chemokines released in CCB may also be unique and specifically promote attraction of neutrophils to haemorrhages, compared to cytokines and chemokines released in HCM, BCB and MCM.

Mononuclear cells

IHC was utilised as a tool to assist in determining the various lineages of cells in the MN leucocyte population.

a) Monocytes-macrophages, MAC-387

In this study, MN cells were mainly mixed with neutrophils in the CCB cases and were the dominant inflammatory cells in the non-CCB cases, where they were mostly restricted to intravascular compartments (leucostasis). MN cells are associated with acute to subacute inflammatory reactions, thus these findings are suggestive of non-CCB cases having longer standing inflammatory responses. The absence of haemorrhage in non-CCB cases indicates that cytokines released in the absence of haemorrhage favours MN cells rather than neutrophils.

As previously mentioned, MAC-387 labels histiocytes, including neutrophils, monocytes, tissue reactive macrophages, eosinophils and epidermis. The vast majority of MN cells were positive for MAC-387 and negative for CD3 and CD20, thus the majority of the MN leucocytes were of monocyte-macrophage origin or reactive macrophages. MAC-387 positive labelling in the CCB cases was strong and widely distributed. Macrophages originate from bone marrow- derived monocytes and circulate haematogenously, with some cells localising in tissues. Given the frequent neutrophils identified on HE staining, the distribution of MN leucocytes, neutrophils and MAC-387 positive labelling

© University of Pretoria

leucocytes, the MAC-387 cells visualised in the CCB cases likely constituted a combination of intravascular monocytes and neutrophils, as well as migrating macrophages and neutrophils. This is indicative of inflammatory cell infiltrates that originate from circulating monocytes and granulocytes sludging in the microvasculature (leucostasis), then migrating intramurally and perivascularly, rather than increased numbers of resident leucocytes. This is similar to the findings in acute HCM in young children and in MCM, where the primary inflammatory cell component was intravascular monocyte accumulation with phagocytosed haemozoin pigment as well as haemozoin laden macrophages in ring haemorrhages (Dorovini-Zis et al., 2011, Carvalho et al., 2000, Miu et al., 2008). Histopathological lesions of HCM in adults consisted of haemozoin-laden monocytes mainly intravascularly, infrequent haemorrhages and Dürck's granulomas (reactive microglia, lymphocytes and astrocytes), signifying a longer-term immune response (Dorovini-Zis et al., 2011). The histological changes seen in CCB cases of this study were more similar to the changes in acute HCM cases in young children than changes in adults with HCM. The mortality rate and accelerated development of disease was rapid in both acute HCM and CCB cases, suggesting similar catastrophic acute progression of these fatal forms of *Babesia* and malaria, which both appear to be centred on endothelial injury and massive cytokine release with subsequent CNS haemorrhage.

Cells of the monocyte-macrophage lineage were present in all study cases, in association with haemorrhages as well as in intact vasculature in the form of leucostasis. The dominance of this cell lineage indicates that CCB in naturally infected *B. rossi* causes significant activation and infiltration of monocyte-macrophage lineage leucocytes in response to cytokine release in the CNS. In HCM, it has been suggested that upregulation of cell adhesion molecules and decreased expression of thrombomodulin in certain organs, such as the brain and placenta, leads to increased unbound thrombin, which binds to and activates the endothelium, to release cytokines (Clark et al., 2008). In HCM, these cytokines, like interleukin-1, tumour necrosis factor, thrombin and monocyte chemotactic protein-1 (MCP-1), favour MN cell infiltration. In dogs infected with *B. rossi*, similar results have been found, where various interleukins and MCP-1 were elevated (Goddard et al., 2016).

The CB study cases had 100% positive immunolabelling with MAC-387 in association with the vasculature, thus indicating the ubiquitous distribution of cells from the

© University of Pretoria

monocyte-macrophage lineage in all *Babesia* infected cases, regardless of whether the cases had developed into complicated babesiosis in the form of CCB or not. The majority of cases (59%) in the CCB and non-CCB groups combined, had severe MAC-387 positive immunolabelling and it was widely distributed in IL, PL and EL areas. Neuropil distribution of MAC-387 positive labelled cells was also present in 55% of cases, of which the majority showed severe immunolabelling in the IL and PL areas. In Pardini's study, on HE staining, monocytes were primarily seen intravascularly and associated with leucostasis while perivascular neutrophils were occasionally present surrounding haemorrhages (Pardini, 2010). IHC, in this study, assisted in highlighting the various cell lines and allowed us to clearly distinguish between them.

Although MAC-387 immunolabelling has not been recorded in HCM, BCB or MCM studies, the findings in this study are comparable to HE stained HCM cases where macrophages were more readily identifiable due to the presence of haemozoin pigment granules in macrophages, as a result of haemoglobin breakdown. Macrophages were most prominent in the white matter of the cerebrum and cerebellum and were concentrated around heavily parasitised thrombosed microvessels with segmental endothelial cell necrosis (Dorovini-Zis et al., 2011).

These findings, as they relate to the distribution of lesions and cellular infiltrates, demonstrate the close relationship between microvascular haemorrhages, endothelial damage and infiltrating macrophages, monocytes and neutrophils in CCB and HCM.

Neuropil inflammation was notably less when compared to vascular infiltrates, which further supports the interpretation that CCB is a vasocentric disease. It is interesting to note that a higher overall percentage of non-CCB cases were MAC-387 positive. This could be a result of low numbers of cases in this group, thus each case reflected as a high percentage. It is also thought that the majority of cases showed MAC-387 positive labelling in the neuropil as a result of the systemic effects of cytokine release and resultant inflammatory reactions, as shown in previous *B. rossi* studies (Leisewitz et al., 2019a).

In the non-CCB cases, the inflammatory cell population was mainly MN, most vasculitis was moderate and the distribution could not be recorded due to a lack of sufficient lesions in this group.

b) Lymphocytes Responses, (CD3+ T-cells and CD20+ B-cells)

To distinguish lymphocytes from other mononuclear leucocytes observed on HE stain, CD3 and CD20 IHC markers were applied. CD3 labels T lymphocytes. The total number

© University of Pretoria

of cases with CD3 positive immunolabelling was low in the CCB cases and absent in the non-CCB group. In the CCB group, rare positive T lymphocytes were located inside intact vasculature, widely distributed or away from lesions. In paediatric HCM cases, CD4 and CD8 were used as T lymphocyte IHC markers and it was found that T lymphocytes were less prominent in paediatric cases compared to adult CM, where "Dürck's granulomas" (localised accumulations of reactive microglia, lymphocytes and astrocytes) were a common histological feature (Winkler et al., 1999, Dorovini-Zis et al., 2011, Trivedi and Chakravarty, 2022). No comprehensive information on CD3 immunolabelling has been published for BCB and MCM.

CD20 labels B lymphocytes, including plasma cells. A low percentage of the study cases had CD20 positive immunolabelling.

The CD3 and CD20 results thus indicate a general paucity of lymphocytic cellular reactions in canine babesiosis and no notable difference between CCB and non-CCB cases. The interpretation of these findings is that the immune reaction in fatal babesiosis is primarily driven by cytokines that cause an acute influx of the monocyte-macrophage and neutrophil lines of inflammatory cells and that dogs do not survive long enough to develop a sub-acute or chronic inflammatory response. T cells are known to be involved in the immune reaction in HCM, therefore, the possibility that the age of some of the tissues limited the ability to detect T cells cannot be excluded with certainty.

c) Microglia and IBA1

Macrophages that are resident in organs or connective tissue first enter these sites as monocytes from the circulating blood under physiological conditions, and not under inflammatory conditions. Resident macrophages then form part of the monocyte-macrophage system. In the brain these resident macrophages are the microglial cells (Ackermann, 2017). IBA1 is an IHC marker that labels tissue macrophages and microglia as well as dendritic cells. It was used in this study to highlight and visualise microglial cells. Numerous resident microglia and dendritic cells were visualised with positive IBA1 labelling. These cells were not included in the score sheets as their distribution, concentration and morphology were considered normal when compared with the control cases. These resident microglial cells were evenly spread and exhibited a ramified shape with fine, highly branched dendrites. True positive IBA1 immunolabelling was attributed to IBA1 positive labelled microglial cells that were unevenly concentrated into clusters and where the cells displayed hypertrophy, typified by large rounder shapes and short, thicker dendrites. Such clusters were noted in

© University of Pretoria

association with the vasculature in all CCB cases and rarely in non-CCB cases. In the neuropil, away from vasculature, positive IBA1 immunolabelling was present in most CCB cases and rarely in non-CCB cases.

These findings paralleled the MAC-387 immuno-labelling with regard to the majority of immune-reactive cells being vasocentric. This further supports the strong vasocentric inflammatory drivers in CCB cases as demonstrated by strong immunoreactivity exhibited by MAC-387 and IBA1 positive labelling cells. This further suggests that the broader cell population labelled by MAC-387 covers the primary immunologically responsive cell populations in the study cases. It is important to note that where CNS pathology occurs and microglial cells are activated, these cells contribute and are a source of cytokines, such as tumour necrosis factor-alpha (TNF-α) and interleukin-6 (IL-6). These proinflammatory cytokines are part of the early inflammatory response and contribute to CNS injury (Tomita et al., 2020).

6.3.2.3 Type of vasculitis and vascular necrosis

Vasculitis was described and classified in this study based on inflammation with or without fibrin exudation and/or necrosis. The findings showed that most CCB cases had necrotizing vasculitis with fibrin exudate than cases with vasculitis in the absence of fibrin exudation and necrosis, while fewer had necrotizing vasculitis in the absence of fibrin and rare cases had vasculitis with fibrin exudation but no necrosis. The non-CCB cases in our study lacked evidence of necrosis and fibrin exudation, although leucocytes were seen to accumulate intravascularly (leucostasis). In contrast, Pardini's study described intravascular and extravascular fibrin polymerisation as a more common finding in non-CCB cases than in CCB cases (Pardini, 2010), but the association between fibrin and vasculitis was not described. Endothelial cell necrosis was described in Pardini's study, but was also not noted in association with vasculitis. In this study, most of the CCB cases had fibrin exudation associated with vasculitis. It is thought that this difference is due to this study including fewer cases and combining inflammation with fibrin exudate, thus creating a larger scope for changes to be recorded in this category. Extravascular fibrin exudate is formed as a direct result of protein "leakage", including fibrinogen, in gaps between endothelial cells or due to endothelial injury in response to inflammation at the microvascular level. The presence of intramural and extravascular fibrin in the microvasculature and in the vicinity of haemorrhages is thus considered to be part of the inflammatory response. Perivascular oedema is possibly associated with leakage of protein-rich fluid from the vasculature.

© University of Pretoria

Vessel walls remained partially intact in most of the CCB cases and were completely lost in some and remained fully intact in the minority of cases. In non-CCB cases, only leucostasis was recorded, i.e. no fibrin or necrosis. The findings related to vasculitis support the theory, shared with that of Pardini, that CCB is primarily a result of endothelial cell injury, causing vessel wall damage and subsequent haemorrhagic lesions, followed by neurological clinical signs, if the patient survives long enough to display clinical signs (Pardini, 2010).

In HCM, vascular dysfunction in the brain has been attributed to various factors, such as vascular occlusion by pRBCs, ischaemia, hypoxia, vasoconstriction and acidosis (Carvalho et al., 2014). The phenomenon of vasoconstriction and vascular occlusion in HCM has seen increased interest and research recently, with the understanding that vascular occlusion alone cannot be the sole contributor to endothelial injury in HCM. Vasoconstriction and vascular dysfunction is now thought to be associated with mediators like nitric oxide, endothelins (Carvalho et al., 2014), as well as a loss of vascular integrity through the breakdown of the endothelial glycocalyx (Bush et al., 2021). There are sufficient histopathological similarities between CCB and HCM, such as haemorrhages, endothelial injury, vasculitis and microvasculature packed with pRBCs clogging up microvasculature, to indicate that mediators of the same family, or with similar effects, are at play. The pathomechanisms around decreased blood flow, vasoconstriction, pro-inflammatory and pro-adhesion changes in endothelium are most likely similar for CCB and HCM. Further research in this area may reveal similar mediators in CCB.

6.3.2.4 Fibrin, thrombi and MSB special stain

On HE approximately half of the cases in this study had visible fibrin deposition, while on MSB special stain this number increased to 80%. Fibrin deposition had a high prevalence in the CCB cases and was in the minority in the non-CCB cases. These findings suggest an increase in fibrin leakage from damaged blood vessels in CCB cases, supporting the suggestion that the primary focus of pathology is in vascular endothelial cells. A previous study on 2 individual complicated canine babesiosis cases found an absence of fibrin on HE staining, but fibrin was identified on MSB stain in both cases and both cases were diagnosed with disseminated intravascular coagulation (DIC) (Moore and Williams, 1979). This highlights the value of using a special stain like

© University of Pretoria

MSB, to increase the visibility of fibrin deposition. Pardini's study evaluated fibrin presence on HE stain and did not include an MSB special stain.

In HCM and MCM, fibrinogen IHC was used to demonstrate fibrinogen distribution and investigate permeability of the blood-brain barrier (Brown et al., 2000). Diffuse parenchymal positive immunolabelling was present in mice that had fatal MCM whereas non-fatal MCM cases were observed to have positive staining restricted to intravascular areas only (Miu et al., 2008). This was thought to indicate that the blood-brain barrier was not compromised in the non-fatal cases. In HCM cases, extravasated fibrinogen showed positive immunolabelling in association with ruptured capillaries and ring haemorrhages, in thrombosis and in microvessels that were heavily sequestered with pRBCs, regardless of whether thrombosis or haemorrhage was present (Dorovini-Zis et al., 2011). MSB special staining in this study and fibrinogen IHC staining in HCM and MCM cases thus show similar results, with increased fibrin/fibrinogen in association with haemorrhages in cerebral forms of babesiosis and malaria.

DIC has been described in *B. rossi* infected dogs with severe multi-organ damage and dysfunction (Moore and Williams, 1979, Goddard et al., 2015), while non-overt DIC (absence of obvious haemorrhages) has also been described in a coagulopathy study, where consumptive coagulopathy due to increased pro-coagulant activation, inhibitor consumption and fibrinolytic activity resulted in fatal *B. rossi* infection (Goddard et al., 2013). No outcome predictors were, however, established based on DIC and coagulopathy findings in these studies.

Thrombi were very rare in this study with only 1 case showing evidence of thrombus formation. This case was one of the non-CCB cases and thrombus formation was present in the meninges. Similarly, Pardini failed to find substantial evidence of thrombosis histologically but on ultrastructure evaluation there was some evidence of fibrin thrombus formation and it was suggested that sludging of erythrocytes may have a similar effect to thrombi, since fibrin thrombi were only present in non-CCB cases. This theory of sludging pRBCs acting as thrombi, has not been proven, however, it is supported in this study, where the single case with thrombus formation was also a non-CCB case.

Thrombi are a prominent feature of paediatric HCM. In the CM pro-inflammatory environment, platelets have been shown to act as bridges between pRBCs and endothelial cells in the absence of cytoadherence receptors (Combes et al., 2006,

© University of Pretoria

Wassmer et al., 2008). This is a possible alternative mechanism behind the sludging of microvasculature, in the absence of active sequestration in CCB.

The results of a coagulopathy study in *B. rossi* infected dogs showed that non-overt DIC was caused by a consumptive coagulopathy due to increased pro-coagulant activation, inhibitor consumption and fibrinolytic activity (Goddard et al., 2013). These findings indicate that thrombosis and infarction are not likely to be key pathological features of CCB, but that a hypercoagulable state in *B. rossi* cases, regardless of whether CCB or non-CCB, may occasionally predispose to thrombosis. Microthrombi are a documented feature of HCM and have been described as typically being central to ring haemorrhages and thought to be a result of disrupted vascular circulation resulting in infarction and malacia (Dorovini-Zis et al., 2011). In this study, as described above, microthrombi were not a feature of the histopathological pattern. Infarction was considered to be a possible secondary lesion CCB cases, but there has been no histological evidence to support this theory in this study or in Pardini's study (Pardini, 2010).

The rare occurrence of thrombus formation in CCB compared to HCM is likely a result of different disease mechanisms. Thrombocytopenia is a common finding in *B. rossi* infections, but it is also noted in human malaria (Horstmann and Dietrich, 1985, Goddard et al., 2015). It thus raises the question as to why CCB cases do not develop thrombi but HCM cases do. In *B. rossi* infected dogs it has been concluded that the absence of bleeding clinically versus obvious haemorrhages at post-mortem is a result of large platelets in circulation during a strong bone marrow response and high concentrations of fibrinogen, despite thrombocytopenia, resulting in DIC (Goddard et al., 2013, Goddard et al., 2015). In human malaria, on the other hand, it has been concluded that DIC is not a factor, but that thrombocytopenia is a result of endothelial damage and that sequestration of microvasculature is a key factor in the mechanism leading to thrombosis in these small vessels (Horstmann and Dietrich, 1985). It was concluded that thrombocytopenia in malaria is not indicative of DIC but may relate to endothelial damage (Dorovini-Zis et al., 2011). Further investigation is needed to determine the exact mechanisms at play in both HCM and CCB.

6.3.2.5 Endothelial cell hypertrophy and VCAM1

Endothelial cell hypertrophy was present in all CCB cases of this study, with variable severity. Similarly, the non-CCB cases showed evidence of endothelial cell hypertrophy in all cases. Endothelial cell reactivity was further investigated using VCAM1 IHC. The difference between the CCB and non-CCB cases was that the majority of the CCB cases

© University of Pretoria

had moderate endothelial hypertrophy whereas most of the non-CCB cases had mild endothelial hypertrophy, indicating that CCB cases had more reactive endothelial cells. Endothelial cell hypertrophy was evaluated ultrastructurally in Pardini's study with some ultrastructural changes indicating reactivity, such as cytoplasmic swelling and formation of pseudopodia, while endothelial cell necrosis was also evident (Pardini, 2010). Similar endothelial cell pycnosis was noted in the individual cases described by Basson and Pienaar (1965). There is significantly less research available regarding endothelial stimulation in inflammatory conditions in dogs, particularly in babesiosis, but the information that is available indicates that babesiosis generally creates a proinflammatory environment at the endothelial level, resulting in haemostasis and endothelial dysfunction. This proinflammatory condition is thought to promote parasite pathogenicity by causing activation of endothelial cells through increased endothelial proteins, such as vascular cellular adhesive molecule 1 (VCAM1), intercellular adhesive molecule1 (ICAM1) and thrombomodulin (Kules et al., 2017).

In studies investigating endothelial stimulation in nonfatal canine babesiosis cases caused by *B. canis* infection, it was found that the proinflammatory condition due to babesia infection resulted in endothelial activation, which was detected by a rise in serum ICAM1 and VCAM1 (Baric Rafaj et al., 2013, Kules et al., 2017). Both ICAM1 and VCAM1 play a critical role during inflammatory conditions in mediating firm adhesions between endothelial cells and leucocytes. These findings indicate that endothelial cell hypertrophy and cellular adhesion molecule activation are features of CCB caused by *B. rossi* infection, as they are in *B. canis* infections.

In BCB cases there were very limited data, but the available literature indicated that there a lack in injury to endothelial cells in experimental BCB cases (Everitt et al., 1986), suggesting a possible link between endothelial cell injury and haemorrhages, given that BCB cases generally lack haemorrhage (Callow and McGavin, 1963).

In HCM, endothelial cell injury has been considered by some authors to be the cause of microvascular thrombosis, leading to petechiae and triggering the coagulation cascade to eventually cause DIC (Dorovini-Zis et al., 2011, Milner Jr et al., 2014, Nishanth and Schlüter, 2019). As previously described, ring haemorrhages in HCM have been associated with central thrombosed, ruptured capillaries (Dorovini-Zis et al., 2011, Milner Jr et al., 2014). This is not a feature that was observed in our CCB cases, where haemorrhages were often associated with vasculitis and lacked evidence of thrombosis.

© University of Pretoria

Other than in haemoprotozoal infections, injury to the endothelial lining has also been shown to be central to organ failure in sepsis, typically associated with severe inflammation (Ince et al., 2016, Moxon et al., 2020). In these instances the causes for endothelial damage have been shown to include factors such as loss of the glycocalyx layer, which acts as a barrier along the endothelial cell lining extracellular histones and limitations on anti-inflammatory factors, such as the effect of glucocorticoids on proinflammatory migration inhibitory factors (Clark and Awburn, 2002, Ince et al., 2016, Moxon et al., 2020). The effect of leucocyte adhesion molecules, like VCAM1, along the endothelial lining allows for leucocytes, such as neutrophils and monocytes, to adhere to the endothelium and to move out of the vasculature via diapedesis, where there is release of cytokines and inflammatory mediators in an attempt to destroy the pathogens. The glycocalyx plays a central role as it shields the leucocyte adhesion molecules from attaching to circulating leucocytes in a healthy individual, but when lost, initiates the mechanism of adhesion and cytokine release (Ince et al., 2016). Glycocalyx loss is mainly associated with the effects of reactive oxygen species, but other effectors include hyperglycaemia, cytokines and bacterial endotoxins (Ince et al., 2016). The absence of the glycocalyx results in exposure of adhesion molecules (such as ICAM1 and VCAM1), which initiates the inflammatory events and a procoagulant state that follows (Ince et al., 2016). The hypertrophic changes and positive VCAM1 immunoreactivity seen in the CCB cases of this study are likely to be a result of similar molecular events as those noted during sepsis.

Extracellular histones are mediators of endothelial cell damage and have been associated with microvascular thrombosis, leakage, blood-brain barrier breakdown and sequestration in HCM cases (Moxon et al., 2020). During sepsis and severe inflammatory conditions, sustained inflammation leads to a prothrombotic, antifibrinolytic state, which can cause disseminated intravascular coagulation (Moxon et al., 2020). As previously discussed, thrombosis was not a common feature in our CCB cases but is a common feature in HCM (Dorovini-Zis et al., 2011) and this is likely a result of different disease mechanisms.

In HCM, certain endothelium-activated biomarkers have been shown to be increased in CM with retinopathy when compared to CM without retinopathy, and even more so when compared to non-cerebral malaria. This indicates that these biomarker proteins are involved in the severity of the disease and can be used as markers for disease severity (Conroy et al., 2010). Endothelial cells themselves are considered highly likely to not

© University of Pretoria

only be the target of inflammation in HCM, resulting in blood-brain barrier (BBB) breakdown and leakage, but likely to also be involved in the innate and adaptive immune responses in an attempt to control and limit effects of *P. falciparum* infection (Pais and Penha-Gonçalves, 2019). Further investigations into a range of endothelium-activated biomarkers in CCB may help understand the exact pathomechanisms at play, as it is clear that the endothelial cells lining the microvasculature are central to the pathophysiology of these diseases.

VCAM-1 labels cytokine activated endothelium. The results in this study showed that the vast majority of CCB cases had positive VCAM-1 immunolabelling versus a minority in the non-CCB, suggesting a likely predisposition to VCAM-1 expression in CCB cases. Interestingly, in other studies of the spleen, lung and bone marrow in *B. rossi* infected dogs from the same geographical area, there were no significant differences in VCAM1 immunoreactivity between babesia and non-babesia infected dogs (Henning et al., 2020, Martin, 2020, Bumby, 2022). This is likely due to a unique mechanism present in the CNS that is not displayed in the other organ systems that were studied.

VCAM-1 and other cell adhesion molecules have been shown to express and be associated with endothelial-adhering pRBCs in HCM studies. It is thought that these adhesion molecules are activated by inflammatory modulators, which in HCM mainly include tumour necrosis factor alpha (TNF-α) and interferon gamma (IFN-γ), in response to inflammatory modulators (Ockenhouse et al., 1992, Turner et al., 1994, Trivedi and Chakravarty, 2022).

6.3.3 Global changes

Global changes in this study included leucostasis, oedema, congestion and parasitaemia.

6.3.3.1 Leucostasis

Leucostasis was present in all CCB and non-CCB cases. There was no predominant anatomical region, severity or distribution in association with leucostasis. This was an expected finding as leucostasis is considered a global change. In both the CCB and non-CCB cases, there was no dominant cell type noted between MN cells and neutrophils. In cattle infected with virulent *B. bovis*, neutrophilic leucostasis was described in the lungs, but the CNS did not show similar neutrophilic leucostasis (Wright et al., 1988). In dogs infected with *B. rossi*, similarly neutrophilic leucostasis has been described (Martin, 2020), but this was not present in the CNS in these cases. Studies

© University of Pretoria

have shown that children with HCM showed monocytic leucostasis in the CNS (Dorovini-Zis et al., 2011), while mice with MCM showed a mixture of monocytic and lymphocytic leucostasis (Carvalho et al., 2000). In our study, given the histological changes noted in the vasculature of the CNS, leucocytosis (i.e. increased leucocytes in the vascular system) is likely the first step and is due to release of inflammatory mediators in response to *Babesia* infection with subsequent increased bone marrow activity and release of leucocytes systemically. The slowing down (stasis) of leucocytes in the CNS specifically, is likely a result of the interaction between cell adhesion molecules and leucocytes in the small calibre blood vessels, together with sludging of pRBCs as previously discussed. VCAM1 activation on endothelial cell membranes may be involved in this mechanism.

6.3.3.2 Oedema

Although oedema is a non-specific lesion, it was noted to be a widely distributed, global lesion in this study, particularly vasogenic oedema, which was present in all CCB cases. The largest proportion of cases had severe vasogenic oedema, moderate cases were fewer and mild cases were in the minority. Vasogenic oedema has also been described in HCM and MCM. In the HCM study of 103 paediatric HCM cases, brain swelling as a result of cerebral oedema was present in all cases (Carvalho et al., 2000, Dorovini-Zis et al., 2011, Milner Jr et al., 2014), however, computed tomography (CT) and magnetic resonance imaging (MRI) have shown that oedema is not consistently present and not necessarily related to death (Medana et al., 2001, Ponsford et al., 2012). In the non-CCB group, all cases showed evidence of vasogenic oedema ranging from mild to severe. Most cases had mild vasogenic oedema; fewer were moderate and very few were severe. Cytotoxic oedema was generally less common and present in less than half of the CCB cases while completely absent in the non-CCB group.

The BBB consists of the vascular endothelial cells with their intercellular tight junctions, the underlying basement membrane as well as astrocyte and pericyte endfeet that maintain and regulate the BBB integrity (Tunon-Ortiz and Lamb, 2019). Vasogenic oedema is considered a result of endothelial damage and subsequent increased vascular permeability with breakdown of the BBB (Trivedi and Chakravarty, 2022). This results in movement of plasma constituents into the perivascular extracellular space and can result in astrocyte cell swelling (Miller and Zachary, 2017). Subsequent accumulation of fluid in the extravascular space can be so severe that intracranial pressure increases to the point where neurological dysfunction occurs and even

© University of Pretoria

herniation of the brain into the foramen magnum (Dorovini-Zis et al., 2011, Tunon-Ortiz and Lamb, 2019). Cerebral oedema was found to be a poor prognostic indicator and was frequently associated with long term neurological deficits or death in children with HCM, but it was uncommon in adults (Seydel et al., 2015). Down-regulation and reduction of paracellular endothelial cell junction proteins at the BBB have been found in paediatric HCM and this is thought to be the underlying cause for breakdown of the BBB and resultant vasogenic oedema in these patients (Tunon-Ortiz and Lamb, 2019). Similar findings have been noted in experimental studies of MCM, where vasogenic oedema was also associated with altered BBB permeability (Szklarczyk et al., 2007). Given the important function of pericytes and astrocytes in the maintenance of the BBB integrity, a more in-depth look at how these cells respond in HCM and CCB may yield some valuable information in unravelling the pathomechanisms in these two diseases. These findings support the hypothesis that endothelial cell damage is central to the pathogenesis of haemorrhagic lesions found in CCB and HCM. In BCB, oedema was described as being variable, but the details pertaining to vasogenic versus neurogenic oedema were not recorded (Callow and McGavin, 1963, Patarroyo et al., 1982).

6.3.3.3 Congestion

Congestion was a typical global, non-specific histological change and was present in all cases in this study (CCB and non-CCB). Congestion has also been described as a common finding in BCB (Bock et al., 2004). In HCM and MCM congestion does not commonly feature as a description of pathological changes, however significant association has been noted in adult patients with increased microvascular congestion (with pRBCs or non-pRBCs) with HCM induced coma (Ponsford et al., 2012). Sequestration of pRBCs is broadly used in HCM, i.e. the accumulation and adherence of pRBCs to each other and to endothelial lining of small calibre blood vessels. Congestion is defined as a passive event, while sequestration is an active event. A number of authors have attributed sequestration to be a consequence of knob or ridge formation on pRBC membranes, with subsequent development of adhesions between pRBCs and between pRBCs and endothelial cells (Aikawa et al., 1992b, Aikawa et al., 1992a, Ockenhouse et al., 1992, Fairhurst and Wellems, 2006, Dorovini-Zis et al., 2011, Milner, 2018). In MCM, congestion and sequestration of pRBCs are not typical histological changes, but leucocyte sequestration (monocytes and lymphocytes mainly) has been described (Miu et al., 2008). Contributions from leucocytes, such as T-helper 1 cells, are thought to contribute to a cytokine storm (Miu et al., 2008).

© University of Pretoria

6.3.3.4 Parasitaemia

Severe parasitaemia cases were present in both the CCB treated and non-treated groups, but represented a higher percentage of the non-treated cases than the treated cases. This supported our expectation that the non-treated CCB cases may have a higher parasitaemia than treated CCB cases due to the effects of anti-babesia medication. A true and statistically sound comparison can, however, not be made based on the small number of cases included in this study, and would require a full experimental design to determine whether there is truly a significant difference in parasitaemia levels between treated and non-treated CCB cases. In *P. falciparum* infected patients, a high parasite burden is usually associated with a more severe form of the disease (Taylor et al., 2004).

6.3.4 Neuronal changes

6.3.4.1 Neuronal injury and neurophagia

Neuronal injury was noted in half of the CCB cases in this study and neurophagia was present in a quarter of cases. These changes were noted at various areas in association with lesions, but no area was predominant. Neuronal injury was less common in the non-CCB group with only one quarter of the cases showing this change, while neurophagia was absent in the non-CCB group. These numbers were higher than Pardini's study, where about one third of CCB cases showed neuronal injury, however, neurophagia was not described in that study. For non-CCB cases, this study showed a relatively high percentage of neuronal injury (25%), compared to Pardini's study where only 5% displayed this change. This is likely due to the case numbers in this group being markedly less (6 cases), compared to 22 non-CCB cases in Pardini's study. The case numbers in this study therefore carried a higher individual percentile value. In BCB, neuronal degeneration was not a typical histological feature (Wright et al., 1988). In HCM, beta-amyloid precursor protein IHC was used to determine axonal injury in cases with early neuronal damage and was found to be closely associated with ring haemorrhages and sequestration (Medana et al., 2002). Similar beta-amyloid precursor protein IHC studies have not been documented in CCB, BCB or MCM, however, evidence of neuronal injury was visible in more CCB than non-CCB cases, indicating that neurons are damaged in the cerebral form of babesiosis, as in the cerebral form of malaria in humans.

© University of Pretoria

The histological neuronal changes observed in these cases are considered to be a result of acute neuronal injury, and in some cases, acute neuronal necrosis. The changes are non-specific and can be the result of a variety of CNS injuries (Garman, 2011, Miller and Zachary, 2017). In this study, the more likely causes are cerebral ischaemia caused by blood loss and hypovolaemic shock, which can be explained by anaemia due to babesiosis, but this alone would not explain the increased numbers affected in CCB compared to non-CCB cases. The other cause, thought to play an important role in these cases, is the effect of inflammatory mediators and their association with neuronal injury and necrosis. This is a very likely link to the other indicators of significant cytokine release in CCB cases, as previously discussed. Other causes of neuronal injury, which were not notable features in this study and are thus less likely to have contributed to neuronal injury, are vascular thrombosis, cardiac failure, bacterial toxins, thermal injury, heavy metals, nutritional deficiencies, such as thiamine deficiency and trauma (Miller and Zachary, 2017).

6.3.4.2 Neuropil inflammation

In our CCB and non-CCB cases, neuropil inflammatory cell infiltration was common, considered to be a global-like change. The cell type was predominantly MN, which was the same as what was found in the vasocentric inflammatory components in our CCB cases, as well as in acute HCM cases in children (Dorovini-Zis et al., 2011). The key to the predominantly macrophage-monocyte inflammatory response is considered to be the result of release of specific cytokines that promote MN cell response, as previously discussed (6.3.2.1) and has been described in *B. rossi* infected dogs and in HCM cases (Clark et al., 2008, Goddard et al., 2016).

6.3.4.3 Spongiosis and LFB special stain

On HE staining, 10/16 CCB (56%) cases had evidence of myelin pallor and on LFB special stain, these 10 cases as well as an additional case had evidence of myelin pallor, bringing the total to 11/16 (69%) of CCB cases. In contrast none of the non-CCB cases displayed evidence of myelin pallor. In HCM, LFB has also been used to highlight myelin damage and in these cases two patterns emerged. One showed discrete areas where total myelin loss was associated with ring haemorrhages and necrotic perivascular zones. The other pattern consisted of patchy, irregular, variably sized, poorly demarcated zones of myelin loss in association with central microvessels filled with sequestrated pRBCs. Similar to findings in our CCB cases, the HCM lesions showed no evidence of macrophages with phagocytosed myelin (Dorovini-Zis et al., 2011). In HCM

© University of Pretoria

cases, inducible nitrous oxide (iNOS) expression and sequestration have been associated with myelin loss. It is likely that similar iNOS release by infiltrating leucocytes in CCB plays a role in causing myelin degeneration and loss. As previously discussed, the findings in this study did not support sequestration as being present in CCB. In mice, similar neurological damage has been noted in optic nerves of experimental MCM cases, due to axonal demyelination and neurodegeneration as a result of compromised blood-nerve barrier (Ma et al., 1997), indicating a similar development of CM and neurological damage in human and mice. The aggressive inflammatory host response to malaria infection favours the occurrence of neurotoxicity and is related to reduced synaptic densities and axon demyelination (Ma et al., 1997, Lima et al., 2021). Myelin loss and spongiosis have not been described in BCB.

6.3.5 Hypoglycaemia as a differential for CCB

6.3.5.1 Neuronal changes in hypoglycaemia versus CCB

Hypoglycaemia occurs in approximately 20% of complicated canine babesiosis cases and is a major differential for neurological signs such as coma, seizures and convulsions in dogs (Nel et al., 2004, Schoeman and Herrtage, 2007a, Rees and Schoeman, 2008, Leisewitz et al., 2019b). In dogs, hypoglycaemia is most often the result of a functioning insulinoma in the pancreas, producing excessive insulin, or an accidental insulin overdose in diabetic patients (Cantile and Youssef, 2016). In cases with acute hypoglycaemic death, cerebral lesions are typically not evident, which is considered a result of delayed histological changes, while biochemical changes are acutely at play and result in death (Cantile and Youssef, 2016). Prolonged hypoglycaemia, however, typically causes visible neuronal degeneration with complete chromatolysis, loss of cytoplasmic margins and fading of the cytoplasm followed by pycnosis, eccentric nuclei and ultimate karyolysis (Cantile and Youssef, 2016). In this study, neuronal changes were generally not as advanced as those described in prolonged hypoglycaemia, yet the changes were also not completely absent, as is described in acute hypoglycaemia. This indicates that the neuronal changes seen in these CCB cases are not typical for either acute or prolonged hypoglycaemia and while hypoglycaemia primarily causes neuronal changes histologically, CCB cases are associated with haemorrhagic and inflammatory histological lesions primarily. Regardless of these factors, hypoglycaemia remains a common finding in complicated canine babesiosis (Nel et al., 2004, Schoeman and Herrtage, 2007a, Rees and Schoeman, 2008, Leisewitz et al., 2019b)

© University of Pretoria

and thus remains a likely contributing factor to neuronal degeneration and other CNS histopathological changes.

6.3.5.2 Hypoglycaemia and microglia

Hypoglycaemia studies have shown inflammatory responses that mainly include the microglial population, which are strongly IBA1-positive, with changes in cell shapes indicative of reactive microglia in the absence of monocyte-macrophage reactivity (Gazit et al., 2004, Tomita et al., 2020). In this study, although IBA1-positive immunoreactivity was noted in most cases, the presence of strong monocyte-macrophage immuno-reactivity to the MAC-387 marker, in combination with increased MN leucocytes on HE staining, are considered indicative of hypoglycaemia not being the primary cause for neuropathology in these cases.

6.3.5.3 Hypoglycaemia as a differential for CNS haemorrhage

CNS haemorrhage has been described in humans suffering from hypoglycaemia, particularly in neonates (Filan et al., 2006, Rozance and Hay, 2006, Yong et al., 2012). Although hypoglycaemia is a common finding in dogs with babesiosis, studies have shown that CNS haemorrhage is not directly associated with hypoglycaemia (Gazit et al., 2004, Tomita et al., 2020).

6.3.5.4 Localised hypoglycaemia

Localised hypoglycaemia could potentially cause pathology due to metabolic competition by pRBCs in close proximity. Glucose levels of the animals chosen in this study were not available, however, previous studies have shown that at least 20% of complicated canine babesiosis cases presented to the OVAH are hypoglycaemia (Nel et al., 2004, Schoeman and Herrtage, 2007b, Rees and Schoeman, 2008, Leisewitz et al., 2019b).

© University of Pretoria

CONCLUSIONS

The aims in this study were:

1) To perform and report detailed microscopic descriptions of the brain in *B.rossi*-infected dogs diagnosed pathologically with cerebral babesiosis and contrast these findings with published data on BCB and HCM.
2) To use IHC staining to semi-quantify and give detailed descriptions of some of the different cell populations and processes within the brain of dogs with canine cerebral babesiosis, including lymphocytes, macrophages, microglia and endothelial cells.

These aims were met. The vascular and neuronal changes in the CCB cases were found to be significantly different ($p < 0.1$) from that of the non-CCB and control cases. Inflammation and global changes were not significantly different ($p > 0.1$) from non-CCB and control cases.

Vascular histopathological changes were the most striking features of the CCB group. Interestingly, the treated CCB cases had more severe and widespread histopathological changes than non-treated CCB cases, particularly with regard to inflammatory changes and less so in the vascular and global changes. However, using the Kruskal-Wallis test, analysis of the data to compare treated and non-treated CCB cases showed that the differences between the two groups were not statistically significant. Low case numbers were likely to have limited statistical analyses of the differences between treated and non-treated CCB cases. Acquiring increased case numbers for both groups may be useful for future studies. The most striking changes are summarised in the table below.

Table 11: Differences between the CCB treated, CCB not treated and non-CCB.

Histological feature	**CCB cases (treated and non-treated)**	**Non-CCB**
Haemorrhage	Frequent, petechiae	Absent
Inflammatory cells	MN and neutrophils mixed, with vascular injury	MN, leucostasis
Vasculitis	Necrotising	Absent, leucostasis only
Fibrin	Common	Rare
Endothelial cell hypertrophy	Moderate	Mild
Myelin pallor	Common, mild	Rare

CCB: canine cerebral babesiosis

© University of Pretoria

Haemorrhages were the key distinguishing feature between CCB and non-CCB cases. The likely pathomechanism is endothelial injury due to a cytokine storm as the primary initiator. Mononuclear cells and neutrophils were the dominant inflammatory cells in CCB cases and centred on haemorrhages, which was interpreted as an indicator of the acute nature of the disease compared to non-CCB cases, where the mononuclear cell population was restricted to the vascular compartment, indicating a more systemic cytokine response to *Babesia* infection. Vasculitis was typically necrotising, with associated fibrin exudate and compromised vascular wall integrity in the CCB cases. This demonstrated the destructive vasocentric nature of this disease, which was highlighted by the lack of vascular wall injury in non-CCB cases. Endothelial cell hypertrophy was more common in CCB cases but not completely absent in non-CCB cases, indicating a combination of endothelial reactivity in severe CNS injury, as occurs in CCB cases, but also systemic endothelial reactivity in non-CCB. Although myelin pallor was more prominent in CCB cases, it is a non-specific change, which does not appear to be a reliable indicator for CCB versus non-CCB cases.

This study did not include ultrastructural microscopy such as atomic force microscopy or electron microscopy. Given our findings of endothelial cell involvement and vasculitis, we suspect that the primary changes were on a molecular level at the endothelial cell surface and most likely at the interface between endothelium and pRBC membranes, but that red cell sequestration is not strongly associated with the pathophysiological mechanism. Macrophage-induced changes involving inflammatory mediators which result in endothelial damage and vascular dysfunction are the most likely mechanisms involved, but have not been fully described as yet. Future studies focusing on the interface between pRBCs and endothelium on an ultrastructural and molecular level would be valuable in further determination of the pathophysiology of CCB.

© University of Pretoria

REFERENCE LIST

ABDULLAHI, S. U., MOHAMMED, A. A., TRIMNELL, A. R., SANNUSI, A. & ALAFIATAYO, R. 1990. Clinical and haematological findings in 70 naturally occurring cases of canine babesiosis. *Journal of Small Animal Practice,* 31**,** 145-147.

ACKERMANN, M. R. 2017. Chapter 3 - Inflammation and Healing. In: J. F. Zachary (ed), *Pathologic Basis of Veterinary Disease (Sixth Edition),.* pp. 73-131, Mosby.

ADASZEK, L., GORNA, M., KLIMIUK, P., KALINOWSKI, M. & WINIARCZYK, S. 2012. A presumptive case of cerebral babesiosis in a dog in Poland caused by a virulent Babesia canis strain. *Tierarztl Prax Ausg K Kleintiere Heimtiere,* 40**,** 367-71.

AIKAWA, M., BROWN, A., SMITH, C. D., TEGOSHI, T., HOWARD, R. J., HASLER, T. H., ITO, Y., PERRY, G., COLLINS, W. E. & WEBSTER, K. 1992a. A primate model for human cerebral malaria: Plasmodium coatneyi-infected rhesus monkeys. *The American journal of tropical medicine and hygiene,* 46**,** 391-397.

AIKAWA, M., PONGPONRATN, E., TEGOSHI, T., NAKAMURA, K., NAGATAKE, T., COCHRANE, A. & OZAKI, L. S. 1992b. A study on the pathogenesis of human cerebral malaria and cerebral babesiosis. *Mem Inst Oswaldo Cruz,* 87 Suppl 3**,** 297-301.

AIKAWA, M., RABBEGE, J., UNI, S., RISTIC, M. & MILLER, L. H. 1985. Structural alteration of the membrane of erythrocytes infected with Babesia bovis. *The American journal of tropical medicine and hygiene,* 34**,** 45-49.

ALLRED, D. R. & AL-KHEDERY, B. 2004. Antigenic variation and cytoadhesion in Babesia bovis and Plasmodium falciparum: different logics achieve the same goal. *Molecular and biochemical parasitology,* 134**,** 27-35.

ALLRED, D. R., CARLTON, J. M.-R., SATCHER, R. L., LONG, J. A., BROWN, W. C., PATTERSON, P. E., O'CONNOR, R. M. & STROUP, S. E. 2000. The ves multigene family of B. bovis encodes components of rapid antigenic variation at the infected erythrocyte surface. *Molecular cell,* 5**,** 153-162.

ALLRED, D. R., GRUENBERG, J. & SHERMAN, I. 1986. Dynamic rearrangements of erythrocyte membrane internal architecture induced by infection with Plasmodium falciparum. *Journal of Cell Science,* 81**,** 1-16.

ANDRIANARIVO, A., BARR, B., ANDERSON, M., ROWE, J., PACKHAM, A., SVERLOW, K. & CONRAD, P. 2001. Immune responses in pregnant cattle and bovine fetuses following experimental infection with Neospora caninum. *Parasitology research,* 87**,** 817-825.

APANASKEVICH, D. A., HORAK, I. & CAMICAS, J.-L. 2007. Redescription of Haemaphysalis (Rhipistoma) elliptica (Koch, 1844), an old taxon of the Haemaphysalis (Rhipistoma) leachi group from East and southern Africa, and of Haemaphysalis (Rhipistoma) leachi (Audouin, 1826)(Ixodida, Ixodidae). *Onderstepoort Journal of Veterinary Research,* 74**,** 181-208.

BARIC RAFAJ, R., KULES, J., SELANEC, J., VRKIC, N., ZOVKO, V., ZUPANCIC, M., TRAMPUS BAKIJA, A., MATIJATKO, V., CRNOGAJ, M. & MRLJAK, V. 2013. Markers of coagulation activation, endothelial stimulation, and inflammation in dogs with babesiosis. *J Vet Intern Med,* 27**,** 1172-8.

BARTLEY, P. M., HAMILTON, C., WILSON, C., INNES, E. A. & KATZER, F. 2016. Detection of Babesia annae DNA in lung exudate samples from Red foxes (Vulpes vulpes) in Great Britain. *Parasites & vectors,* 9**,** 84.

© University of Pretoria

BARTOLONI, A. & ZAMMARCHI, L. 2012. Clinical aspects of uncomplicated and severe malaria. *Mediterranean journal of hematology and infectious diseases,* 4.

BARUCH, D., GORMELY, J., MA, C., HOWARD, R. & PASLOSKE, B. 1996. Plasmodium falciparum erythrocyte membrane protein 1 is a parasitized erythrocyte receptor for adherence to CD36, thrombospondin, and intercellular adhesion molecule 1. *Proceedings of the National Academy of Sciences,* 93**,** 3497-3502.

BASSON, J. 1965. Canine babesiosis: a report on the pathology of three cases with special reference to the'cerebral'form. *Journal of the South African Veterinary Association,* 36**,** 333-341.

BASSON, P. & PIENAAR, J. 1965. Canine babesiosis: a report on the pathology of three cases with special reference to the'cerebral'form. *Journal of the South African Veterinary Association,* 36**,** 333-341.

BOCK, R., JACKSON, L., DE VOS, A. & JORGENSEN, W. 2004. Babesiosis of cattle. *Parasitology,* 129 Suppl**,** S247-69.

BOTHA, H. 1964. The cerebral form of babesiosis in dogs. *Journal of the South African Veterinary Association,* 35**,** 27-28.

BROWN, H., CHAU, T., MAI, N., DAY, N., SINH, D., WHITE, N., HIEN, T., FARRAR, J. & TURNER, G. 2000. Blood–brain barrier function in cerebral malaria and CNS infections in Vietnam. *Neurology,* 55**,** 104-111.

BROWN, W. & PALMER, G. 1999. Designing blood-stage vaccines against Babesia bovis and B. bigemina. *Parasitology Today,* 15**,** 275-281.

BUMBY, M. M. 2022. *Cytological and histopathological bone marrow findings in dogs with natural Babesia rossi infection.* Masters thesis, Dept of Paraclinical Sciences, Faculty of Veterinary Science, University of Pretoria.

BUSH, M. A., ANSTEY, N. M., YEO, T. W., FLORENCE, S. M., GRANGER, D. L., MWAIKAMBO, E. D. & WEINBERG, J. B. 2021. Vascular Dysfunction in Malaria: Understanding the Role of the Endothelial Glycocalyx. *Frontiers in Cell and Developmental Biology,* 9.

CALLOW, L. & MCGAVIN, M. 1963. Cerebral babesiosis due to Babesia argentina. *Australian Veterinary Journal,* 39**,** 15-21.

CANTILE, C. & YOUSSEF, S. 2016. Chapter 4 - Nervous system. In: M.G. Maxie (ed), *Jubb, Kennedy & Palmer's Pathology of Domestic Animals: Volume 1, 6th edn*, pp. 250-406, Elsevier.

CARRET, C., WALAS, F., CARCY, B., GRANDE, N., PRECIGOUT, E., MOUBRI, K., SCHETTERS, T. & GORENFLOT, A. 1999. Babesia canis canis, Babesia canis vogeli, Babesia canis rossi: differentiation of the three subspecies by a restriction fragment length polymorphism analysis on amplified small subunit ribosomal RNA genes. *Journal of eukaryotic microbiology*.

CARVALHO, L., LENZI, H. L., PELAJO-MACHADO, M., OLIVEIRA, D. N., DANIEL-RIBEIRO, C. T. & FERREIRA-DA-CRUZ, M. 2000. Plasmodium berghei: cerebral malaria in CBA mice is not clearly related to plasma TNF levels or intensity of histopathological changes. *Experimental parasitology,* 95**,** 1-7.

CARVALHO, L. J. D. M., MOREIRA, A. D. S., DANIEL-RIBEIRO, C. T. & MARTINS, Y. C. 2014. Vascular dysfunction as a target for adjuvant therapy in cerebral malaria. *Memorias do Instituto Oswaldo Cruz,* 109**,** 577-588.

CHIMELLI, L. 2011. A morphological approach to the diagnosis of protozoal infections of the central nervous system. *Pathology research international,* 2011.

© University of Pretoria

CLARK, I. & AWBURN, M. 2002. Migration inhibitory factor in the cerebral and systemic endothelium in sepsis and malaria. *Critical care medicine,* 30**,** S263-S267.

CLARK, I. A., AL YAMAN, F. M. & JACOBSON, L. S. 1997. The biological basis of malarial disease. *International journal for parasitology,* 27**,** 1237-1249.

CLARK, I. A., ALLEVA, L. M., BUDD, A. C. & COWDEN, W. B. 2008. Understanding the role of inflammatory cytokines in malaria and related diseases. *Travel medicine and infectious disease,* 6**,** 67-81.

COLLETT, M. 2000. Survey of canine babesiosis in South Africa. *Journal of the South African Veterinary Association,* 71**,** 180-186.

COMBES, V., COLTEL, N., FAILLE, D., WASSMER, S. C. & GRAU, G. E. 2006. Cerebral malaria: role of microparticles and platelets in alterations of the blood–brain barrier. *International journal for parasitology,* 36**,** 541-546.

COMMINS, M., GOODGER, B., WALTISBUHL, D. & WRIGHT, I. 1988. Babesia bovis: studies of parameters influencing microvascular stasis of infected erythrocytes. *Research in veterinary science,* 44**,** 226-228.

CONROY, A. L., PHIRI, H., HAWKES, M., GLOVER, S., MALLEWA, M., SEYDEL, K. B., TAYLOR, T. E., MOLYNEUX, M. E. & KAIN, K. C. 2010. Endothelium-based biomarkers are associated with cerebral malaria in Malawian children: a retrospective case-control study. *PloS one,* 5**,** e15291.

COOKE, B. M., MOHANDAS, N., COWMAN, A. F. & COPPEL, R. L. 2005. Cellular adhesive phenomena in apicomplexan parasites of red blood cells. *Veterinary parasitology,* 132**,** 273-295.

CRAIG, A. G., GRAU, G. E., JANSE, C., KAZURA, J. W., MILNER, D., BARNWELL, J. W., TURNER, G., LANGHORNE, J. & MALARIA", P. O. T. H. R. M. O. A. M. F. R. O. S. 2012. The role of animal models for research on severe malaria. *PLoS pathogens,* 8**,** e1002401.

DAVID, P. H., HOMMEL, M., MILLER, L. H., UDEINYA, I. J. & OLIGINO, L. D. 1983. Parasite Sequestration in Plasmodium falciparum Malaria: Spleen and Antibody Modulation of Cytoadherence of Infected Erythrocytes. *Proceedings of the National Academy of Sciences of the United States of America,* 80**,** 5075-5079.

DE CASTRO, J. J. 1997. Sustainable tick and tickborne disease control in livestock improvement in developing countries. *Veterinary parasitology,* 71**,** 77-97.

DE SOUZA, J. B., HAFALLA, J. C., RILEY, E. M. & COUPER, K. N. 2010. Cerebral malaria: why experimental murine models are required to understand the pathogenesis of disease. *Parasitology,* 137**,** 755-772.

DE SOUZA, J. B. & RILEY, E. M. 2002. Cerebral malaria: the contribution of studies in animal models to our understanding of immunopathogenesis. *Microbes and Infection,* 4**,** 291-300.

DE VILLIERS, L. 2018. *A comparison between manual count, flow cytometry and qPCR as a means of determining Babesia rossi parasitaemia in naturally infected dogs,* Masters thesis, Dept of Companion Animal Clinical Studies, Faculty of Veterinary Science, University of Pretoria.

DE VOS, A., DE WAAL, D. & JACKSON, L. 2004. Bovine babesiosis. In: J.A.W. Coetzer and R.C. Trustin, *Infectious diseases of livestock, Volume One, 2nd edn,* pp.406-424, Oxford University Press.

DEFAUW, P., SCHOEMAN, J. P., LEISEWITZ, A. L., GODDARD, A., DUCHATEAU, L., ARESU, L., MEYER, E. & DAMINET, S. 2020. Evaluation of acute kidney injury in dogs with complicated or uncomplicated Babesia rossi infection. *Ticks and tick-borne diseases,* 11**,** 101406.

© University of Pretoria

DEPOIX, D., CARCY, B., JUMAS-BILAK, E., PAGES, M., PRECIGOUT, E., SCHETTERS, T., RAVEL, C. & GORENFLOT, A. 2002. Chromosome number, genome size and polymorphism of European and South African isolates of large Babesia parasites that infect dogs. *Parasitology,* 125**,** 313-321.

DOROVINI-ZIS, K., SCHMIDT, K., HUYNH, H., FU, W., WHITTEN, R. O., MILNER, D., KAMIZA, S., MOLYNEUX, M. & TAYLOR, T. E. 2011. The neuropathology of fatal cerebral malaria in malawian children. *The American journal of pathology,* 178**,** 2146-2158.

ELSHEIKHA, H. M. & KHAN, N. A. 2010. Protozoa traversal of the blood–brain barrier to invade the central nervous system. *FEMS microbiology reviews,* 34**,** 532-553.

EVERITT, J. I., SHADDUCK, J. A., STEINKAMP, C. & CLABAUGH, G. 1986. Experimental Babesia bovis infection in Holstein calves. *Vet Pathol,* 23**,** 556-62.

FAIRHURST, R. M. & WELLEMS, T. E. 2006. Modulation of malaria virulence by determinants of Plasmodium falciparum erythrocyte membrane protein-1 display. *Current opinion in hematology,* 13**,** 124-130.

FILAN, P. M., INDER, T. E., CAMERON, F. J., KEAN, M. J. & HUNT, R. W. 2006. Neonatal hypoglycemia and occipital cerebral injury. *The Journal of pediatrics,* 148**,** 552-555.

GARMAN, R. H. 2011. Histology of the central nervous system. *Toxicologic pathology,* 39**,** 22-35.

GAZIT, V., BEN-ABRAHAM, R., COLEMAN, R., WEIZMAN, A. & KATZ, Y. 2004. Cysteine-induced hypoglycemic brain damage: an alternative mechanism to excitotoxicity. *Amino Acids,* 26**,** 163-168.

GODDARD, A., LEISEWITZ, A. L., KJELGAARD-HANSEN, M., KRISTENSEN, A. T. & SCHOEMAN, J. P. 2016. Excessive Pro-Inflammatory Serum Cytokine Concentrations in Virulent Canine Babesiosis. *PLoS One,* 11**,** e0150113.

GODDARD, A., LEISEWITZ, A. L., KRISTENSEN, A. T. & SCHOEMAN, J. P. 2015. Platelet indices in dogs with Babesia rossi infection. *Veterinary Clinical Pathology,* 44**,** 493-497.

GODDARD, A., WIINBERG, B., SCHOEMAN, J. P., KRISTENSEN, A. T. & KJELGAARD-HANSEN, M. 2013. Mortality in virulent canine babesiosis is associated with a consumptive coagulopathy. *Vet J,* 196**,** 213-7.

GRAU, G., PIGUET, P., GRETENER, D., VESIN, C. & LAMBERT, P. 1988. Immunopathology of thrombocytopenia in experimental malaria. *Immunology,* 65**,** 501.

GROVES, M., DENNIS, G., AMYX, H. & HUXSOLL, D. 1975. Transmission of Ehrlichia canis to dogs by ticks (Rhipicephalus sanguineus). *American journal of veterinary research,* 36**,** 937-940.

GUPTA, N. K., BANSAL, S. B., JAIN, U. C. & SAHARE, K. 2013. Study of thrombocytopenia in patients of malaria. *Tropical parasitology,* 3**,** 58.

HANSEN, D. S., BERNARD, N. J., NIE, C. Q. & SCHOFIELD, L. 2007. NK cells stimulate recruitment of CXCR3+ T cells to the brain during Plasmodium berghei-mediated cerebral malaria. *The Journal of Immunology,* 178**,** 5779-5788.

HENNING, A., CLIFT, S. J. & LEISEWITZ, A. L. 2020. The pathology of the spleen in lethal canine babesiosis caused by Babesia rossi. *Parasite Immunology,* 42**,** e12706.

HO, M. & WHITE, N. J. 1999. Molecular mechanisms of cytoadherence in malaria. *American Journal of Physiology-Cell Physiology,* 276**,** C1231-C1242.

© University of Pretoria

HOCHMAN, S. E., MADALINE, T. F., WASSMER, S. C., MBALE, E., CHOI, N., SEYDEL, K. B., WHITTEN, R. O., VARUGHESE, J., GRAU, G. E. & KAMIZA, S. 2015. Fatal pediatric cerebral malaria is associated with intravascular monocytes and platelets that are increased with HIV coinfection. *MBio,* 6**,** e01390-15.

HOMER, M. J., AGUILAR-DELFIN, I., TELFORD, S. R., 3RD, KRAUSE, P. J. & PERSING, D. H. 2000. Babesiosis. *Clin Microbiol Rev,* 13**,** 451-69.

HORSTMANN, R. & DIETRICH, M. 1985. Haemostatic alterations in malaria correlate to parasitaemia. *Blut,* 51**,** 329-335.

HORTOBAGYI, T., WISE, S., HUNT, N., CARY, N., DJUROVIC, V., FEGAN-EARL, A., SHORROCK, K., ROUSE, D. & AL-SARRAJ, S. 2007. Traumatic axonal damage in the brain can be detected using β-APP immunohistochemistry within 35 min after head injury to human adults. *Neuropathology and applied neurobiology,* 33**,** 226-237.

HUNT, N. H., GRAU, G. E., ENGWERDA, C., BARNUM, S. R., VAN DER HEYDE, H., HANSEN, D. S., SCHOFIELD, L. & GOLENSER, J. 2010. Murine cerebral malaria: the whole story. *Trends in parasitology,* 26**,** 272-274.

HUTCHINGS, C. L., LI, A., FERNANDEZ, K. M., FLETCHER, T., JACKSON, L. A., MOLLOY, J. B., JORGENSEN, W. K., LIM, C. T. & COOKE, B. M. 2007. New insights into the altered adhesive and mechanical properties of red blood cells parasitized by Babesia bovis. *Molecular microbiology,* 65**,** 1092-1105.

INCE, C., MAYEUX, P. R., NGUYEN, T., GOMEZ, H., KELLUM, J. A., OSPINA-TASCÓN, G. A., HERNANDEZ, G., MURRAY, P. & DE BACKER, D. 2016. The endothelium in sepsis. *Shock (Augusta, Ga.),* 45**,** 259.

IRWIN, P. J. 2009. Canine babesiosis: from molecular taxonomy to control. *Parasit Vectors,* 2 Suppl 1**,** S4.

IRWIN, P. J. 2010. Canine babesiosis. *Vet Clin North Am Small Anim Pract,* 40**,** 1141-56.

JACOBSON, L. S. 2006. The South African form of severe and complicated canine babesiosis: clinical advances 1994-2004. *Vet Parasitol,* 138**,** 126-39.

JACOBSON, L. S. & CLARK, I. A. 1994. The pathophysiology of canine babesiosis: new approaches to an old puzzle. *J S Afr Vet Assoc,* 65**,** 134-45.

KALARIA, R., FERRER, I. & LOVE, S. 2018. Chapter 2 - Vascular disease, hypoxia and related conditions. In: S. Love, A. Perry, J. Ironside and H. Budka (eds), *Greenfield's neuropathology: Volume 1, 9th edn,* pp. 59-209, CRC Press.

KJEMTRUP, A. M. & CONRAD, P. A. 2006. A review of the small canine piroplasms from California: Babesia conradae in the literature. *Veterinary parasitology,* 138**,** 112-117.

KÖSTER, L. S., LOBETTI, R. G. & KELLY, P. 2015. Canine babesiosis: a perspective on clinical complications, biomarkers, and treatment. *Veterinary medicine: research and reports,* 6**,** 119.

KRAUSE, P. J., DAILY, J., TELFORD, S. R., VANNIER, E., LANTOS, P. & SPIELMAN, A. 2007. Shared features in the pathobiology of babesiosis and malaria. *Trends Parasitol,* 23**,** 605-10.

KULES, J., GOTIC, J., MRLJAK, V. & BARIC RAFAJ, R. 2017. Blood markers of fibrinolysis and endothelial activation in canine babesiosis. *BMC Vet Res,* 13**,** 82.

LACKNER, P., BEER, R., HEUSSLER, V., GOEBEL, G., RUDZKI, D., HELBOK, R., TANNICH, E. & SCHMUTZHARD, E. 2006. Behavioural and histopathological

© University of Pretoria

alterations in mice with cerebral malaria. *Neuropathology and applied neurobiology,* 32**,** 177-188.
LAVAN, R., TUNCELI, K., DE SWARDT, H., CHELCHINSKEY, C., ABATZIDIS, M. & ARMSTRONG, R. 2018. Canine babesiosis treatment rates in South African veterinary clinics between 2011 and 2016. *Parasites & vectors,* 11**,** 1-5.
LAWLER, P. R. & LAWLER, J. 2012. Molecular basis for the regulation of angiogenesis by thrombospondin-1 and-2. *Cold Spring Harbor perspectives in medicine,* 2**,** a006627.
LEISEWITZ, A., GODDARD, A., DE GIER, J., VAN ENGELSHOVEN, J., CLIFT, S., THOMPSON, P. & SCHOEMAN, J. P. 2019a. Disease severity and blood cytokine concentrations in dogs with natural Babesia rossi infection. *Parasite immunology,* 41**,** e12630.
LEISEWITZ, A., GUTHRIE, AJ** & BERRY, W. 1996. Evaluation of the effect of whole-blood transfusion on the oxygen status and acid-base balance of Babesia canis infected dogs using the oxygen status algorithm. *Journal of the South African Veterinary Association,* 67**,** 20-26.
LEISEWITZ, A. L., GODDARD, A., CLIFT, S., THOMPSON, P. N., DE GIER, J., VAN ENGELSHOVEN, J. M. & SCHOEMAN, J. P. 2019b. A clinical and pathological description of 320 cases of naturally acquired Babesia rossi infection in dogs. *Veterinary parasitology,* 271**,** 22-30.
LEVINE, N. D. 1988. *The protozoan phylum Apicomplexa. Volume I. Volume II*, CRC Press, Inc.
LIMA, M. N., FREITAS, R. J., PASSOS, B. A., DARZE, A. M. G., CASTRO-FARIA-NETO, H. C. & MARON-GUTIERREZ, T. 2021. Neurovascular interactions in malaria. *Neuroimmunomodulation,* 28**,** 108-117.
LOU, J., LUCAS, R. & GRAU, G. E. 2001. Pathogenesis of cerebral malaria: recent experimental data and possible applications for humans. *Clinical microbiology reviews,* 14**,** 810-820.
MA, N., MADIGAN, M. C., CHAN-LING, T. & HUNT, N. H. 1997. Compromised blood-nerve barrier, astrogliosis, and myelin disruption in optic nerves during fatal murine cerebral malaria. *Glia,* 19**,** 135-151.
MACPHERSON, G., WARRELL, M., WHITE, N., LOOAREESUWAN, S. & WARRELL, D. 1985. Human cerebral malaria. A quantitative ultrastructural analysis of parasitized erythrocyte sequestration. *The American journal of pathology,* 119**,** 385.
MADDER, M., THYS, E., ACHI, L., TOURÉ, A. & DE DEKEN, R. 2011. Rhipicephalus (Boophilus) microplus: a most successful invasive tick species in West-Africa. *Experimental and Applied Acarology,* 53**,** 139-145.
MAEGRAITH, B., GILLES, H. & DEVAKUL, K. 1957. Pathological Processes in Babesia canis Infections. *Zeitschrift fur Tropenmedizin und Parasitologie,* 8**,** 485-514.
MAIER, A. G., COOKE, B. M., COWMAN, A. F. & TILLEY, L. 2009. Malaria parasite proteins that remodel the host erythrocyte. *Nature Reviews Microbiology,* 7**,** 341-354.
MALHERBE, W. 1956. The manifestations and diagnosis of Babesia infections. *Annals of the New York Academy of Sciences,* 64**,** 128-146.
MALHERBE, W. & PARKIN, B. 1951. Atypical symptomatology in Babesia canis infection. *Journal of the South African Veterinary Association,* 22**,** 25-36.
MANEERAT, Y., VIRIYAVEJAKUL, P., PUNPOOWONG, B., JONES, M., WILAIRATANA, P., PONGPONRATN, E., TURNER, G. & UDOMSANGPETCH,

© University of Pretoria

R. 2000. Inducible nitric oxide synthase expression is increased in the brain in fatal cerebral malaria. *Histopathology,* 37**,** 269-277.

MARTIN, C. A. 2020. *Pathology of complicated Babesia rossi-associated acute lung injury and respiratory distress syndrome in dogs,* Masters thesis, Dept of Paraclinical Sciences, Faculty of Veterinary Science, University of Pretoria.

MATJILA, P., PENZHORN, B., BEKKER, C., NIJHOF, A. & JONGEJAN, F. 2004. Confirmation of occurrence of Babesia canis vogeli in domestic dogs in South Africa. *Veterinary Parasitology,* 122**,** 119-125.

MATJILA, P. T., CARCY, B., LEISEWITZ, A. L., SCHETTERS, T., JONGEJAN, F., GORENFLOT, A. & PENZHORN, B. L. 2009. Preliminary evaluation of the BrEMA1 gene as a tool for associating babesia rossi genotypes and clinical manifestation of canine Babesiosis. *J Clin Microbiol,* 47**,** 3586-92.

MATJILA, P. T., LEISEWITZ, A. L., JONGEJAN, F. & PENZHORN, B. L. 2008. Molecular detection of tick-borne protozoal and ehrlichial infections in domestic dogs in South Africa. *Veterinary parasitology,* 155**,** 152-157.

MCCALL, M. B. & SAUERWEIN, R. W. 2010. Interferon-γ—central mediator of protective immune responses against the pre-erythrocytic and blood stage of malaria. *Journal of leukocyte biology,* 88**,** 1131-1143.

MEDANA, I. M., CHAUDHRI, G., CHAN-LING, T. & HUNT, N. H. 2001. Central nervous system in cerebral malaria:'Innocent bystander'or active participant in the induction of immunopathology? *Immunology and cell biology,* 79**,** 101-120.

MEDANA, I. M., DAY, N. P., HIEN, T. T., MAI, N. T. H., BETHELL, D., PHU, N. H., FARRAR, J., ESIRI, M. M., WHITE, N. J. & TURNER, G. D. 2002. Axonal injury in cerebral malaria. *The American journal of pathology,* 160**,** 655-666.

MEDANA, I. M., DAY, N. P., SACHANONTA, N., MAI, N. T., DONDORP, A. M., PONGPONRATN, E., HIEN, T. T., WHITE, N. J. & TURNER, G. D. 2011. Coma in fatal adult human malaria is not caused by cerebral oedema. *Malaria journal,* 10**,** 1-14.

MEDANA, I. M. & TURNER, G. D. 2006. Human cerebral malaria and the blood–brain barrier. *International journal for parasitology,* 36**,** 555-568.

MEHLHORN, H. & SCHEIN, E. 1985. The piroplasms: life cycle and sexual stages. *Advances in parasitology,* 23**,** 37-103.

MILLER, L. H., BARUCH, D. I., MARSH, K. & DOUMBO, O. K. 2002. The pathogenic basis of malaria. *Nature,* 415**,** 673-679.

MILLER, M. A. & ZACHARY, J. F. 2017. Chapter 1 - Mechanisms and Morphology of Cellular Injury, Adaptation, and Death. *Pathologic Basis of Veterinary Disease (Sixth Edition).* Mosby.

MILNER, D. A. 2018. Malaria pathogenesis. *Cold Spring Harbor perspectives in medicine,* 8**,** a025569.

MILNER JR, D. A., WHITTEN, R. O., KAMIZA, S., CARR, R., LIOMBA, G., DZAMALALA, C., SEYDEL, K. B., MOLYNEUX, M. E. & TAYLOR, T. E. 2014. The systemic pathology of cerebral malaria in African children. *Frontiers in cellular and infection microbiology,* 4.

MIU, J., MITCHELL, A. J., MÜLLER, M., CARTER, S. L., MANDERS, P. M., MCQUILLAN, J. A., SAUNDERS, B. M., BALL, H. J., LU, B. & CAMPBELL, I. L. 2008. Chemokine gene expression during fatal murine cerebral malaria and protection due to CXCR3 deficiency. *The Journal of Immunology,* 180**,** 1217-1230.

© University of Pretoria

MONROE, A., WILLIAMS, N. A., OGOMA, S., KAREMA, C. & OKUMU, F. 2022. Reflections on the 2021 World Malaria Report and the future of malaria control. Springer.

MOORE, D. & WILLIAMS, M. 1979. Disseminated intravascular coagulation: a complication of Babesia canis infection in the dog. *Journal of the South African Veterinary Association,* 50**,** 265-275.

MOSIER, D. A. 2017. Chapter 2 - Vascular Disorders and Thrombosis. In: J. F. Zachary (ed), *Pathologic Basis of Veterinary Disease (Sixth Edition),* pp. 44-72, Mosby.

MOTA, M. M., PRADEL, G., VANDERBERG, J. P., HAFALLA, J. C., FREVERT, U., NUSSENZWEIG, R. S., NUSSENZWEIG, V. & RODRíGUEZ, A. 2001. Migration of Plasmodium sporozoites through cells before infection. *Science,* 291**,** 141-144.

MOXON, C. A., GIBBINS, M. P., MCGUINNESS, D., MILNER JR, D. A. & MARTI, M. 2020. New insights into malaria pathogenesis. *Annual Review of Pathology: Mechanisms of Disease,* 15**,** 315-343.

MUHLNICKEL, C. J., JEFFERIES, R., MORGAN-RYAN, U. M. & IRWIN, P. J. 2002. Babesia gibsoni infection in three dogs in Victoria. *Australian Veterinary Journal,* 80**,** 606-610.

NEL, M., LOBETTI, R. G., KELLER, N. & THOMPSON, P. N. 2004. Prognostic value of blood lactate, blood glucose, and hematocrit in canine babesiosis. *J Vet Intern Med,* 18**,** 471-6.

NEWTON, C. R., HIEN, T. T. & WHITE, N. 2000. Cerebral malaria. *Journal of Neurology, Neurosurgery & Psychiatry,* 69**,** 433-441.

NIJHOF, A. M., PENZHORN, B. L., LYNEN, G., MOLLEL, J. O., MORKEL, P., BEKKER, C. P. & JONGEJAN, F. 2003. Babesia bicornis sp. nov. and Theileria bicornis sp. nov.: tick-borne parasites associated with mortality in the black rhinoceros (Diceros bicornis). *Journal of Clinical microbiology,* 41**,** 2249-2254.

NISHANTH, G. & SCHLÜTER, D. 2019. Blood–brain barrier in cerebral malaria: pathogenesis and therapeutic intervention. *Trends in parasitology,* 35**,** 516-528.

NYANGIWE, N., HORAK, I. G., VAN DER MESCHT, L. & MATTHEE, S. 2017. Range expansion of the economically important Asiatic blue tick, Rhipicephalus microplus, in South Africa. *Journal of the South African Veterinary Association,* 88**,** 1-7.

O'CONNOR, R. M., LONG, J. A. & ALLRED, D. R. 1999. Cytoadherence of Babesia bovis-infected erythrocytes to bovine brain capillary endothelial cells provides an in vitro model for sequestration. *Infect Immun,* 67**,** 3921-8.

OAKLEY, M. S., GERALD, N., MCCUTCHAN, T. F., ARAVIND, L. & KUMAR, S. 2011. Clinical and molecular aspects of malaria fever. *Trends in parasitology,* 27**,** 442-449.

OCKENHOUSE, C. F., TEGOSHI, T., MAENO, Y., BENJAMIN, C., HO, M., KAN, K. E., THWAY, Y., WIN, K., AIKAWA, M. & LOBB, R. R. 1992. Human vascular endothelial cell adhesion receptors for Plasmodium falciparum-infected erythrocytes: roles for endothelial leukocyte adhesion molecule 1 and vascular cell adhesion molecule 1. *The Journal of experimental medicine,* 176**,** 1183-1189.

OKOH, A. E. 1978. A case of cerebral babesiosis in the dog. *Bull Anim Health Prod Afr,* 26**,** 118-9.

OOSTHUIZEN, M. C., ALLSOPP, B. A., TROSKIE, M., COLLINS, N. E. & PENZHORN, B. L. 2009. Identification of novel Babesia and Theileria species in

© University of Pretoria

South African giraffe (Giraffa camelopardalis, Linnaeus, 1758) and roan antelope (Hippotragus equinus, Desmarest 1804). *Veterinary parasitology,* 163**,** 39-46.

PAIS, T. F. & PENHA-GONÇALVES, C. 2019. Brain endothelium: the "innate immunity response hypothesis" in cerebral malaria pathogenesis. *Frontiers in immunology,* 9**,** 3100.

PARDINI, A. D. 2010. *The pathology and pathogenesis of canine cerebral babesiosis,* Masters thesis, Dept of Paraclinical Sciences, Faculty of Veterinary Science, University of Pretoria.

PARRODI, F., WRIGHT, I., BOURNE, A. & DOBSON, C. 1989. In vitro adherence of bovine erythrocytes infected with Babesia bovis to thrombospondin and laminin. *International journal for parasitology,* 19**,** 567-569.

PATARROYO, J. H., VARGAS, M. I. & BICUDO, P. L. 1982. Description of lesions in cattle in a natural outbreak of Babesia bovis infection in Brazil. *Vet Parasitol,* 11**,** 301-8.

PENET, M.-F., VIOLA, A., CONFORT-GOUNY, S., LE FUR, Y., DUHAMEL, G., KOBER, F., IBARROLA, D., IZQUIERDO, M., COLTEL, N. & GHARIB, B. 2005. Imaging experimental cerebral malaria in vivo: significant role of ischemic brain edema. *Journal of Neuroscience,* 25**,** 7352-7358.

PENZHORN, B. L. 2011. Why is Southern African canine babesiosis so virulent? An evolutionary perspective. *Parasit Vectors,* 4**,** 51.

PENZHORN, B. L. 2020. Don't let sleeping dogs lie: unravelling the identity and taxonomy of Babesia canis, Babesia rossi and Babesia vogeli. *Parasites & vectors,* 13**,** 1-9.

PENZHORN, B. L., KJEMTRUP, A. M., LÓPEZ-REBOLLAR, L. M. & CONRAD, P. A. 2001. Babesia leo n. sp. from lions in the Kruger National Park, South Africa, and its relation to other small piroplasms. *Journal of Parasitology,* 87**,** 681-685.

PENZHORN, B. L., VORSTER, I., HARRISON-WHITE, R. F. & OOSTHUIZEN, M. C. 2017. Black-backed jackals (Canis mesomelas) are natural hosts of Babesia rossi, the virulent causative agent of canine babesiosis in sub-Saharan Africa. *Parasit Vectors,* 10**,** 124.

PIERCY, S. 1947. Hyper-acute canine babesia (tick fever). *The Veterinary record,* 59**,** 612.

PONSFORD, M. J., MEDANA, I. M., PRAPANSILP, P., HIEN, T. T., LEE, S. J., DONDORP, A. M., ESIRI, M. M., DAY, N. P., WHITE, N. J. & TURNER, G. D. 2012. Sequestration and microvascular congestion are associated with coma in human cerebral malaria. *Journal of Infectious Diseases,* 205**,** 663-671.

PURCHASE, H. S. 1947. Cerebral babesiosis in dogs. *Vet Rec,* 59**,** 269.

RAUTENBACH, Y., GODDARD, A., THOMPSON, P. N., MELLANBY, R. J. & LEISEWITZ, A. L. 2017. A flow cytometric assessment of the lymphocyte immunophenotypes in dogs naturally infected with Babesia rossi. *Veterinary parasitology,* 241**,** 26-34.

REES, P. & SCHOEMAN, J. P. 2008. Plasma insulin concentrations in hypoglycaemic dogs with Babesia canis rossi infection. *Veterinary parasitology,* 152**,** 60-66.

REYERS, F., LEISEWITZ, A. L., LOBETTI, R. G., MILNER, R. J., JACOBSON, L. S. & VAN ZYL, M. 1998. Canine babesiosis in South Africa: more than one disease. Does this serve as a model for falciparum malaria? *Ann Trop Med Parasitol,* 92**,** 503-11.

ROBERTS, D. D., SHERWOOD, J. A., SPITALNIK, S. L., PANTON, L. J., HOWARD, R. J., DIXIT, V. M., FRAZIER, W. A., MILLER, L. H. & GINSBURG, V. 1985.

© University of Pretoria

Thrombospondin binds falciparum malaria parasitized erythrocytes and may mediate cytoadherence. *Nature,* 318**,** 64-66.

ROGERS, R. J. 1971. Observations on the pathology of babesia argentina infections in cattle. *Aust Vet J,* 47**,** 242-7.

ROWE, J. A., MOULDS, J. M., NEWBOLD, C. I. & MILLER, L. H. 1997. P. falciparum rosetting mediated by a parasite-variant erythrocyte membrane protein and complement-receptor 1. *Nature,* 388**,** 292-295.

ROZANCE, P. J. & HAY, W. W. 2006. Hypoglycemia in newborn infants: features associated with adverse outcomes. *Neonatology,* 90**,** 74-86.

SCHEEPERS, E., LEISEWITZ, A. L., THOMPSON, P. N. & CHRISTOPHER, M. M. 2011. Serial haematology results in transfused and non-transfused dogs naturally infected with Babesia rossi. *Journal of the South African Veterinary Association,* 82**,** 136-143.

SCHETTERS, T. P. & ELING, W. 1999. Can Babesia infections be used as a model for cerebral malaria? *Parasitology today,* 15**,** 492-497.

SCHOEMAN, J. P. 2009. Canine babesiosis. *Onderstepoort J Vet Res,* 76**,** 59-66.

SCHOEMAN, J. P. & HERRTAGE, M. E. 2007a. The response of the pituitary-adrenal and pituitary-thyroidal axes to the plasma glucose perturbations in Babesia canis rossi babesiosis. *J S Afr Vet Assoc,* 78**,** 215-20.

SCHOEMAN, J. P. & HERRTAGE, M. E. 2007b. The response of the pituitary-adrenal and pituitary-thyroidal axes to the plasma glucose perturbations in Babesia canis rossi babesiosis. *Journal of the South African Veterinary Association,* 78**,** 215-220.

SEYDEL, K. B., KAMPONDENI, S. D., VALIM, C., POTCHEN, M. J., MILNER, D. A., MUWALO, F. W., BIRBECK, G. L., BRADLEY, W. G., FOX, L. L. & GLOVER, S. J. 2015. Brain swelling and death in children with cerebral malaria. *New England Journal of Medicine,* 372**,** 1126-1137.

SHABANGU, N., PENZHORN, B. L., OOSTHUIZEN, M. C., VORSTER, I., VAN SCHALKWYK, O. L., HARRISON-WHITE, R. F. & MATJILA, P. T. 2021. A shared pathogen: Babesia rossi in domestic dogs, black-backed jackals (Canis mesomelas) and African wild dogs (Lycaon pictus) in South Africa. *Veterinary Parasitology,* 291**,** 109381.

SHORTT, H. 1973. Babesia canis: the life cycle and laboratory maintenance in its arthropod and mammalian hosts. *International Journal for Parasitology,* 3**,** 119-148.

SMITH, J. D., ROWE, J. A., HIGGINS, M. K. & LAVSTSEN, T. 2013. Malaria's deadly grip: cytoadhesion of P lasmodium falciparum-infected erythrocytes. *Cellular microbiology,* 15**,** 1976-1983.

SNOW, R. W. 2015. Global malaria eradication and the importance of Plasmodium falciparum epidemiology in Africa. *BMC Medicine,* 13**,** 23.

STROBL, A., KÜNZEL, F., TICHY, A. & LESCHNIK, M. 2020. Complications and risk factors regarding the outcomes of canine babesiosis in Central Europe–A retrospective analysis of 240 cases. *Acta Veterinaria Hungarica,* 68**,** 160-168.

SUVARNA, S. & LAYTON, C. 2018. *Bancroft's theory and practice of histological techniques, 7th edn. Churchill Livingstone Elsevier*, Oxford.

SZKLARCZYK, A., STINS, M., MILWARD, E., RYU, H., FITZSIMMONS, C., SULLIVAN, D. & CONANT, K. 2007. Glial activation and matrix metalloproteinase release in cerebral malaria. *Journal of neurovirology,* 13**,** 2-10.

© University of Pretoria

TAYLOR, D. W., PARRA, M., CHAPMAN, G. B., STEARNS, M. E., RENER, J., AIKAWA, M., UNI, S., ALEY, S. B., PANTON, L. J. & HOWARD, R. J. 1987. Localization of Plasmodium falciparum histidine-rich protein 1 in the erythrocyte skeleton under knobs. *Molecular and biochemical parasitology,* 25**,** 165-174.

TAYLOR, T. E., FU, W. J., CARR, R. A., WHITTEN, R. O., MUELLER, J. G., FOSIKO, N. G., LEWALLEN, S., LIOMBA, N. G. & MOLYNEUX, M. E. 2004. Differentiating the pathologies of cerebral malaria by postmortem parasite counts. *Nature medicine,* 10**,** 143-145.

TOMITA, N., NAKAMURA, T., SUNDEN, Y., MIYATA, H. & MORITA, T. 2020. Temporal analysis of histopathology and cytokine expression in the rat cerebral cortex after insulin-induced hypoglycemia. *Neuropathology,* 40**,** 240-250.

TØNNESEN, M., PENZHORN, B., BRYSON, N., STOLTSZ, W. & MASIBIGIRI, T. 2004. Displacement of Boophilus decoloratus by Boophilus microplus in the Soutpansberg region, Limpopo province, South Africa. *Experimental & applied acarology,* 32**,** 199-208.

TRIVEDI, S. & CHAKRAVARTY, A. 2022. Neurological Complications of Malaria. *Current Neurology and Neuroscience Reports***,** 1-15.

TUNON-ORTIZ, A. & LAMB, T. J. 2019. Blood brain barrier disruption in cerebral malaria: Beyond endothelial cell activation. *PLoS Pathogens,* 15**,** e1007786.

TURNER, G. 1997. Cerebral malaria. *Brain Pathology,* 7**,** 569-582.

TURNER, G. D., MORRISON, H., JONES, M., DAVIS, T. M., LOOAREESUWAN, S., BULEY, I. D., GATTER, K. C., NEWBOLD, C. I., PUKRITAYAKAMEE, S. & NAGACHINTA, B. 1994. An immunohistochemical study of the pathology of fatal malaria: evidence for widespread endothelial activation and a potential role for intercellular adhesion molecule-1 in cerebral sequestration. *The American journal of pathology,* 145**,** 1057.

UDOMSANGPETCH, R., AIKAWA, M., BERZINS, K., WAHLGREN, M. & PERLMANN, P. 1989. Cytoadherence of knobless Plasmodium falciparum-infected erythrocytes and its inhibition by a human monoclonal antibody. *Nature,* 338**,** 763-765.

UILENBERG, G. 2006. Babesia—a historical overview. *Veterinary parasitology,* 138**,** 3-10.

UILENBERG, G., FRANSSEN, F., PERIE, N. & SPANJER, A. 1989. Three groups of Babesia canis distinguished and a proposal for nomenclature. *Veterinary Quarterly,* 11**,** 33-40.

USMANI-BROWN, S., HALPERIN, J. J. & KRAUSE, P. J. 2013. Neurological manifestations of human babesiosis. *Handb Clin Neurol,* 114**,** 199-203.

WASSMER, S. C., TAYLOR, T., MACLENNAN, C. A., KANJALA, M., MUKAKA, M., MOLYNEUX, M. E. & GRAU, G. E. 2008. Platelet-induced clumping of Plasmodium falciparum-infected erythrocytes from Malawian patients with cerebral malaria—possible modulation in vivo by thrombocytopenia. *The Journal of infectious diseases,* 197**,** 72-78.

WELZL, C., LEISEWITZ, A., JACOBSON, L., VAUGHAN-SCOTT, T. & MYBURGH, E. 2001. Systemic inflammatory response syndrome and multiple-organ damage/dysfunction in complicated canine babesiosis. *Journal of the South African Veterinary Association,* 72**,** 158-162.

WHITE, N. J. & ASHLEY, E. A. 2022. Chapter 224 - Malaria. In*:* LOSCALZO, J., FAUCI, A., KASPER, D., HAUSER, S., LONGO, D. & JAMESON, J. L. (eds.) *Harrison's Principles of Internal Medicine, 21st edn,* New York, NY: McGraw-Hill Education.

© University of Pretoria

WINKLER, S., WILLHEIM, M., BAIER, K., SCHMID, D., AICHELBURG, A., GRANINGER, W. & KREMSNER, P. 1999. Frequency of cytokine-producing T cells in patients of different age groups with Plasmodium falciparum malaria. *The Journal of infectious diseases,* 179**,** 209-216.

WRIGHT, I., GOODGER, B. & CLARK, I. 1988. Immunopathophysiology of Babesia bovis and Plasmodium falciparum infections. *Parasitology Today,* 4**,** 214-218.

YONG, A. W., MORRIS, Z., SHULER, K., SMITH, C. & WARDLAW, J. 2012. Acute symptomatic hypoglycaemia mimicking ischaemic stroke on imaging: a systemic review. *Bmc neurology,* 12**,** 1-12.

ZAHLER, M., SCHEIN, E., RINDER, H. & GOTHE, R. 1998. Characteristic genotypes discriminate between Babesia canis isolates of differing vector specificity and pathogenicity to dogs. *Parasitology Research,* 84**,** 544-548.

ZINTL, A., MULCAHY, G., SKERRETT, H. E., TAYLOR, S. M. & GRAY, J. S. 2003. Babesia divergens, a bovine blood parasite of veterinary and zoonotic importance. *Clinical microbiology reviews,* 16**,** 622-636.

© University of Pretoria

APPENDICES

Appendix A: Check sheet template and abbreviations used on check sheets

APPENDIX A

CCB -APPENDIX HISTOPATHOLOGY DATASHEET

TEMPLATE

Criteria	S-number:										Comments
Signalment											
Hx of nervous signs (absent / Present)											
RT-qPCR results (2017 cases)											
Brain histopathology											**Score**
Autolysis	☐ Absent	☐ Mild	☐ Moderate	☐ Severe							
Microscopic lesions present?	☐ Absent	☐ Present									
Lesion distribution (histological)	☐ Absent	☐ Focal	☐ Multifocal	☐ Coalescing	☐ Diffuse						
		☐ Grey matter	☐ White matter	☐ Mixed							
		☐ Deep sulci	☐ Superficial sulci	☐ Undetermined							
Haemorrhage	☐ Absent	☐ Petechiae	☐ Ecchymoses	☐ Suffusive	☐ Ring haemorrhages						
Vasculitis	Inflammatory cellular infiltrate (types of cells), severity and distribution, as identified on HE		Absent = A; Intralesional = IL; Perilesional = PL; Extralesional = EL								
			Mononuclear (MN) ☐	☐ Mild (1)	☐ Moderate (2)	☐ Severe (3)	☐ IL	☐ PL	☐ EL		
			Neutrophils A (0) ☐	☐ Mild (1)	☐ Moderate (2)	☐ Severe (3)	☐ IL	☐ PL	☐ EL		
	Type of vasculitis		☐ Necrotising	☐ Fibrinoid	☐ Necrotic debris						
			☐ Inflammatory	☐ Perivascular	☐ Vascular wall	☐ Intravascular					
	Vascular necrosis		☐ Absent (0)	☐ Wall intact (1)	☐ Wall partially intact (2)	☐ Wall not intact (dissolution) (3)	☐ IL	☐ PL	☐ EL		
	Fibrin	HE	☐ Absent (0)	☐ Present (1)							
		MSB	☐ Absent (0)	☐ Perivascular	☐ Vascular wall	☐ Intravascular	☐ Mixed				
				☐ Mild (1)	☐ Moderate (2)	☐ Severe (3)	☐ IL	☐ PL	☐ EL		
	Thrombi	☐ Absent (0)	☐ Mild (1)	☐ Moderate (2)	☐ Severe (3)	☐ White matter	☐ Grey matter	☐ Meninges			
			☐ Mononuclear	☐ Neutrophils			☐ IL	☐ PL	☐ EL		
	Endothelial cell	Hypertrophy	☐ Absent (0)	☐ Mild (1)	☐ Moderate (2)	☐ Severe (3)					
	IMP	CD3	☐ Absent (0)	☐ Mild (1)	☐ Moderate (2)	☐ Severe (3)	☐ IL	☐ PL	☐ EL		
			Enter details on distribution wrt vasculature, eg. Perivascular, intravascular, vascular wall								
		CD20	☐ Absent (0)	☐ Mild (1)	☐ Moderate (2)	☐ Severe (3)	☐ IL	☐ PL	☐ EL		
			Enter details on distribution wrt vasculature, eg. Perivascular, intravascular, vascular wall								
		MAC387	☐ Absent (0)	☐ Mild (1)	☐ Moderate (2)	☐ Severe (3)	☐ IL	☐ PL	☐ EL		
			Enter details on distribution wrt vasculature, eg. Perivascular, intravascular, vascular wall								
		IBA-1	☐ Absent (0)	☐ Mild (1)	☐ Moderate (2)	☐ Severe (3)	☐ IL	☐ PL	☐ EL		
			Enter details on distribution wrt vasculature, eg. Perivascular, intravascular, vascular wall								
		VCAM1	☐ Absent (0)	☐ Mild (1)	☐ Moderate (2)	☐ Severe (3)	☐ IL	☐ PL	☐ EL		
			Enter details on distribution wrt vasculature, eg. Perivascular, intravascular, vascular wall								
Leucostasis	☐ Absent (0)	White matter	☐ Mild (1)	☐ Moderate (2)	☐ Severe (3)	☐ Mononuclear	☐ Neutrophils		☐ IL	☐ PL	☐ EL	
		Grey matter	☐ Mild (1)	☐ Moderate (2)	☐ Severe (3)	☐ Mononuclear	☐ Neutrophils		☐ IL	☐ PL	☐ EL	
		Meninges	☐ Mild (1)	☐ Moderate (2)	☐ Severe (3)	☐ Mononuclear	☐ Neutrophils		☐ IL	☐ PL	☐ EL	
Oedema	Vasogenic	☐ Absent (0)	☐ Mild (1)	☐ Moderate (2)	☐ Severe (3)				☐ IL	☐ PL	☐ EL	
	Cytotoxic	☐ Absent (0)	☐ Present (1)						☐ IL	☐ PL	☐ EL	
Congestion	☐ Absent (0)	☐ Present (1)									
Parasitaemia (use oil)	Degree of parasitaemia (intravascular)	☐ Absent (0)	☐ Low number (1)	☐ Moderate number (2)	☐ High number (3)						
	pRBC aggregates in capillaries	☐ Absent (0)	☐ Present (1)						☐ IL	☐ PL	☐ EL	

© University of Pretoria

APPENDIX A

CCB -APPENDIX HISTOPATHOLOGY DATASHEET
TEMPLATE

Neuronal and neuropil changes	Neuronal injury	☐ Absent	☐ Present				☐ IL	☐ PL	☐ EL	
	Neurophagia	☐ Absent	☐ Present				☐ IL	☐ PL	☐ EL	
	Neuropil inflammatory cellular infiltration (HE)	Mononuclear	☐ Absent (0)	☐ Scant (1)	☐ Obvious (2)		☐ IL	☐ PL	☐ EL	
		Neutrophils	☐ Absent (0)	☐ Scant (1)	☐ Obvious (2)		☐ IL	☐ PL	☐ EL	
	IMP	CD3	☐ Absent (0)	☐ Mild (1)	☐ Moderate (2)	☐ Severe (3)	☐ IL	☐ PL	☐ EL	
		CD20	☐ Absent (0)	☐ Mild (1)	☐ Moderate (2)	☐ Severe (3)	☐ IL	☐ PL	☐ EL	
		MAC387	☐ Absent (0)	☐ Mild (1)	☐ Moderate (2)	☐ Severe (3)	☐ IL	☐ PL	☐ EL	
		IBA-1	☐ Absent (0)	☐ Mild (1)	☐ Moderate (2)	☐ Severe (3)	☐ IL	☐ PL	☐ EL	
Spongiosis	☐ Absent (0)	Distribution	☐ Grey matter	☐ White matter	☐ Mixed		☐ IL	☐ PL	☐ EL	
		Demyelination (LFB)	☐ Mild (1)	☐ Moderate (2)	☐ Severe (3)		☐ IL	☐ PL	☐ EL	
			☐ Primary	☐ Secondary			☐ IL	☐ PL	☐ EL	
IMP in association with lesions	CD3	☐ Absent (0)	☐ Intact vasculature (yes/no)	☐ Haemorrhage (yes/no)	☐ Myelin damage (yes/no) *link with LFB	☐ Axonal damage (yes/no)	☐ IL	☐ PL	☐ EL	
	CD20	☐ Absent (0)	☐ Intact vasculature (yes/no)	☐ Haemorrhage (yes/no)	☐ Myelin damage (yes/no) *link with LFB	☐ Axonal damage (yes/no)	☐ IL	☐ PL	☐ EL	
	IBA-1	☐ Absent (0)	☐ Phagocytosed Babesia parasites (yes/no)	☐ Haemorrhage (yes/no)	☐ Leucostasis (yes/no)		☐ IL	☐ PL	☐ EL	
	MAC387	☐ Absent (0)	☐ Acute lesion/s (define "acute lesions")	☐ Haemorrhage (yes/no)	☐ Longer-standing / sub-acute lesion/s (define)	☐ Chronic lesion/s (define)	☐ IL	☐ PL	☐ EL	
	VCAM-1	☐ Absent (0)	☐ Intact vasculature (yes/no)	☐ Haemorrhage (yes/no)	☐ Myelin damage (yes/no) *link with LFB	☐ Axonal damage (yes/no)	☐ IL	☐ PL	☐ EL	

ADDITIONAL NOTES

Do Von Kossa's? ☐ Yes ☐ No
Do Smooth muscle actin (SMA)* ☐ Yes ☐ No

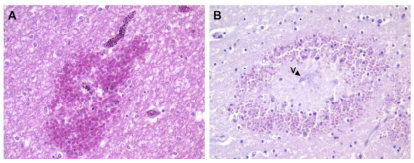
Total scores:
Haemorrhage and IMP (descriptive)
Inflammation (max = 34)
Neuronal changes (max = 3)
Vasculature (max =16)
Global changes (max = 18)
[TOTAL 71]

© University of Pretoria

Appendix B: Histopathology grading and scoring criteria

PARAMETER	GRADING/ SCORE	CRITERIA
AUTOLYSIS		
Severity	Mild	Anatomical architecture easily distinguishable, cellular morphology well-defined.
	Moderate	Anatomical architecture still easily distinguishable, cellular morphology not well-defined, red blood cells still preserved, small numbers of putrefactive (Clostridial) bacteria may be present in some fields.
	Severe	Cellular morphology cannot be defined, anatomical architecture barely distinguishable, red blood cells lysed and difficult to identify, numerous putrefactive (Clostridial) bacteria present.
HISTOPATHOLOGY	(All changes in comparison with normal control brain).	
Lesion definition: Haemorrhage with or without spongiosis and/or malacia. Score and describe the WORST lesion/s per area or histological change.		
Microscopic lesions	Absent	No evidence of microscopic lesions when scanning on 40x and 100x magnification.
	Present	Evidence of microscopic lesions, regardless of severity or distribution.
Lesion distribution (histologic) *Note: macroscopic distribution (see discussion) will be based on A. Pardini's thesis; use full set wax blocks to check macro and describe. Scanned all blocks that were chosen based on macro lesions. Chose block with worst lesions (haemorrhage).*	Absent Focal Multifocal Coalescing Diffuse	No evidence of microscopic lesions. Single well circumscribed area affected. Multiple non-overlapping areas affected Multiple overlapping areas affected. Entire section of tissue OR all specific anatomical sites affected
General distribution of pathological changes wrt lesion	Intralesional (IL)	Predominantly (>50%) present within the lesion.
	Perilesional (PL)	Predominantly (>50%) present at the edge of the lesion.
	Extralesional (EL)	Predominantly (>50%) present away from the lesion.
Grey versus white matter	Grey matter White matter Mixed	>50% of the lesions are in the grey matter. >50% of the lesions are in the white matter. Distribution between the grey and white matter varies to the extent that neither is dominant.
Anatomical distribution	Deep sulci	Majority of the lesion/s present occur in the deeper half of the sulci.
	Superficial sulci	Majority of the lesion/s present occur in the superficial half of the sulci.
	Undetermined	The anatomical location was unclear or no predominant area wrt sulci.

© University of Pretoria

Haemorrhage= Extravasated erythrocytes (Ponsford et al., 2012, Medana and Turner, 2006) Petechiae Ring haemorrhage 	Absent (0) Petechiae Ecchymoses Suffusive Ring haemorrhages	No evidence of haemorrhage. Extravasated erythrocytes are restricted to less than one half of the approximate diameter of the cerebellar molecular layer (1-2mm in diameter). Extravasated erythrocytes fill up between one half and the full approximate diameter of the cerebellar molecular layer (up to 2-3cm in diameter). Extravasated erythrocytes fill up more than the full approximate diameter of the cerebellar molecular layer (larger than 3cm in diameter, notable macroscopically). Vasocentric haemorrhages which surround a central small to medium sized blood vessel, surrounded by a zone of clearing (and astroglial response). There is an outer zone of erythrocytes and leucocytes which have been extravasated from the ruptured vessel. May contain fibrin platelet thrombi in the vascular lumen.
Vasculitis –cellular infiltration and severity (see annotation*). Purpose is to try and identify the inflammatory cell type/s based on HE morphology, but IMP will follow for clarity. (400 x magnification, when checking at least 3 FOV)	Absent (0) Mild (1) Moderate (2) Severe (3) Mononuclear Neutrophils	No evidence of inflammatory cell infiltrate. Single leucocytes present within (intramural) or surrounding the vascular wall, without notable expansion of the blood vessel wall/s; 1/4 of vessel walls affected. One layer of leucocytes present within the vascular wall (intramural), resulting in slight expansion of the vascular wall. 2/4 of vessel walls affected. More than one layer of leucocytes present within the vascular wall (intramural), resulting in marked expansion of the vascular wall. 3/4 to whole of vessel walls affected. Lymphocytes (T or B), plasma cells, monocytes or macrophages predominate. Neutrophils predominate and are distinguished from other granulocytes (eosinophils, mast cells or basophils) based on histomorphology.
Vasculitis – type (400 x magnification, when checking at least 3 FOV)	Absent Necrotising Inflammatory	No evidence of inflammatory cell infiltrate associated with the vessel walls. Smudged eosinophilia (**fibrinoid**) change to the vessel walls. Smudged eosinophilia (fibrinoid) with evidence of **necrotic debris**, loss of detail and crispness, endothelial nuclei pycnotic, swollen or absent. Predominantly inflammatory infiltration, without evidence of necrotising changes (see vasculitis distribution below).
Vasculitis – distribution (iro vascular wall) *See leucostasis.*	Absent Perivascular Intravascular	No evidence of inflammatory cell infiltrate associated with the vessel walls. Inflammation predominantly (>50%) present in perivascular areas **(see annotation*).** Inflammation predominantly (>50%) present within the vessel walls **(see annotation*).**
Vascular necrosis	Absent (0) Wall intact (1) Wall partially intact (2)	No evidence of vessel wall changes. Homogenous eosinophilia and rarefaction of vessel walls, but vascular wall remains intact. Homogenous eosinophilia and rarefaction of vessel walls, with loss of vascular wall multifocally while the remainder of the vascular walls are still visible. May see endothelial nuclear pycnosis and karryorrhexis.

© University of Pretoria

	Wall not intact (dissolution) (3)	Smudged full circumference of vessel walls with loss of detail, pycnotic endothelial nuclei, karyolysis and cellular debris.
Vasculitis - distribution (location iro lesion)	Absent	No evidence of inflammatory cell infiltrate associated with the vessel walls.
	Intralesional (IL)	Inflammation predominantly (>50%) present within the lesion.
	Perilesional (PL)	Inflammation predominantly (>50%) present at the edge of the lesion.
	Extralesional (EL)	Inflammation predominantly (>50%) present away from the lesion.
	Mixed	Distribution of inflammation is so mixed that no predominant area can be identified.
Fibrin (HE)	Absent (0) Present (1)	No evidence of fibrin exudate. Suspect fibrin exudate. Note location and suspicion – to be confirmed on special stain (MSB).
Fibrin - severity (vascular, MSB special stain)	Absent (0) Mild (1)	No evidence of fibrinous exudate. Affecting less than a third of the blood vessels (under 100x magnification, estimated over 10 x FOV).
	Moderate (2)	Affecting more than a third to two thirds of the blood vessels (under 100x magnification, estimated over 10 x FOV).
	Severe (3)	Affecting more than two thirds of the blood vessels (under 100x magnification, estimated over 10 x FOV).
Fibrin – distribution (vascular, MSB special stain)	Intravascular	Majority (>50%) of the fibrin present, is located in the vascular lumen.
	Vascular wall	Majority (>50%) of the fibrin present, is located in the vascular wall/s.
	Perivascular	Majority (>50%) of the fibrin present, is located outside vascular walls and/or lumens.
	Mixed	Fibrin present is not concentrated in a specific location. Specify/describe which areas are affected. Make note in space provided.
Thrombi – distribution (location iro lesion)	Absent Intralesional (IL)	No evidence of thrombi. Thrombi are predominantly (>50%) present within the lesion.
	Perilesional (PL)	Thrombi are predominantly (>50%) present at the edge of the lesion.
	Extralesional (EL)	Thrombi are predominantly (>50%) present away from the lesion.
	Mixed	Distribution of thrombi is so mixed that no predominant area can be identified.
Thrombi	Absent (0) Mild (1)	No evidence of thrombi. 1-2 thrombi identified in total for all histology sections per case.
	Moderate (2)	3-5 thrombi identified in total for all histology sections per case.
	Severe (3)	≥ 6 thrombi identified in total for all histology sections per case.
	Cellular infiltrate	Identify and describe predominant cellular component of thrombus/thrombi, based on HE (IMP will confirm later).
	Distribution	Identify and describe predominant location of thombus/thrombi (white matter, grey matter, meninges or mixed).
Endothelial cell hypertrophy	Absent (0) Mild (1)	No evidence of endothelial cell hypertrophy. Less than one third of endothelial cells display nuclear activation/hypertrophy.

© University of Pretoria

✓ Endothelial hypertrophy = nucleus width is double or more than the normal thickness. ✓ Use 100x magnification to scan for changes and check details of at least 5 blood vessels (IL, PL and EL) at 400x magnification. ✓ Will check on IMP (VCAM1)	Moderate (2) Severe (3)	One to two thirds of endothelial cells display nuclear activation/hypertrophy. More than two thirds of endothelial cells display nuclear activation/hypertrophy.
Leucostasis **(see annotation 1)** ✓ Use similar sized vessels ✓ Use 100x magnification to scan and check details of at least 5 blood vessels per IL, PL and EL at 400x magnification.	Absent Mild Moderate Severe Cellular infiltrate Distribution	No evidence of leucostasis. Less than one third of the blood vessels display leucostasis at 400 x magnification, when checking at least 3 FOV. One to two thirds of the blood vessels display leucostasis at 400 x magnification, when checking at least 3 FOV. More than two thirds of the blood vessels display leucostasis at 400 x magnification, when checking at least 3 FOV. Identify and describe predominant cellular component (mononuclear or PMN) in leucostatic blood vessels, based on HE (IMP will confirm later). Identify and describe predominant location of leucostasis (white matter, grey matter, meninges or mixed).
Oedema (vasogenic) = amorphous clear to eosinophilic extravascular fluid. ✓ Use similar sized vessels ✓ Use 100x magnification to scan and check details of at least 5 blood vessels per IL, PL and EL at 400x magnification.	Absent (0) Mild (1) Moderate (2) Severe (3)	No evidence of oedema. Slight expansion (1x capillary wall thickness) of the perivascular or perineuronal (approximately half average neuron diameter) areas by oedema fluid. Moderate expansion (2-3x capillary wall thickness) of the perivascular or perineuronal (approximately half to single average neuron diameter) areas by oedema fluid. Marked expansion (>3x capillary wall thickness) of the perivascular or perineuronal (approximately more than one neuron diameter) areas by oedema fluid.
Oedema (cytotoxic) **= amorphous clear to eosinophilic perineuronal fluid.** ✓ Check at least 5 FOV in IL, PL and EL	Absent (0) Present (1)	No evidence of perineuronal oedema. Perineuronal oedema is present around most neurons (>50%)
Congestion (intravascular accumulation of RBCs)	Absent (0) Present (1)	No evidence of congestion/hyperaemia. Congestion is present in most blood vessels (>50%) in all available histology sections. **Note: check venules, arterioles and capillaries. If present in arterioles make a note (= hyperaemia).**
Parasitaemia - percentage Approximately 5mm areas chosen: - **Intralesional (IL)** - **Perilesional (PL)** - **Extralesional (EL)** (Proportion parasitised erythrocytes calculated based on total. Count at least 150 RBCs)	Absent (0) Low number (1) Moderate number (2) High number (3)	No evidence of parasite erythrocytes. Less than 20% of the erythrocytes are parasitised. Between 20% and 50% of the erythrocytes are parasitised. More than 50% of the erythrocytes are parasitised.
pRBCs (parasitised RBCs) aggregates in capillaries	Absent (0)	Lack of agglutination in pRBCs in capillaries.

© University of Pretoria

Note: focus on capillaries. Aggregates = intravascular slowing and/or clumping of red blood cells NB: definition = excludes active tethering!	Present (1)	>50% of pRBCs in intact capillaries show intravascular agglutination at 400x magnification, within 3 FOV.
Neuronal injury ✓ Use 100x magnification to scan for changes and check details at 400x magnification ✓ Check at least 5 FOV in IL, PL and EL ✓ No score ✓ Neuronal cellular changes: 1. Hypereosinophilia 2. Peripheralisation of nissl substance with irregular granular cytoplasm 3. Shrunken cytoplasm 4. Neurophagia 5. Pycnosis, karyolysis, karryorrhexis or chromatolysis **(should see at least 3 of above criteria)**	Absent Present	No evidence of neuronal degeneration. Neuronal injury is present, specify location (IL, PL or EL)
Neurophagia ✓ Neurophagic nodules form around an injured neuron ✓ Use 100x magnification to scan for changes and check details at 400x magnification ✓ Check at least 5 FOV in IL, PL and EL ✓ No score	Absent Present	No evidence of neurophagia is observed. Neurophagic nodules are observed, specify location (IL, PL and EL)
Neuropil inflammatory cell infiltrate ✓ Per HPF at 400 x magnification, when checking at least 3 FOV. ✓ Identify and describe predominant cellular component in leucostatic blood vessels, based on HE (IMP will confirm later).	Absent (0) Scant (1) Obvious (2) Mononuclear Neutrophils	No evidence of inflammatory cell infiltrate. Up to 5 leucocytes present in neuropil. More than 5 leucocytes present in neuropil. Lymphocytes (T or B), plasma cells, monocytes, macrophages Neutrophils predominate and are distinguished from other granulocytes (eosinophils, mast cells or basophils) based on histomorphology.
Demyelination (LFB) ✓ Primary demyelination = absence of blue-staining myelin sheaths, silver impregnated axons remain intact. ✓ Secondary demyelination = concomitant loss of axons and myelin sheaths. *(Macrophages may contain myelin debris).*	Absent (0) Mild (1) Moderate (2) Severe (3)	No evidence of LFB staining. Demyelination observed in less than one third of neuropil at 400x magnification, when checking 3 FOV. Demyelination observed in less than one to two thirds of neuropil at 400x magnification, when checking 3 FOV. Demyelination observed in more than two thirds of neuropil at 400x magnification, when checking 3 FOV.
Spongiosis - distribution ✓ vacuolation of myelin sheaths ✓ astroglial swelling ✓ Perivascular, perineuronal and periglial spaces expanded by oedema.	Absent (0) Grey matter White matter Mixed	No evidence of spongiosis. >50% of the lesions are in the grey matter. >50% of the lesions are in the white matter. Distribution between the grey and white matter varies to the extent that neither is dominant.

© University of Pretoria

Spongiosis – severity ✓ **400x magnification, when checking 3 FOV.**	Absent Mild (1) Moderate (2) Severe (3)	No evidence of spongiosis. Spongiosis observed in less than one third of neuropil Spongiosis observed in one to two thirds of neuropil. Spongiosis observed in more than two thirds of neuropil

IMMUNOHISTOCHEMISTRY

Immunoperoxidase reactivity ***Vasculitis * Neuronal changes** *** Association with lesions** - CD3, CD20, MAC387, IBA-1 and VCAM1 - At least 3 x hotspots / case with 50-100 cells / hotspot - Vasocentric / PL areas are good areas to use - Avoid haemorrhagic areas - Count % positive labelling cells out of total of 300 leucocytes *Take photos to count, using 20x or 40x magnification.*	Absent (0) Mild (1) Moderate (2) Severe (3)	No immunolabelling was present. <20% cells labelled clearly per HPF. 20-50% cells labelled clearly per HPF. >50% cells labelled clearly per HPF.

Notes on IMP markers:
CD3 = T lymphocytes [Dako]
CD20 = B lymphocytes including plasma cells [Thermo Fisher Scientific]
MAC387 = monocytes-macrophages / mature granulocytes (including neutrophils) / recently migrated (extravascular) mononuclear leucocytes / reactive tissue macrophages / tissue eosinophils [Dako]
IBA1 = tissue macrophages / microglia and dendritic cells (can be intravascular, but primarily extravascular in CCB) [Abcam]
VCAM-1 = cytokine activated endothelium [Thermo Fisher Scientific]

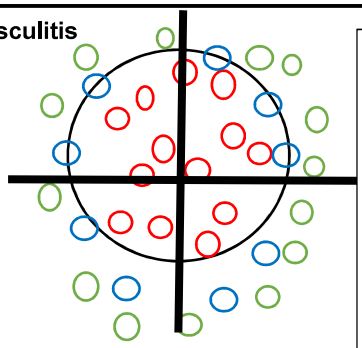
SCORING SYSTEMS:

1) HAEMORRHAGE - Haemorrhage size (descriptive)	**2) VASCULATURE (Max = 16)** - Fibrin (MSB) - Vascular necrosis - Endothelial hypertrophy (HE) - VCAM 1
3) INFLAMMATION (Max = 34) - Vascular - Neuropil - IHC (CD3, CD20, MAC387, IBA-1, VCAM1)	**4) GLOBAL (Max = 18)** - Leucostasis - Oedema - Congestion - Parasitaemia
5) NEURONAL CHANGES (Max = 3) - Neuronal injury - Demyelination (LFB) - Spongiosis	**ABSENT = O** Mild / Present / Scant / Low number = 1 Moderate / Obvious / Moderate number = 2 Severe / High number = 3

High power field (400x magnification)
FOV: Field of view
HE: Haematoxylin - eosin staining
LFB: Luxol fast blue stain
MSB: Martius scarlet blue stain
PMN: Polymorphonuclear cells (granulocytes = neutrophils, eosinophils, basophils, mast cells)

© University of Pretoria

Annotation 1*Vasculitis



Distribution:

- Perivascular (leucocytes outside vessel wall)
- Vascular wall (leucocytes within vessel wall)
- Intravascular (leucocytes inside vessel lumen) = leucostasis

Severity scoring

Divide into quarters:

- Mild = 1/4 affected
- Moderate = 2/4 affected
- Severe =3/4 to whole vessel affected

© University of Pretoria

Appendix C: Master summary check sheet for all cases (see attached)

© University of Pretoria

UNIVERSITEIT VAN PRETORIA
UNIVERSITY OF PRETORIA
YUNIBESITHI YA PRETORIA

APPENDIX A

CCB -APPENDIX HISTOPATHOLOGY DATASHEET

TEMPLATE

Criteria	S-number:	Comments
Signalment		
Hx of nervous signs (absent / Present)		
RT-qPCR results (2017 cases)		

Brain histopathology										Score
Autolysis	☐ Absent	☐ Mild	☐ Moderate	☐ Severe						
Microscopic lesions present?	☐ Absent	☐ Present								
Lesion distribution (histological)	☐ Absent	☐ Focal	☐ Multifocal	☐ Coalescing	☐ Diffuse					
		☐ Grey matter	☐ White matter	☐ Mixed						
		☐ Deep sulci	☐ Superficial sulci	☐ Undetermined						
Haemorrhage	☐ Absent	☐ Petechiae	☐ Ecchymoses	☐ Suffusive	☐ Ring haemorrhages					
Vasculitis	Inflammatory cellular infiltrate (types of cells), severity and distribution, as identified on HE		Absent = A; Intralesional = IL; Perilesional = PL; Extralesional = EL							
			Mononuclear A (0) ☐	☐ Mild (1)	☐ Moderate (2)	☐ Severe (3)	☐ IL	☐ PL	☐ EL	
			Neutrophils A (0) ☐	☐ Mild (1)	☐ Moderate (2)	☐ Severe (3)	☐ IL	☐ PL	☐ EL	
	Type of vasculitis		☐ Necrotising	☐ Fibrinoid	☐ Necrotic debris					
			☐ Inflammatory	☐ Perivascular	☐ Vascular wall	☐ Intravascular				
	Vascular necrosis		☐ Absent (0)	☐ Wall intact (1)	☐ Wall partially intact (2)	☐ Wall not intact (dissolution) (3)	☐ IL	☐ PL	☐ EL	
	Fibrin	HE	☐ Absent (0)	☐ Present (1)						
		MSB	☐ Absent (0)	☐ Perivascular	☐ Vascular wall	☐ Intravascular	☐ Mixed			
				☐ Mild (1)	☐ Moderate (2)	☐ Severe (3)	☐ IL	☐ PL	☐ EL	
	Thrombi	☐ Absent (0)	☐ Mild (1)	☐ Moderate (2)	☐ Severe (3)	☐ White matter	☐ Grey matter	☐ Meninges		
			☐ Mononuclear	☐ Neutrophils			☐ IL	☐ PL	☐ EL	
	Endothelial cell	Hypertrophy	☐ Absent (0)	☐ Mild (1)	☐ Moderate (2)	☐ Severe (3)				
	IMP	CD3	☐ Absent (0)	☐ Mild (1)	☐ Moderate (2)	☐ Severe (3)	☐ IL	☐ PL	☐ EL	
			Enter details on distribution wrt vasculature, eg. Perivascular, intravascular, vascular wall							
		CD20	☐ Absent (0)	☐ Mild (1)	☐ Moderate (2)	☐ Severe (3)	☐ IL	☐ PL	☐ EL	
			Enter details on distribution wrt vasculature, eg. Perivascular, intravascular, vascular wall							
		MAC387	☐ Absent (0)	☐ Mild (1)	☐ Moderate (2)	☐ Severe (3)	☐ IL	☐ PL	☐ EL	
			Enter details on distribution wrt vasculature, eg. Perivascular, intravascular, vascular wall							
		IBA-1	☐ Absent (0)	☐ Mild (1)	☐ Moderate (2)	☐ Severe (3)	☐ IL	☐ PL	☐ EL	
			Enter details on distribution wrt vasculature, eg. Perivascular, intravascular, vascular wall							
		VCAM1	☐ Absent (0)	☐ Mild (1)	☐ Moderate (2)	☐ Severe (3)	☐ IL	☐ PL	☐ EL	
			Enter details on distribution wrt vasculature, eg. Perivascular, intravascular, vascular wall							
Leucostasis	☐ Absent (0)	White matter	☐ Mild (1)	☐ Moderate (2)	☐ Severe (3)	☐ Mononuclear	☐ Neutrophils		☐ IL	☐ PL	☐ EL	
		Grey matter	☐ Mild (1)	☐ Moderate (2)	☐ Severe (3)	☐ Mononuclear	☐ Neutrophils		☐ IL	☐ PL	☐ EL	
		Meninges	☐ Mild (1)	☐ Moderate (2)	☐ Severe (3)	☐ Mononuclear	☐ Neutrophils		☐ IL	☐ PL	☐ EL	
Oedema	Vasogenic	☐ Absent (0)	☐ Mild (1)	☐ Moderate (2)	☐ Severe (3)				☐ IL	☐ PL	☐ EL	
	Cytotoxic	☐ Absent (0)	☐ Present (1)						☐ IL	☐ PL	☐ EL	
Congestion	☐ Absent (0)	☐ Present (1)								
Parasitaemia (use oil)	Degree of parasitaemia (intravascular)	☐ Absent (0)	☐ Low number (1)	☐ Moderate number (2)	☐ High number (3)					
	pRBC aggregates in capillaries	☐ Absent (0)	☐ Present (1)						☐ IL	☐ PL	☐ EL	

© University of Pretoria

UNIVERSITEIT VAN PRETORIA
UNIVERSITY OF PRETORIA
YUNIBESITHI YA PRETORIA

APPENDIX A

CCB -APPENDIX HISTOPATHOLOGY DATASHEET

TEMPLATE

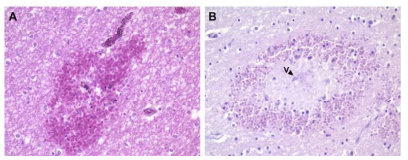
Neuronal and neuropil changes	Neuronal injury	☐ Absent	☐ Present				☐ IL	☐ PL	☐ EL
	Neurophagia	☐ Absent	☐ Present				☐ IL	☐ PL	☐ EL
	Neuropil inflammatory cellular infiltration (HE)	Mononuclear	☐ Absent (0)	☐ Scant (1)	☐ Obvious (2)		☐ IL	☐ PL	☐ EL
		Neutrophils	☐ Absent (0)	☐ Scant (1)	☐ Obvious (2)		☐ IL	☐ PL	☐ EL
	IMP	CD3	☐ Absent (0)	☐ Mild (1)	☐ Moderate (2)	☐ Severe (3)	☐ IL	☐ PL	☐ EL
		CD20	☐ Absent (0)	☐ Mild (1)	☐ Moderate (2)	☐ Severe (3)	☐ IL	☐ PL	☐ EL
		MAC387	☐ Absent (0)	☐ Mild (1)	☐ Moderate (2)	☐ Severe (3)	☐ IL	☐ PL	☐ EL
		IBA-1	☐ Absent (0)	☐ Mild (1)	☐ Moderate (2)	☐ Severe (3)	☐ IL	☐ PL	☐ EL
Spongiosis	☐ Absent (0)	Distribution	☐ Grey matter	☐ White matter	☐ Mixed		☐ IL	☐ PL	☐ EL
		Demyelination (LFB)	☐ Mild (1)	☐ Moderate (2)	☐ Severe (3)		☐ IL	☐ PL	☐ EL
			☐ Primary	☐ Secondary			☐ IL	☐ PL	☐ EL
IMP in association with lesions	CD3	☐ Absent (0)	☐ Intact vasculature (yes/no)	Haemorrhage (yes/no) ☐	Myelin damage (yes/no) *link with LFB ☐	☐ Axonal damage (yes/no)	☐ IL	☐ PL	☐ EL
	CD20	☐ Absent (0)	☐ Intact vasculature (yes/no)	Haemorrhage (yes/no) ☐	Myelin damage (yes/no) *link with LFB ☐	☐ Axonal damage (yes/no)	☐ IL	☐ PL	☐ EL
	IBA-1	☐ Absent (0)	☐ Phagocytosed Babesia parasites (yes/no)	Haemorrhage (yes/no) ☐	☐ Leucostasis (yes/no)		☐ IL	☐ PL	☐ EL
	MAC387	☐ Absent (0)	Acute lesion/s (define "acute lesions") ☐	Haemorrhage (yes/no) ☐	☐ Longer-standing / sub-acute lesion/s (define)	☐ Chronic lesion/s (define)	☐ IL	☐ PL	☐ EL
	VCAM-1	☐ Absent (0)	☐ Intact vasculature (yes/no)	Haemorrhage (yes/no) ☐	Myelin damage (yes/no) *link with LFB ☐	☐ Axonal damage (yes/no)	☐ IL	☐ PL	☐ EL

ADDITIONAL NOTES

Do Von Kossa's? ☐ Yes ☐ No
Do Smooth muscle actin (SMA)? ☐ Yes ☐ No

Total scores:
Haemorrhage and IMP (descriptive)
Inflammation (max = 34)
Neuronal changes (max = 3)
Vasculature (max =16)
Global changes (max = 18)
[TOTAL 71]

© University of Pretoria

PARAMETER	GRADING/ SCORE	CRITERIA
AUTOLYSIS		
Severity	Mild	Anatomical architecture easily distinguishable, cellular morphology well-defined.
	Moderate	Anatomical architecture still easily distinguishable, cellular morphology not well-defined, red blood cells still preserved, small numbers of putrefactive (Clostridial) bacteria may be present in some fields.
	Severe	Cellular morphology cannot be defined, anatomical architecture barely distinguishable, red blood cells lysed and difficult to identify, numerous putrefactive (Clostridial) bacteria present.
HISTOPATHOLOGY	(All changes in comparison with normal control brain).	
Lesion definition: Haemorrhage with or without spongiosis and/or malacia. **Score and describe the WORST lesion/s per area or histological change.**		
Microscopic lesions	Absent	No evidence of microscopic lesions when scanning on 40x and 100x magnification.
	Present	Evidence of microscopic lesions, regardless of severity or distribution.
Lesion distribution (histologic) *Note: macroscopic distribution (see discussion) will be based on A. Pardini's thesis; use full set wax blocks to check macro and describe. Scanned all blocks that were chosen based on macro lesions. Chose block with worst lesions (haemorrhage).*	Absent Focal Multifocal Coalescing Diffuse	No evidence of microscopic lesions. Single well circumscribed area affected. Multiple non-overlapping areas affected Multiple overlapping areas affected. Entire section of tissue OR all specific anatomical sites affected
General distribution of pathological changes wrt lesion	Intralesional (IL) Perilesional (PL) Extralesional (EL)	Predominantly (>50%) present within the lesion. Predominantly (>50%) present at the edge of the lesion. Predominantly (>50%) present away from the lesion.
Grey versus white matter	Grey matter White matter Mixed	>50% of the lesions are in the grey matter. >50% of the lesions are in the white matter. Distribution between the grey and white matter varies to the extent that neither is dominant.
Anatomical distribution	Deep sulci Superficial sulci Undetermined	Majority of the lesion/s present occur in the deeper half of the sulci. Majority of the lesion/s present occur in the superficial half of the sulci. The anatomical location was unclear or no predominant area wrt sulci.
Haemorrhage= Extravasated erythrocytes Prapansilp, P, et al 2013  Petechia Ring haemorrhage	Absent (0) Petechiae Ecchymoses Suffusive Ring haemorrhages	No evidence of haemorrhage. Extravasated erythrocytes are restricted to less than one half of the approximate diameter of the cerebellar molecular layer (1-2mm in diameter). Extravasated erythrocytes fill up between one half and the full approximate diameter of the cerebellar molecular layer (up to 2-3cm in diameter). Extravasated erythrocytes fill up more than the full approximate diameter of the cerebellar molecular layer (larger than 3cm in diameter, notable macroscopically). Vasocentric haemorrhages which surround a central small to medium sized blood vessel, surrounded by a zone of clearing (and astroglial response). There is an outer zone of erythrocytes and leukocytes which have been extravasated from the ruptured vessel. May contain fibrin platelet thrombi in the vascular lumen.
Vasculitis –cellular infiltration and severity (see annotation*). Purpose is to try and identify the inflammatory cell type/s based on HE morphology, but IMP will follow for clarity. (400 x magnification, when checking at least 3 FOV)	Absent (0) Mild (1) Moderate (2) Severe (3) Mononuclear Neutrophils	No evidence of inflammatory cell infiltrate. Single leukocytes present within (intramural) or surrounding the vascular wall, without notable expansion of the blood vessel wall/s; 1/4 of vessel walls affected. One layer of leukocytes present within the vascular wall (intramural), resulting in slight expansion of the vascular wall. 2/4 of vessel walls affected. More than one layer of leukocytes present within the vascular wall (intramural), resulting in marked expansion of the vascular wall. 3/4 to whole of vessel walls affected. Lymphocytes (T or B), plasma cells, monocytes or macrophages predominate. Neutrophils predominate and are distinguished from other granulocytes (eosinophils, mast cells or basophils) based on histomorphology.

© University of Pretoria

Vasculitis – type (400 x magnification, when checking at least 3 FOV)	Absent Necrotising Inflammatory	No evidence of inflammatory cell infiltrate associated with the vessel walls. Smudged eosinophilia (**fibrinoid**) change to the vessel walls. Smudged eosinophilia (fibrinoid) with evidence of **necrotic debris**, loss of detail and crispness, endothelial nuclei pycnotic, swollen or absent. Predominantly inflammatory infiltration, without evidence of necrotising changes (see vasculitis distribution below).
Vasculitis – distribution (iro vascular wall) *See leucostasis.*	Absent Perivasculitis Vasculitis Intravascular	No evidence of inflammatory cell infiltrate associated with the vessel walls. Inflammation predominantly (>50%) present in perivascular areas **(see annotation*).** Inflammation predominantly (>50%) present within the vessel walls **(see annotation*).**
Vascular necrosis	Absent (0) Wall intact (1) Wall partially intact (2) Wall not intact (dissolution) (3)	No evidence of vessel wall changes. Homogenous eosinophilia and rarefaction of vessel walls, but vascular wall remains intact. Homogenous eosinophilia and rarefaction of vessel walls, with loss of vascular wall multifocally while the remainder of the vascular walls are still visible. May see endothelial nuclear pycnosis and karyorrhexis. Smudged full circumference of vessel walls with loss of detail, pycnotic endothelial nuclei, karyolysis and cellular debris.
Vasculitis - distribution (location iro lesion)	Absent Intralesional (IL) Perilesional (PL) Extralesional (EL) Mixed	No evidence of inflammatory cell infiltrate associated with the vessel walls. Inflammation predominantly (>50%) present within the lesion. Inflammation predominantly (>50%) present at the edge of the lesion. Inflammation predominantly (>50%) present away from the lesion. Distribution of inflammation is so mixed that no predominant area can be identified.
Fibrin (HE)	Absent (0) Present (1)	No evidence of fibrin exudate. Suspect fibrin exudate. Note location and suspicion – to be confirmed on special stain (MSB).
Fibrin - severity (vascular, MSB special stain)	Absent (0) Mild (1) Moderate (2) Severe (3)	No evidence of fibrinous exudate. Affecting less than a third of the blood vessels (under 100x magnification, estimated over 10 x FOV). Affecting more than a third to two thirds of the blood vessels (under 100x magnification, estimated over 10 x FOV). Affecting more than two thirds of the blood vessels (under 100x magnification, estimated over 10 x FOV).
Fibrin – distribution (vascular, MSB special stain)	Intravascular Vascular wall Perivascular Mixed	Majority (>50%) of the fibrin present, is located in the vascular lumen. Majority (>50%) of the fibrin present, is located in the vascular wall/s. Majority (>50%) of the fibrin present, is located outside vascular walls and/or lumens. Fibrin present is not concentrated in a specific location. Specify/describe which areas are affected. Make note in space provided.
Thrombi – distribution (location iro lesion)	Absent Intralesional (IL) Perilesional (PL) Extralesional (EL) Mixed	No evidence of thrombi. Thrombi are predominantly (>50%) present within the lesion. Thrombi are predominantly (>50%) present at the edge of the lesion. Thrombi are predominantly (>50%) present away from the lesion. Distribution of thrombi is so mixed that no predominant area can be identified.
Thrombi	Absent (0) Mild (1) Moderate (2) Severe (3) Cellular infiltrate Distribution	No evidence of thrombi. 1-2 thrombi identified in total for all histology sections per case. 3-5 thrombi identified in total for all histology sections per case. ≥ 6 thrombi identified in total for all histology sections per case. Identify and describe predominant cellular component of thrombus/thrombi, based on HE (IMP will confirm later). Identify and describe predominant location of thombus/thrombi (white matter, grey matter, meninges or mixed).
Endothelial cell hypertrophy ✓ Endothelial hypertrophy = nucleus width is double or more than the normal thickness. ✓ Use 100x magnification to scan for changes and check details of at least 5 blood vessels (IL, PL and EL) at 400x magnification. ✓ Will check on IMP (VCAM1)	Absent (0) Mild (1) Moderate (2) Severe (3)	No evidence of endothelial cell hypertrophy. Less than one third of endothelial cells display nuclear activation/hypertrophy. One to two thirds of endothelial cells display nuclear activation/hypertrophy. More than two thirds of endothelial cells display nuclear activation/hypertrophy.

© University of Pretoria

Leucostasis **(see annotation 1)** ✓ Use similar sized vessels ✓ Use 100x magnification to scan and check details of at least 5 blood vessels per IL, PL and EL at 400x magnification.	Absent Mild Moderate Severe Cellular infiltrate Distribution	No evidence of leucostasis. Less than one third of the blood vessels display leucostasis at 400 x magnification, when checking at least 3 FOV. One to two thirds of the blood vessels display leucostasis at 400 x magnification, when checking at least 3 FOV. More than two thirds of the blood vessels display leucostasis at 400 x magnification, when checking at least 3 FOV. Identify and describe predominant cellular component (mononuclear or PMN) in leucostatic blood vessels, based on HE (IMP will confirm later). Identify and describe predominant location of leucostasis (white matter, grey matter, meninges or mixed).
Oedema (vasogenic) = amorphous clear to eosinophilic extravascular fluid. ✓ Use similar sized vessels ✓ Use 100x magnification to scan and check details of at least 5 blood vessels per IL, PL and EL at 400x magnification.	Absent (0) Mild (1) Moderate (2) Severe (3)	No evidence of oedema. Slight expansion (1x capillary wall thickness) of the perivascular or perineuronal (approximately half average neuron diameter) areas by oedema fluid. Moderate expansion (2-3x capillary wall thickness) of the perivascular or perineuronal (approximately half to single average neuron diameter) areas by oedema fluid. Marked expansion (>3x capillary wall thickness) of the perivascular or perineuronal (approximately more than one neuron diameter) areas by oedema fluid.
Oedema (cytotoxic) **= amorphous clear to eosinophilic perineuronal fluid.** ✓ Check at least 5 FOV in IL, PL and EL	Absent (0) Present (1)	No evidence of perineuronal oedema. Perineuronal oedema is present around most neurons (>50%)
Congestion (intravascular accumulation of rbc's)	Absent (0) Present (1)	No evidence of congestion/hyperaemia. Congestion is present in most blood vessels (>50%) in all available histology sections. **Note: check venules, arterioles and capillaries. If present in arterioles make a note** **(= hyperaemia).**
Parasitaemia - percentage Approximately 5mm areas chosen: - **Intralesional (IL)** - **Perilesional (PL)** - **Extralesional (EL)** (Proportion parasitised erythrocytes calculated based on total. Count at least 150 rbc's)	Absent (0) Low number (1) Moderate number (2) High number (3)	No evidence of parasite erythrocytes. Less than 20% of the erythrocytes are parasitized. Between 20% and 50% of the erythrocytes are parasitized. More than 50% of the erythrocytes are parasitized.
pRBC's (parasitised rbc's) aggregates in capillaries Note: focus on capillaries. Aggregates = intravascular slowing and/or clumping of red blood cells NB: definition = excludes active tethering!	Absent (0) Present (1)	Lack of agglutination in pRBC's in capillaries. >50% of pRBC's in intact capillaries show intravascular agglutination at 400x magnification, within 3 FOV.
Neuronal injury ✓ Use 100x magnification to scan for changes and check details at 400x magnification ✓ Check at least 5 FOV in IL, PL and EL ✓ No score ✓ Neuronal cellular changes: 1. Hypereosinophilia 2. Peripheralisation of nissl substance with irregular granular cytoplasm 3. Shrunken cytoplasm 4. Neurophagia 5. Pycnosis, karyolysis, karyorrhexis or chromatolysis **(should see at least 3 of above criteria)**	Absent Present	No evidence of neuronal degeneration. Neuronal injury is present, specify location (IL, PL or EL)

© University of Pretoria

Neurophagia ✓ Neurophagic nodules form around an injured neuron ✓ Use 100x magnification to scan for changes and check details at 400x magnification ✓ Check at least 5 FOV in IL, PL and EL ✓ No score	Absent Present	No evidence of neurophagia is observed. Neurophagic nodules are observed, specify location (IL, PL and EL)
Neuropil inflammatory cell infiltrate ✓ Per HPF at 400 x magnification, when checking at least 3 FOV. ✓ Identify and describe predominant cellular component in leucostatic blood vessels, based on HE (IMP will confirm later).	Absent (0) Scant (1) Obvious (2) Mononuclear Neutrophils	No evidence of inflammatory cell infiltrate. Up to 5 leukocytes present in neuropil. More than 5 leukocytes present in neuropil. Lymphocytes (T or B), plasma cells, monocytes, macrophages Neutrophils predominate and are distinguished from other granulocytes (eosinophils, mast cells or basophils) based on histomorphology. eosinophils, mast cells and basophils
Demyelination (LFB) ✓ Primary demyelination = absence of blue-staining myelin sheaths, silver impregnated axons remain intact. ✓ Secondary demyelination = concommitant loss of axons and myelin sheaths. *(Macrophages may contain myelin debris).*	Absent (0) Mild (1) Moderate (2) Severe (3)	No evidence of LFB staining. Demyelination observed in less than one third of neuropil at 400x magnification, when checking 3 FOV. Demyelination observed in less than one to two thirds of neuropil at 400x magnification, when checking 3 FOV. Demyelination observed in more than two thirds of neuropil at 400x magnification, when checking 3 FOV.
Spongiosis - distribution ✓ vacuolation of myelin sheaths ✓ astroglial swelling ✓ Perivascular, perineuronal and periglial spaces expanded by oedema.	Absent (0) Grey matter White matter Mixed	No evidence of spongiosis. >50% of the lesions are in the grey matter. >50% of the lesions are in the white matter. Distribution between the grey and white matter varies to the extent that neither is dominant.
Spongiosis – severity ✓ **400x magnification, when checking 3 FOV.**	Absent Mild (1) Moderate (2) Severe (3)	No evidence of spongiosis. Spongiosis observed in less than one third of neuropil Spongiosis observed in one to two thirds of neuropil. Spongiosis observed in more than two thirds of neuropil
IMMUNOHISTOCHEMISTRY		
Immunoperoxidase reactivity ***Vasculitis * Neuronal changes** *** Association with lesions** - CD3, CD20, MAC387, IBA-1 and VCAM1 - At least 3 x hotspots / case with 50-100 cells / hotspot - Vasocentric / PL areas are good areas to use - Avoid haemorrhagic areas - Count % positive labelling cells out of total of 300 leukocytes *Take photos to count, using 20x or 40x magnification.*	Absent (0) Mild (1) Moderate (2) Severe (3)	No immunolabelling was present. <20% cells labelled clearly per HPF. 20-50% cells labelled clearly per HPF. >50% cells labelled clearly per HPF.

Notes on IMP markers:

CD3 = T lymphocytes [Dako]

CD20 = B lymphocytes including plasma cells [Thermo Fisher Scientific]

MAC387 = monocytes-macrophages / mature granulocytes (including neutrophils) / recently migrated (extravascular) mononuclear leukocytes / reactive tissue macrophages / tissue eosinophils [Dako]

IBA1 = tissue macrophages / microglia and dendritic cells (can be intravascular, but primarily extravascular in CCB) [Abcam]

VCAM-1 = cytokine activated endothelium [Thermo Fisher Scientific]

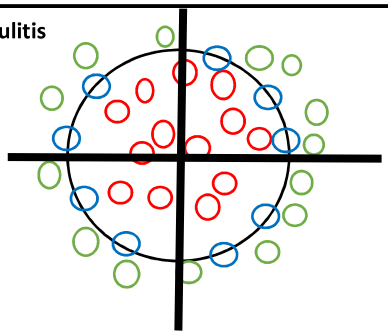
© University of Pretoria

SCORING SYSTEMS:

1) HAEMORRHAGE - Haemorrhage size (descriptive)	**2) VASCULATURE (Max = 16)** - Fibrin (MSB) - Vascular necrosis - Endothelial hypertrophy (HE) - VCAM 1
3) INFLAMMATION (Max = 34) - Vascular - Neuropil - IHC (CD3, CD20, MAC387, IBA-1, VCAM1)	**4) GLOBAL (Max = 18)** - Leucostasis - Oedema - Congestion - Parasitaemia
5) NEURONAL CHANGES (Max = 3) - Neuronal injury - Demyelination (LFB) - Spongiosis	**ABSENT = O** **MILD / PRESENT / SCANT / LOW NUMBER = 1** **MODERATE / OBVIOUS / MODERATE NUMBER = 2** **SEVERE / HIGH NUMBER = 3**

High power field (400x magnification)
FOV: Field of view
HE: Haematoxylin - eosin staining
LFB: Lucsol fast blue stain
MSB: Martius scarlet blue stain
PMN: Polymorphonuclear cells (granulocytes = neutrophils, eosinophils, basophils, mast cells)

Annotation 1*Vasculitis



Distribution:
- Perivascular (leucocytes outside vessel wall)
- Vascular wall (leucocytes within vessel wall)
- Intravascular (leucocytes inside vessel lumen) = leucostasis

Severity scoring
Divide into quarters:
- Mild = 1/4 affected
- Moderate = 2/4 affected
- Severe =3/4 to whole vessel affected

© University of Pretoria

Appendix C

	CCB Rx											CCB Not Rx						Non CCB				Control		
	1. S201-98	2. S598-97	3. S975-97	4. S965-97	5. S2575-97	6. S426-98	7. S1112-98	8. S1268-98	9. S1215-97	10. S3157-96	11. S1894-17	12. S1391-97	13. S923-97	14. S305-98	15. S2535-97	16. S1926-17		17. S2849-96	18. S2788-96	19. S1959-97	20. S3583-17	21. S1939-15 (7E)	22. S1939-15 (5D)	23. S1939-15 (8D)
Microscopic lesions present? (Y / N) & distrib	Y; MF, GM	Y; MF, Mixed	Y; MF, GM	Y; MF, Mixed	Y; MF, Mixed	Y; MF, GM	Y; F, Mixed	Y; MF, GM	Y; F, mixed	Y; MF, Mixed	Y; MF, mixed	Y; MF, mixed	Y; MF, mixed	Y; F, WM	Y; M, mixed	Y; MF, GM		N	N	N	N	N	N	N
Haemorrhage (P / E / S)	P, E & S	P	P	E	P	P>E	E>P	P	P	P>E	P	P	P	P	P	P		N	N	N	N	N	N	N
Inflamm cells (Neut / MN)	Neut>MN	MN=Neut	MN = Neut	Neut > MN	MN = Neut	MN = Neut	Neut > MN	MN = Neut	MN	Neut>MN	MN=Neut	MN>Neut	MN>Neut	MN=Neut	MN>Neut	MN=Neut		MN=Neut	MN>Neut	MN>Neut	MN>Neut	N	N	N
Inflamm cells, severity, (m, Mod, S)	S>Mod	m	S	S > m	m	S	S > Mod	S	Mod	S>Mod	Mod	Mod>m	Mod>m	m	Mod>m	Mod		m	Mod	Mod	S	N	N	N
Inflamm cells, distribution (IL, PL, EL)	PL	IL	IL	PL	IL	IL, PL	IL, PL	IL	Intrav (stasis)	PL	PL	IL, PL, EL	IL, PL, EL	IL	Intrav (stasis)	IL		Intrav (stasis)	Intrav (stasis)	Intrav (stasis)	Intrav (stasis)	N	N	N
Type vasculitis (Necr / Fibrin / Inflam)	Fib + infl	Inflam	Fib + Inflam	Necr + Infl	Necr+Fibr+Infl	Necr+Fibr+Infl	Fibr+Inflam	Inflam	Inflam	Necr, Fibr, Infla	Fibr, infl	Fibr, infl	Fibr, infl	Necr, Inflam	Infl (intrav)	Necr, fibrin, Infl		Inflam (intrav)	Inflam (intrav)	Inflam (intrav)	Inflam (intrav)	N	N	N
Type vasculitis (Periv/ Vas wall / Intrav)	Vas wall	Vas wall	Vas wall	Vas wall	Vas wall	Periv + Vas wall	Periva+ Vas wall	Vas wall	Vas wall	Perivas	Perivas	Vas wall	Vas wall	Perivasc	Intrav	Vas wall		Intrav (stasis)	Intrav (stasis)	Intrav (stasis)	Intrav (stasis)	N	N	N
Vascular necrosis and distrib (Intact / Partial / Complete) and IL, PL, EL	Partial; PL	Intact	Partial; IL	Partial; IL, PL	Complete, IL	Complete; IL, PL	Partial; IL, PL	Compl; IL	Complete; IL	Partial; PL	Partial; IL	Partial; IL, PL	Partial; IL, PL	Compl, IL	Intact	Partial, IL, PL		Intact	Intact	Intact	Intact	N	N	N
Fibrin HE (Y /N)	Y	N	Y	N	Y	Y	Y	N	N	Y	Y	Y	Y	N	N	Y		N	N	N	Y	N	N	N
Fibrin MSB (m, Mod, S & distrib)	Mod, PL	m, IL	Mod; IL, PL	Mod; PL, EL	Mod; IL, PL	Mod; IL, PL	Mod; IL, PL	Mod; IL	N	Mod, PL	m; IL	Mod; IL, PL	Mod; IL, PL, EL	m; IL	Mod; IL, PL, EL	Mod, PL, EL		N	N	N	Mod	N	N	N
Fibrin MSB (Periv/Vas wall/Intrav / Mixed)	Mixed	Periv	Mixed	Mixed	Mixed	Mixed	Mixed	Periv	N	Mixed	Vas wall	Vas wall	Intravas	Intravas	Intrav	Intrav		N	N	N	Intrav	N	N	N
Thrombi (Y/N)	N	N	N	N	N	N	N	N	N	N	N	N	N	N	N	N		N	N	N	m; Men, Neut	N	N	N
Endothelial hypertrophy HE (m, Mod, S)	S	Mod	Mod	m	Mod	Mod	Mod	Mod	Mod	Mod	m	Mod	Mod	Mod	m	Mod		Mod	m	m	S	N	N	N
Leucostasis location (GM / WM / Men)	GM>WM & Men	GM = WM	GM>Men	GM=WM=Men	GM= WM	GM=WM=Men	GM=WM>Men	GM> WM& Men	WM=GM=Men	GM>WM&Men	GM=WM	GM=WM	GM=WM	GM=WM	GM=WM=Men	GM>WM& Men		GM	GM&Men>WM	Men>GM>WM	Men>GM& WM	N	N	N
Leucostasis cell type (MN / Neut)	MN = Neut	MN = Neut (WM); MN (GM)	MN>Neut	MN = Neut (WM & GM); MN = Men	MN = Neut	MN = Neut	MN = Neut	MN=Neut	MN (WM&GM) MN=Neut (Men)	Neut (GM&WM) MN (Men)	Neut (WM) MN (GM)	MN=Neut	MN=Neut	MN=Neut	MN	MN=Neut		M=Neut	MN	MN=Neut	MN & Neut (Men); MN (GM&WM)	N	N	N
Leucostasis severity (m, Mod, S)	m (WM & Men); Mod (GM)	m	S (GM); m (Men)	m	Mod	Mod	S (GM+WM); Mod (Men)	Mod (GM); m (WM&Men)	m	Mod (GM) m (WM&Men)	m (GM&WM)	S (GM&WM)	S (GM&WM)	m	Mod	Mod (GM) > m (WM&Men)		m	Mod (GM&Men) m (WM)	S (Men) Mod (GM) m (WM)	Mod (Men) *thrombi m (GM&WM)	N	N	N
Leucostasis distrib (IL, PL, EL)	IL, PL & EL (global)	IL = PL	GM = IL; Men = EL	GM&WM = IL; Men = EL	PL	GM&WM = PL Men = IL, PL, EL (global)	GM&WM = PL; Men = EL	GM=IL,PL WM&Men=PL (global)	IL (GM&WM) PL, EL (Men)	GM&WM = IL Men = PL	GM&WM = IL	IL, PL, EL (global)	IL, PL, EL (global)	EL	IL, PL, EL	GM (PL, EL) WM (IL, PL) Men (EL)		N	N	N	Thrombi (Men)	N	N	N
Oedema Vasogenic (m, Mod, S)	S	S	Mod	Mod	m	S	Mod	S	m	Mod	m	S	S	S	m	m		Mod	m	S	Mod	N	N	N
Oedema Cytotoxic (Y/N)	Y	Y	Y	Y	N	Y	N	Y	N	N	N	N	N	Y	N	N		N	N	N	N	N	N	N
Congestion (Y / N)	Y	Y	Y	Y	Y	Y	Y	Y	Y	Y	Y	Y	Y	Y	Y	Y		Y	Y	Y	Y	N	N	N
Parasitaemia severity (low, mod, high)	Mod	L	H	L	H	Mod	Mod	H	L	L	L	H	H	H	Mod	L		Mod	H	H	L	N	N	N
Parasitaemia aggregates (Y/N)	Y	N	Y	N	Y	Y	Y	Y	N	N	N	Y	Y	Y	Y	N		Y	Y	Y	N	N	N	N
Neuronal injury (Y / N) & distrib	N	Y; IL, PL, EL	Y; PL	Y; IL, PL	Y; IL, PL & EL	Y; PL	Y; IL	Y; IL, PL	N	Y, PL	N	N	N	N	N	N		Y	N	N	N	N	N	N
Neurophagia (Y/N) & distrib	N	N	N	N	Y; IL	Y; PL	Y; IL, PL	Y; IL, PL	N	N	N	N	N	N	N	N		N	N	N	N	N	N	N
Neuropil inflamm (None/Scant /Obvious)	O	N	O	O	O	O	O	O	N	O	Sc	N	N	Sc	Sc	N		O	Sc	O	Sc	N	N	N
Neuropil inflamm (MN / Neut & distrib)	MN=Neut (IL, PL)	N	MN=Neut	MN=Neut; IL	MN > Neut; IL	MN=Neut; PL	MN=Neut	MN=Neut	N	MN=Neut	MN=Neut	N	N	MN=Neut	MN	N		MN>Neut	MN	MN>Neut	MN	N	N	N
Spongiosis (N/ GM / WM / Mix)	N	N	Mix	Mix	Mix	Mix	Mix	Mix	N	WM	GM	N	N	Mix	Mix	N		N	N	N	N	N	N	N
Spongiosis LFB	N	N	m	m	m	Mod	m	m	N	m	m	N	N	m	m	m		N	N	N	N	N	N	N
Spongiosis distrib (IL, PL, EL)	N	N	PL	IL, PL, EL	IL, PL, EL	PL, EL	PL	IL, PL	N	PL	IL	N	N	PL, EL	IL, PL, EL	PL, EL		N	N	N	N	N	N	N
	1. S201-98	2. S598-97	3. S975-97	4. S965-97	5. S2575-97	6. S426-98	7. S1112-98	8. S1268-98	9. S1215-97	10. S3157-96	11. S1894-17	12. S1391-97	13. S923-97	14. S305-98	15. S2535-97	16. S1926-17		17. S2849-96	18. S2788-96	19. S1959-97	20. S3583-17	21. S1939-15 (7E)	22. S1939-15 (5D)	23. S1939-15 (8D)
CD3 Vascular (Severity + Distrib)	N	N	N	N	N	m; EL	m; IL, PL, EL	N	N	N	N	N	N	N	N	N		N	N	N	N	N	N	N
CD3 Neuropil (Severity + Distrib)	N	N	N	N	N	N	N	N	N	N	N	N	N	N	N	N		N	N	N	N	N	N	N
CD20 Vascular (Severity + Distrib)	N	N	N	N	N	N	N	N	m; EL	N	N	N	N	N	m; EL	N		m; intrav	N	N	N	N	N	N
CD20 Neuropil (Severity + Distrib)	N	N	N	N	N	N	N	N	N	N	N	N	N	N	N	N		N	N	N	N	N	N	N
MAC387 Vascular (Severity + Distrib)	S; PL	S; IL, PL& EL	S; IL, PL & EL	S; IL, PL	Mod; IL, PL	S; IL	m; EL	S; IL, PL	S; IL, PL; EL	Mod; PL, EL	S; IL, PL, EL	m; PL, EL	m; PL, EL	S; IL, PL, EL	S; IL, PL, EL	Mod; IL, PL & EL		m; intrav	Mod; intrav	Mod; intrav	S; Intrav*thrombi	N	N	N
MAC387 Neuropil (Severity + Distrib)	S; IL, PL	N	S; IL	S; IL, PL	N	S; IL	N	S; IL, PL	S; IL, PL; EL	Mod; PL, EL	m; PL	N	N	N	N	m, IL		N	Mod; intrav	Mod; intrav	S; Intrav	N	N	N
IBA-1 Vascular (Severity + Distrib)	m; PL, EL	m; PL, EL	m, IL, PL & EL	m; PL, EL	Mod; IL, PL&EL	S; PL	Mod; EL	Mod; EL	Mod; EL	m; PL, EL	Mod; IL, PL, EL	M; PL, EL	Mod; PL, EL	m; IL, PL	m; IL, PL, EL	Mod; IL, PL & EL		N	N	N	m; Intrav*thrombi	N	N	N
IBA-1 Neuropil (Severity + Distrib)	m; PL, EL	m; PL, EL	m; EL	m; PL	N	S; PL	m; PL	S; IL, PL	N	m; PL, EL	m; PL	N	N	N	N	m, IL		N	N	N	m; Intrav	N	N	N
VCAM-1 Vascular (Severity + Distrib)	m; PL, EL	N	Mod; IL, PL	m, IL, PL, EL	m; IL, PL, EL	Mod; IL, PL	m; PL,IL	m; PL	N	m; PL	N	m; PL	m, PL	m; PL	m; IL, PL, EL	Mod; IL, PL & EL		N	N	N	m; *thrombi	N	N	N

Key:
N = none
m = mild
Mod = moderate
S = severe
IL = intralesional
PL = perilesional
EL = extralesional
O = obvious
Sc = scant
MN = mononuclear leucocytes
Neut = neutroophils
GM = grey matter
WM = white matter
Men = meninges
MF = multifocal
Intrav = intravascular
Infl = inflammation

© University of Pretoria

UNIVERSITEIT VAN PRETORIA
UNIVERSITY OF PRETORIA
YUNIBESITHI YA PRETORIA